이학박사학위논문

# 성별에 따른 사회적 고립의 영향과 시냅스 변화에 대한 연구

Studies on sexual dimorphism in social isolation and synaptic changes

2020년 8월


서울대학교 대학원

생명과학부

최 자 은

# ABSTRACT

## Studies on sexual dimorphism in social isolation and synaptic changes

Ja Eun Choi

School of Biological Sciences

The Graduate School

Seoul National University

Social animals prefer socially connected state and consume considerable energy to maintain the social bonds. To study social connections, many researchers have used the concept of social pain. Disconnection of social bond, which is social isolation, is one type of social pain (Eisenberger, 2012). When socially isolated, a strong motivation to seek social interactions occur in humans (Baumeister and Leary, 1995) as well as in rodents (Matthews et al., 2016). Numerous social isolation studies have been performed by modulating the duration of isolation in accordance with the

objectives, from as short as one day to as long as several months (Matthews et al., 2016; Zelikowsky et al., 2018). It is observed that sociability itself shows a sex-dependent phenotype (Borland et al., 2019; Brancato et al., 2017), which the sexual dimorphism is also detected in the isolated mice (Oliver et al., 2020). In human studies, it is reported that social isolation affects men and women differently (McLean et al., 2011; Vandervoort, 2000). Even though numerous researches have observed the sexual dimorphism in sociability, the underlying mechanism of "why and how" still remains largely unclear. Moreover, it is not investigated about the circuit-specific and synapse-specific perspective on how sociability is differently modulated by isolation in sex dependent manner.

The dopamine system in the brain is known to be related with reward, including rewards linked with sociability (Gunaydin et al., 2014). Extensive studies on the function of ventral tegmental area (VTA), a traditional brain region in the mesolimbic dopamine system, is being researched. Recently, the dorsal raphe nucleus (DRN), which is a distinct brain region containing the dopaminergic neurons, is receiving attention for the independent role of dopamine neurons (Lin et al., 2020; Matthews et al., 2016). However, the role of DRN dopaminergic neuron ($DRN^{TH}$) on circuit level and the consequences on sex-specific sociability remain largely unknown.

I observed that only the male mice showed increased sociability after 24 hours of social isolation. Using optogenetics and chemogenetics combined with immediate early gene (IEG)-based tagging system, I further manipulated the total

population and the isolation-activated neuronal ensembles of $DRN^{TH}$ and NAc shell ($NAc^{sh}$) and modulated isolation-induced sociability. I also found that synaptic strengthening between the isolation-activated neurons in $DRN^{TH}$ and $NAc^{sh}$ has occurred and this strengthening is needed for sociability increase. These findings will provide information on how isolation-induced sociability changes are modulated from synaptic level in sexual dimorphic way.

.....

Keywords : Social isolation, Sociability, Dorsal raphe nucleus, Nucleus accumbens, synapse

*Student Number : 2015-20451*

# CONTENTS

# LIST OF FIGURES

# CHAPTER I

# INTRODUCTION

# BACKGROUND

Maintaining social connections in socially innate animals is important throughout the life time. Thus, social disconnection is a powerful social pain and one type of social pain is the social isolation. Furthermore, sex differences in sociability are also seen in nature. Despite the various phenotypes revealed related to social isolation, remarkably little is known about the circuit-specific details and the neurobiological role of DRN dopaminergic neurons in social isolation and its sexual dimorphic outputs. This study presents the first evidence on how social isolation is regulated from synaptic level to behavioral level.

## Social isolation

Mice are highly social species that participate in social behaviors. Social isolation is a paradigm which separates the cagemates into individuals (Figure 1). Mice kept in the isolated state can be as short as 24 hours to as long as several months. Also, the age of the mice being isolated is known to be critical for the various effect. Therefore, researchers choose the duration of social isolation and the age of the mice being isolated by their experimental objectives.

Manipulation of social environment such as isolation leads to disruptions in various behavioral phenotypes; anxiety (Huang et al., 2017; Karkhanis et al., 2014;

Zelikowsky et al., 2018), depression (Oliver et al., 2020), cognition (Li et al., 2017) and sociability (Matthews et al., 2016; Zelikowsky et al., 2018). In molecular level, social isolation leads to changes in the level of NMDA receptor, monoamines and Tac2 expression in various brain regions (Krupina et al., 2020; Li et al., 2017; Zelikowsky et al., 2018). Sexual dimorphism is one of the phenotypes observed is the sociability, which is reported from human (Asher and Aderka, 2018) to mice (Greenberg et al., 2013; Oliver et al., 2020).

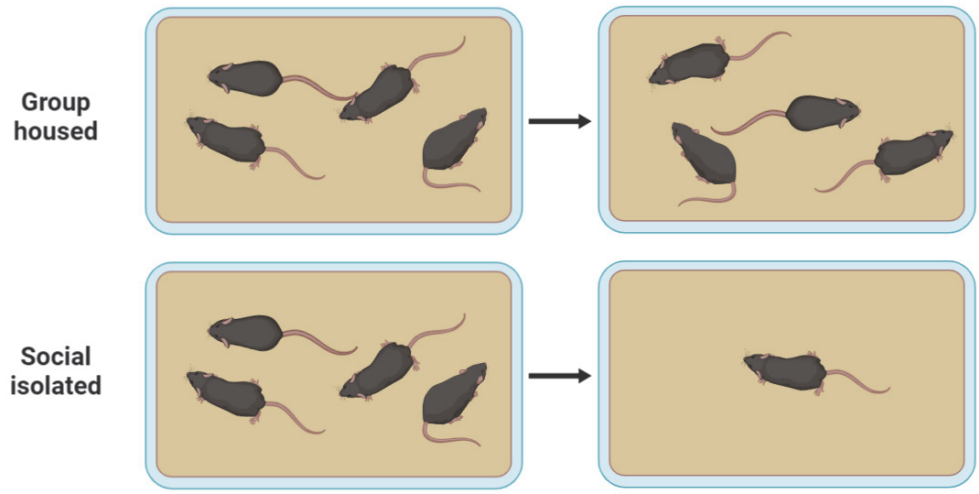


**Figure 1. Schematic image of group housed and social isolated mice**

Illustration of group housing and social isolation. Before moving the mice to a new cage, they were kept in the homecage for at least two weeks for adaptation. Group housing were performed by moving all the littermates to a new cage for 24 hours. Social isolation was performed by moving one mouse to each new cages for 24 hours.

## Dorsal raphe nucleus (DRN)

The DRN is a heterogeneous structure which is consisted with several cell types (Calizo et al., 2011; Huang et al., 2019; Seo et al., 2019). Serotonergic neurons are the most abundant cell type and provide majority of the serotonergic projections throughout the brain (Fernandez et al., 2016; Ishimura et al., 1988; Ren et al., 2018). Related to serotonergic neurons and sociability, a recent research from Malenka's lab has revealed that serotonergic projections from DRN to nucleus accumbens modifies social interaction (Walsh et al., 2018).

Even though the most well-known brain region in the mesolimbic dopamine system is the ventral tegmental area (VTA), distinct brain region containing the dopaminergic neurons exists in the DRN. The existence of dopaminergic neuronal population in the DRN has been described from several decades (Stratford and Wirtshafter, 1990; Trulson et al., 1985). Recently, the role of dopamine neurons in DRN ($DRN^{TH}$) have been receiving attention (Lin et al., 2020; Matthews et al., 2016), but is still a field of the unknown.

The DRN is one of the region related with social isolation. In 2016, Matthews and colleagues reported that the dopaminergic neurons of DRN represents the state of loneliness by 24-hours of isolation (Matthews et al., 2016). Four years after, another research group reported that the serotonergic neurons of DRN are affected in a chronic isolated state (Oliver et al., 2020).

## Nucleus accumbens (NAc)

The NAc can be divided into two sub-regions by structure with distinct projections, the NAc core and the NAc shell ($NAc^{sh}$) (Di Ciano et al., 2008). The neuronal cell type can also be classified into sub-populations according to the expression of dopamine receptors; D1-type and D2-type medium spiny neurons (MSNs). Since D1-MSNs and D2-MSNs have distinguished projections throughout the brain (Smith et al., 2013), various functions are related with the NAc. The NAc is studied to be related with motivation, addiction, reward, and reinforcement learning. In addition, it is also known to regulate social behaviors (Dolen et al., 2013; Gunaydin et al., 2014; Wallace et al., 2009). Moreover, a recent study from Eric J. Nestler's lab revealed the transcriptomes of NAc cell types and found sex differences in the molecule level (Kronman et al., 2019).

## Immediate early genes (IEGs)

Immediate early genes (IEGs) are used as neuronal activity markers. Even though FosB is the most well studied IEGs in striatal circuits (Grueter et al., 2013), there are studies revealing the role of c-fos (Badiani et al., 1998; Bertran-Gonzalez et al., 2008; Chandra et al., 2015; Ferguson and Robinson, 2004). Several researches have reported that cocaine induces a change in c-fos expression in the striatum (Bertran-Gonzalez et al., 2008) or c-fos expression modulation can change the response to cocaine (Zhang et al., 2006).

## Description of behavioral tests

The most widely used behavioral task to examine sociability is the three-chamber test. Therefore, in this study, three-chamber test was mainly used (Figure 2). Test mouse is allowed to freely move in the apparatus for 10 minutes, which is the habituation session. After the habituation, an unfamiliar juvenile mouse is placed under one cup, and an object is placed under the other cup. Then the test mouse is tested for the preference to the unfamiliar juvenile mouse for 10 minutes, which is the test session. The time of sniffing to each cup is analyzed and regarded as sociability. The velocity and the distance moved of test mouse can also be analyzed for anxiety index.

Juvenile interaction test is another behavioral task for examining sociability (Figure 3). Test mouse is placed in a new cage with new beddings for one minute to explore the context. Then, an unfamiliar juvenile stranger mouse is gently introduced into the apparatus. The interaction time of the test mouse is analyzed for 5 minutes.

This study used open field test to measure the anxiety level of the test mouse (Figure 4). The test mouse is placed in the center of the apparatus for 10 minutes of exploration. The total distance moved and time spent in the center is analyzed and regarded as the anxiety level.

**Figure 2. Schematic image of three-chamber test.**

Illustration of test mouse undergoing three-chamber test. An object is placed under one side of the chamber and an unfamiliar juvenile mouse in placed under other side of the chamber. Sociability was represented by counting the sniffing time to the stranger mouse by the total interaction time to each sides.

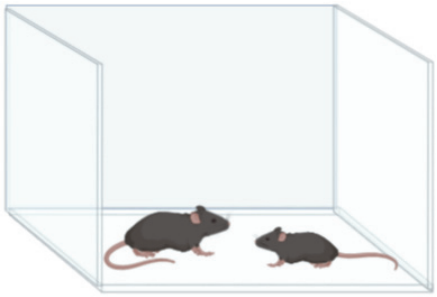

**Figure 3. Schematic image of juvenile interaction test.**

Illustration of test mouse interacting with unfamiliar juvenile mouse. The test mouse is exposed to the stranger mouse and the interaction time was presented as sociability.

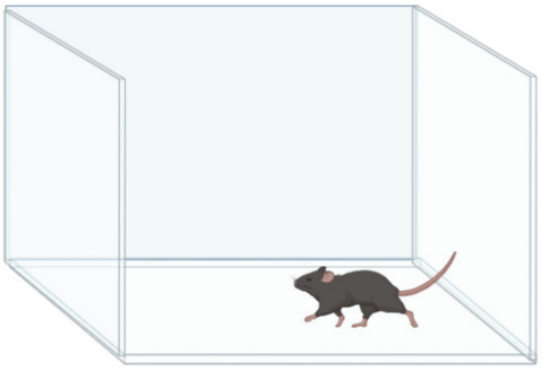

**Figure 4. Schematic image of open field test (OFT).**

Illustration of test mouse undergoing open field test. The test mouse in put in a chamber and was allowed to move freely. The time spent in the center was calculated with the total time spent in the chamber, which represented the anxiety of the mouse.

# PURPOSE OF THIS STUDY

Maintaining social connections in social creatures are important. Therefore, socially innate animals prefer socially connected state. Evidence from human studies and animal studies mention the action of dopamine on behaviors (Calipari et al., 2017; Hasbi et al., 2020), especially on sociability (Berkman et al., 1993; Newmann and Behavior, 1986; Trainor, 2011; Vandervoort, 2000). In addition, sexual dimorphism in sociability is observed in humans (McLean et al., 2011; Vandervoort, 2000), as in mice. However, the basic questions about how and where the sex-dependent social-isolation-induced phenotypes exist have not been pursued. In this thesis, I present for the first time on how social isolation is regulated from synaptic level to behavioral level.

In chapter II, I begin by observing sexual dimorphism in sociability after 24-hours of social isolation. I focused on the dopaminergic neurons in DRN and its monosynaptic connections with the $NAc^{sh}$ to reveal the underlying mechanism. I utilized optogenetic tools to activate or inhibit the $DRN^{TH}$-$NAc^{sh}$ circuit after social isolation to see whether this neural circuit modulates social-isolation-induced sociability.

In chapter III, I narrowed down the neural ensembles from total population to the isolation-activated cells and further manipulated these neurons. I tested whether inhibiting only the isolation-activated neurons can attenuate the isolation-

induced sociability. Then, I observed neuronal excitability, one of electrophysiological properties, and compared the isolation-activated with isolation-non-activated cells. Next, I further narrowed down to the synaptic level. I applied the dual-eGRASP technique and examined the synaptic density between isolation-activated $DRN^{TH}$ and $NAc^{sh}$ after social isolation. Finally, I inhibited the $DRN^{TH}$ neurons when being social isolated for 24-hours to see whether the activation of $DRN^{TH}$ neurons are necessary for the induction of isolation-induced sociability changes.

In this thesis, I address the underlying mechanism of social isolation and its sex-dependent phenotypes from synaptic level to behavioral level. Furthermore, I propose that the activated neuronal ensembles by social isolation are necessary for isolation-induced sociability, as engrams' role in memory.

# CHAPTER II

# Sexual dimorphism in 24-hours of social isolation is regulated by $DRN^{TH}$ and $NAc^{sh}$ neurons

# INTRODUCTION

Social animals, both human and mice, spend substantial amount of time to be socially connected. Thus, disconnecting the social bond raise social pain and one type of social disconnection is the “social isolation”. Moreover, sex may play a role in the responsiveness to social isolation, as previous study has reported that men were more isolated than women (Vandervoort, 2000). Rodents, also, prefer housing in a group rather than housing in an isolated state. However, less is revealed about the “where” and “how” the brain is regulating the social isolation induced changes, especially related with sociability. Moreover, the basic questions about sexual dimorphisms underlying social isolation have not been pursued.

In this chapter, I observed sex-dependent phenotypes in sociability changes after 24-hours of social isolation. Only the isolated male mice showed an increase in sociability following social isolation. In addition, I characterized the dopaminergic neurons projecting from DRN to $NAc^{sh}$ by screening the axonal projections, performing patch clamp recordings, and tracing monosynaptic connections in retrograde way. Finally, I optogenetically manipulated $DRN^{TH}$ to $NAc^{sh}$ circuit and confirmed that this neural circuit modulates isolation-induced sociability increase only in the male mice.

# EXPERIMENTAL PROCEDURES

## Animals

TH-cre male and female mice were maintained in a C57BL/6J background. Animals were housed with food and water *ad libitum* on a 12-hour light-dark cycle. For labeling TH positive neurons in DRN, I used tdTomato reporter mice. All procedures were approved by the Institutional Animal Care and Use Committee (IACUC) of Seoul National University.

## AAVs

Adeno-Associated Viruses serotype 1 were used in all the experiments of chapter 2. For optogenetic modulation of dopaminergic neurons, $pAAV_1$-Ef1a-DIO-eYFP ($1x10^9$ GC) or $pAAV_1$-Ef1a-DIO-ChR2-eYFP ($1x10^9$ GC) or $pAAV_1$-Ef1a-DIO-eNpHR-eYFP ($1x10^9$ GC) were used (Kang et al., 2015).

## Stereotaxic surgery

Both TH-cre males and females were anaesthetized with a ketamine/xylazine solution and positioned on a stereotaxic apparatus (Stoelting Co.). The virus was injected into DRN through 32gauge needle with Hamilton syringe at a rate of 0.1 μl/min and total injection volume was 1 μl. A tip of the needle was

positioned 0.05 mm below the target coordinate right before the injection for 2 minutes. After the injection, the needle stayed in place for extra 7 minutes and was withdrawn slowly (AP: -4.2/ ML: 0/ DV: -3.3). For bilateral optic cannula implantations, cannula (custom and Newdoon) was implanted 0.5mm above $NAc^{sh}$ and was held in place with dental cement (AP: +1.5/ ML: ±0.65/ DV: -4.5). Coordinates for virus injection in $NAc^{sh}$ (AP: +1.5/ ML: ±0.65/ DV-4.5).

## Behavioral task

Both male and female mice were kept in homecage after AAV injection. Each cage was moved to a new cage with new beddings at least two weeks before being group housed or social isolated. For every behavior task using optogenetics, mice were quickly put into the anesthesia chamber with isoflurane and the patch cord was connected to the optic cannula. All stranger mice were three to five weeks old with matched sex to the test mice.

For three-chamber test, habituation in the apparatus was performed for ten minutes, with laser off. After habituation period, an unfamiliar juvenile mouse was placed under one cup, and an object was placed under the other. Ten minutes of test period was performed with laser on or off.

For juvenile interaction test, the test mouse was placed in a cage with new beddings for one minute, with laser off. Then, an unfamiliar juvenile stranger mouse was introduced into the apparatus. Test period for interaction was performed for five

minutes with laser on or off.

For open field test, the test mouse was placed in the center and were left to explore the chamber for 10 minutes, with laser on or off.

## Brain clearing

SeeDB2 was followed published protocols (Ke et al., 2016). The brain sample was perfused with 4'C chilled 1x PBS and 4% paraformaldehyde in 1x PBS. Perfused brains were fixed in 4% PFA for 12 hours. Sample were sliced by vibratome into 1mm thickness for clearing. All SeeDB2 incubation procedures were performed at room temperature.

## Immunohistochemistry

Brains were post-fixed in 4% paraformaldehyde (PFA) at 4 °C overnight and transferred to 30% sucrose for 2 days at 4 °C. Brains were embedded in OCT mounting medium and sections were cut in 40 μ thick using a cryostat (Leica). For immunohistochemistry, primary antibodies rabbit anti-TH (AB152; Millipore) were diluted 1:500 in blocking solution and incubated for 24h at 4 °C. Secondary antibodies in blocking solution were incubated for 2h at room temperature, and sections were mounted with vectashield. Images were viewed under a Zeiss LSM 700 confocal microscope.

## Electrophysiology

Adult mice of both sexes were anesthetized with isoflurane and brains were quickly dissected. N-methyl-D-glucamine (NMDG) solution (93 mM NMDG, 2.5 mM KCl, 1.2 mM $NaH_2PO_4$, 30 mM, $NaHCO_3$, 20 mM HEPES, 25 mM Glucose, 5 mM sodium ascorbate, 2 mM Thiourea, 3mM sodium pyruvate, 10 mM $MgSO_4$, 0.5 mM $CaCl_2$) was used during brain slicing and recovery. Transverse slices of DRN (250 μm) or NAc (300μm) was prepared in ice-cold NMDG solution with vibratome then was recovered in 32℃ NMDG solution for 6~7 minutes. After at least 1h recovery in ACSF (124 mM NaCl, 2.5 mM KCl, 1 mM $NaH_2PO_4$, 25 mM $NaHCO_3$, 10 mM glucose, 2 mM $CaCl_2$, and 2 mM $MgSO_4$), slice was placed to the recording chamber perfused with 32℃ ACSF. To obtain reliable recordings, patched cells were stabilized for at least 3 minutes. Only cells with a change in access resistance <20% were included in the analysis. The recording pipettes (2~4 MΩ) were filled with an internal solution containing 145 mM K-gluconate, 5 mM NaCl, 10 mM HEPES, 1 mM $MgCl_2$, 0.2 mM EGTA, 2 mM MgATP, and 0.1 mM $Na_3GTP$ (280 ~ 300 mOsm, adjust to pH 7.2 with KOH). Current injections were performed in 25pA step with 500ms duration.

## Ovariectomy

Juvenile female mice (5~7 weeks of age) were ovariectomized under

subcutaneous injections of ketamine. Fallopian tubes were traced and both ovaries were removed, then the skin was sutured. For the control group, the cagemates of ovariectomized mice were selected and were performed with sham surgery. After 3 to 4 weeks of recovery in the homecage, ovariectomized group and sham group went under behavior tasks.

# RESULTS

## Sexual dimorphism in sociability is observed after 24-hours of social isolation

To examine whether 24-hours of social isolation affects sociability and to check the immediate effect of social isolation, I performed three-chamber test in two different time points; 2-hour and 24-hour. I hypothesized that if sociability is changed by 24-hour social isolation with specific circuit and synapses strengthened, the 2-hour time point will have no behavioral phenotypes since it is not yet strengthened. Moreover, I tested with male and female mice to see whether sexual differences are observed by social isolation.

When the male mice were isolated for 24-hours, significant increase in sociability was detected compared to 2-hour isolated males (Figure 5B). In contrast, the group housed males showed no changes in sociability both in 2-hour and 24-hour (Figure 5A). Strikingly, the sociability of female mice was tolerant to social isolation, both at 2-hour and 24-hour (Figure 5C and 5D).

Interestingly, in case of anxiety, social isolation induced higher anxiety only in the female mice (Figure 6A and 6C) without changes in total distance moved (Figure 6B and 6D). This results can be interpreted as sexual dimorphic effect of 24-hour social isolation, which goes together with the sex-specific effect of chronic social isolation (Huang et al., 2017).

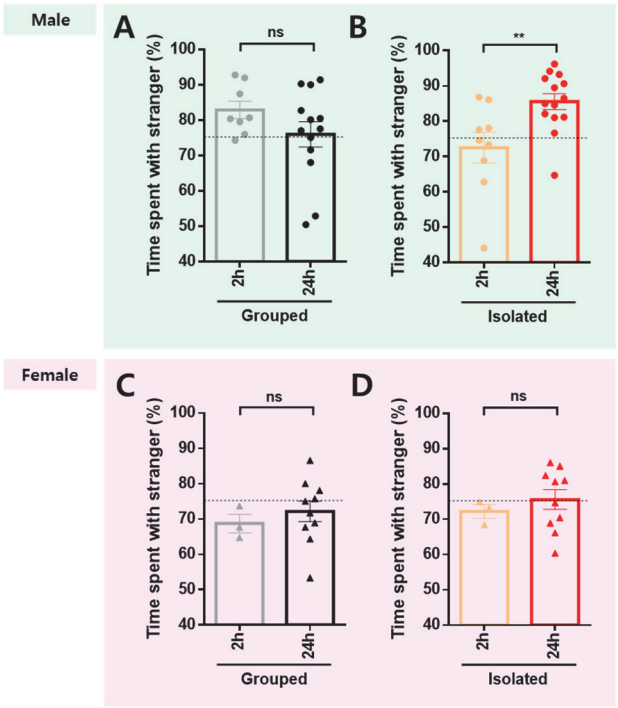


**Figure 5. Sociability changes after 2-hours or 24-hours of social isolation in male and female mice.**

(A, B) In male mice, sociability does not differ between the time of group housed. However, social interaction time was significantly increased in 24-hour isolated males than 2-hour isolated male. (Figure 5A; 2h, n=8; 24h, n=13; 2h, 82.90 ± 2.482; 24h, 75.99 ± 3.575; unpaired *t*-test; $p = 0.1818$; Figure 5B; 2h, n=9; 24h, n=14; 2h, 72.49 ± 4.351; 24h, 85.53 ± 2.221; unpaired *t*-test; $^{**}p = 0.0078$)

(C, D) In female mice, group housing nor social isolation does not alter the sociability. (Figure 5C; 2h, n=3; 24h, n=10; 2h, 68.73 ± 2.625; 24h, 72.16 ± 2.927; unpaired *t*-test; $p = 0.5570$; Figure 5D; 2h, n=3; 24h, n=10; 2h, 72.19 ± 1.938; 24h, 75.56 ± 2.776; unpaired *t*-test; $p = 0.5391$)

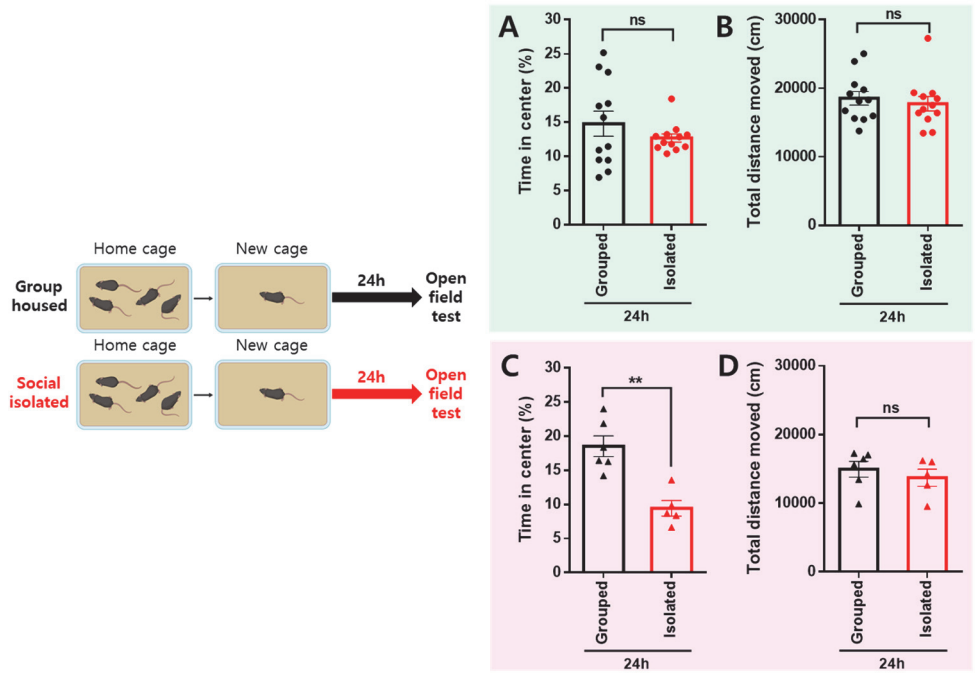


**Figure 6. The anxiety level after 24-hours of social isolation.**

(A, B) In male mice, social isolation for 24-hours did not alter the anxiety level nor the total distance moved. (Figure 6A; grouped, n=12; isolated, n=12; grouped, 14.79 ± 1.832; isolated, 12.71 ± 0.6035; unpaired *t*-test; $p = 0.2927$; Figure 6B; grouped, n=12; isolated, n=12; grouped, 18537 ± 985.6; isolated, 17745 ± 1041; unpaired *t*-test; $p = 0.5858$)

(C, D) In female mice, 24-hours after social isolation significantly increased the anxiety level with no changes in the total distance moved. (Figure 6C; grouped, n=6; isolated, n=5; grouped, 18.52 ± 1.519; isolated, 9.427 ± 1.159; unpaired *t*-test; $^{**}p = 0.0013$; Figure 6D; grouped, n=6; isolated, n=5; grouped, 14952 ± 1159; isolated, 13713 ± 1231; unpaired *t*-test; $p = 0.4836$)

## Characterization of $DRN^{TH}$ to $NAc^{sh}$ circuit.

Alterations to the dopamine system may underlie the observed male-specific sociability increase following 24-hours of social isolation. This hypothesis has been provided through various studies reporting that social isolation modulates dopaminergic neurons (Barik et al., 2013; Krishnan et al., 2007; Matthews et al., 2016). The ventral tegmental area (VTA), one of the most well-known brain region in the mesolimbic dopamine system, is intensely investigated and various functions of the VTA are being revealed. However, distinct brain region containing the dopaminergic neurons, the dorsal raphe nucleus (DRN), is yet to be discovered. Recently, the role of dopamine neurons in DRN ($DRN^{TH}$) have been receiving attention (Matthews et al., 2016), but is still a field of the unknown.

Therefore, I labeled the $DRN^{TH}$ neurons by injecting AAV-DIO-eYFP in TH-cre mouse to observe the axonal projections. Interestingly, I could detect a strong projection to the NAc (Figure 7A). Next, I examined the functional connections between $DRN^{TH}$ and $NAc^{sh}$ by performing patch clamp recording (Figure 7B). 36 out of 39 $NAc^{sh}$ neurons showed laser-induced EPSC (Figure 7C) and had an average of 50pA response (Figure 7D).

I further performed retrograde tracing to characterize the circuit. Bilateral injection of CAV-cre into the $NAc^{sh}$ in tdTomato reporter mice allowed to label the monosynaptic-connected cells from the $NAc^{sh}$ (Figure 8A). Combination with immunohistochemistry, I could discriminate the dopaminergic monosynaptic neurons with the other connections. Co-labeling of DRN slices for tyrosine

hydroxylase (TH) revealed that neurons projecting from the DRN to $NAc^{sh}$ are 42% dopaminergic (Figure 8B). The connection between DRN and $NAc^{sh}$ was similar to previous study (Ekstrand et al., 2014).

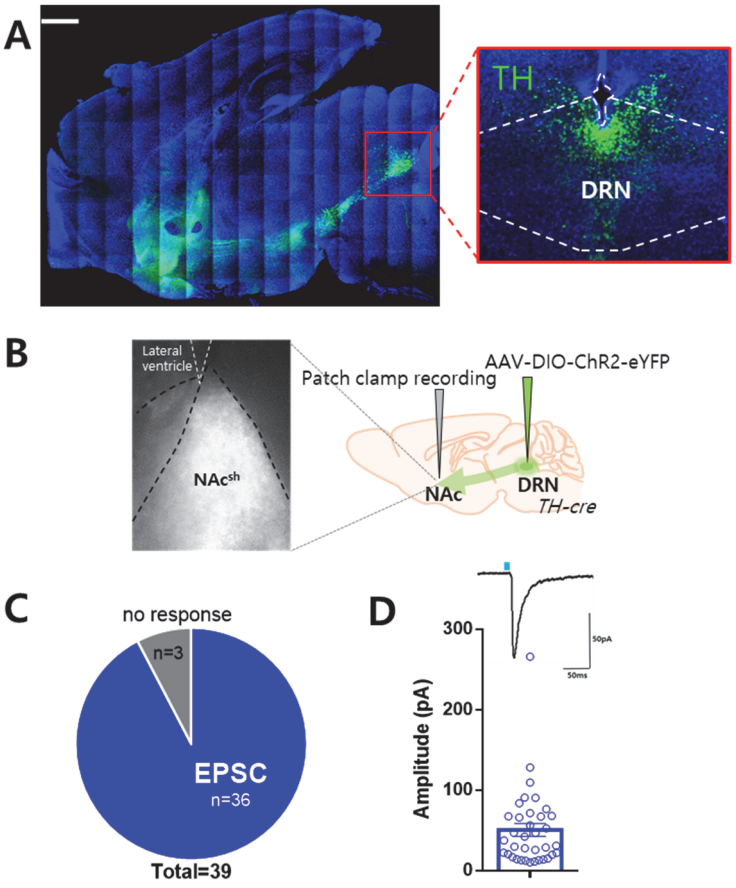


**Figure 7. Whole brain projection of DRN$^{TH}$ and the functional connection with NAc$^{sh}$ neurons.**

(A) Whole brain projection of DRN$^{TH}$ neurons and their distribution in the DRN.

(B) Experimental schema for patch clamp recording and representative image of DRN$^{TH}$ neurons labeled with ChR2-eYFP.

(C) 36 out of 39 neurons in the NAc$^{sh}$ showed light-induced EPSC responses.

(D) Example trace of light-induced peak in DRN$^{TH}$ neuron and the average amplitude. (36 cells from 7 mice)

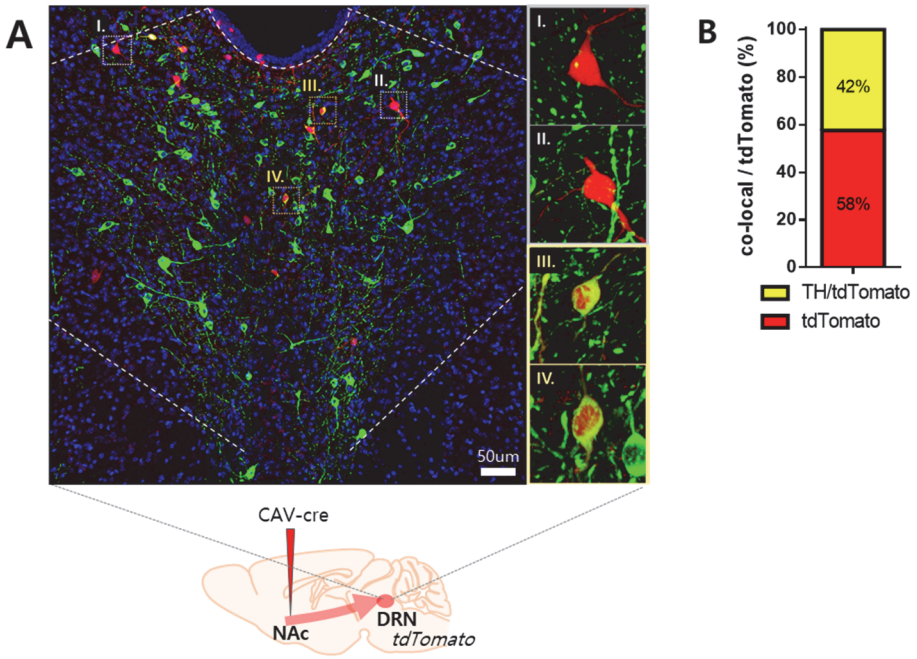


**Figure 8. Cell type characterization of DRN$^{TH}$ to NAc$^{sh}$ circuit.**

(A) Experimental scheme for labeling monosynaptic pre-connections of the NAc$^{sh}$ and the representative image of TH immunostaining in DRN slice

(B) Among the tdTomato cells that were monosynaptially labeled in the DRN, about 42% of the cells were TH positive

## Optogenetic inhibition of $DRN^{TH}$ to $NAc^{sh}$ circuit attenuates social isolation-induced sociability increase.

Socially isolated male mice showed significant increase in sociability. Therefore, I wanted to test whether modulation of the $DRN^{TH}$ to $NAc^{sh}$ circuit could change the sociability induced by isolation. To do so, I injected AAV-DIO-eYFP or AAV-DIO-eNpHR-eYFP into the DRN of TH-cre mice and implanted optic fibres bilaterally into the $NAc^{sh}$ (Figure 9A). In the male mice, terminal inhibition of $DRN^{TH}$ neurons significantly decreased the sociability increase by social isolation (Figure 9C and 9D). This behavioral change was not due to the anxiety level changes (Figure 9E). Interestingly, no changes in sociability were observed in female mice (Figure 9G and 9H). To confirm whether this optogenetic manipulation was specific to social isolation, I performed the same experiment in the group house mice. Surprisingly, the group housed male mice with $DRN^{TH}$ terminals inhibited in the $NAc^{sh}$, did not spend less time interacting with the stranger mouse (Figure 9F), by comparison to social isolated male mice in which exhibited reduced sociability (Figure 9C). Photo-inhibition of $DRN^{TH}$ neuron terminals in the $NAc^{sh}$ did not elicit alterations in the social interaction time in the female mice that were group house also (Figure 9J). Collectively, the sociability decreases by optogenetically inhibiting $DRN^{TH}$ to $NAc^{sh}$ was unique to male mice and only after social isolation. These findings suggest that social isolation-induced sociability increase and the sociability decrease by inhibition of $DRN^{TH}$ to $NAc^{sh}$ circuit show sexual dimorphism.

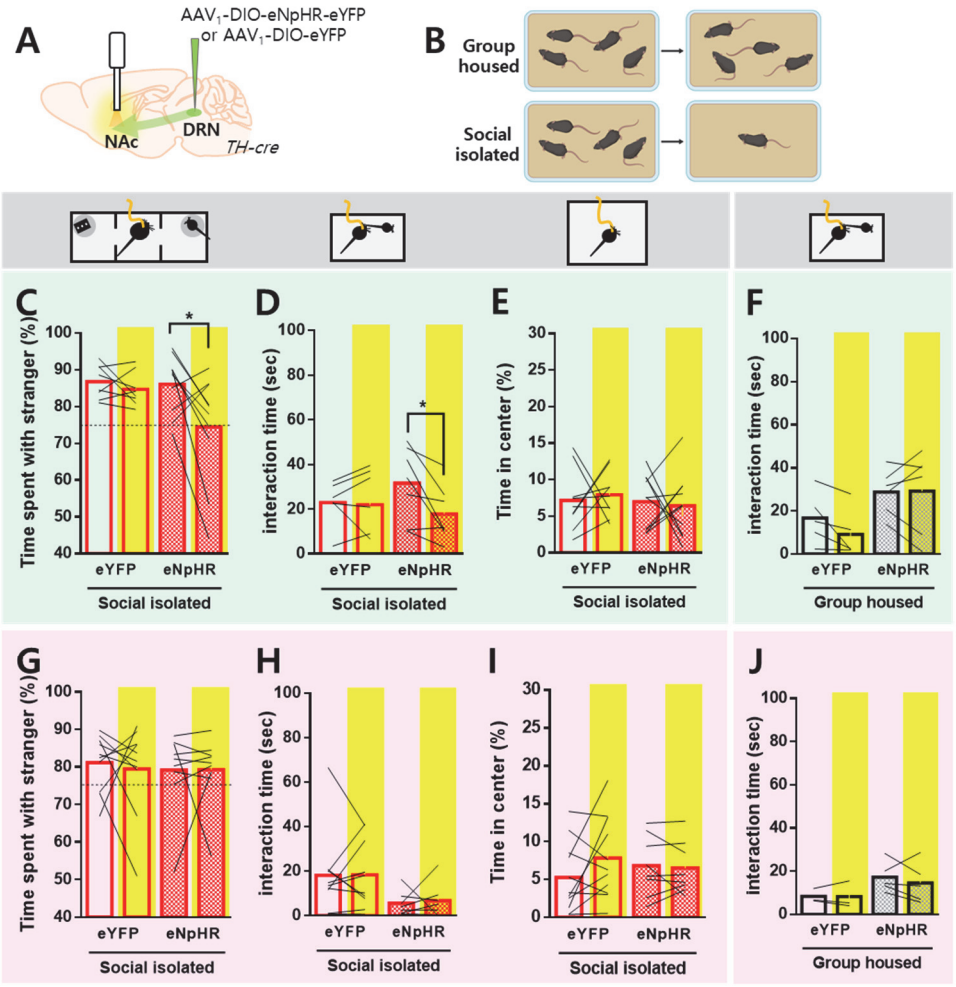


**Figure 9. Inhibition of DRN$^{TH}$ to NAc$^{sh}$ after social isolation decreases interaction time only in male mice.**

(A) Experimental schema for photo-inhibition of DRN$^{TH}$ terminals in NAc$^{sh}$.

(B) Schematic image of group housed and social isolated mice

(C, D) In socially isolated male mice, inhibition of DRN$^{TH}$ neurons projecting to the NAc$^{sh}$ significantly suppresses social interaction time in three-chamber test (C) and

juvenile interaction test (D) (Figure 9C; eYFP, n=8; paired *t*-test; $p = 0.3424$; eNpHR, n=10; paired *t*-test; $*p = 0.0410$; Figure 9D; eYFP, n=6; paired *t*-test; $p = 0.6937$; eNpHR, n=7; paired *t*-test; $*p = 0.0265$)

(E) Inhibition of $DRN^{TH}$ to NAc terminals does not alter the open field test. (eYFP, n=9; paired *t*-test; $p = 0.7110$; eNpHR, n=10; paired *t*-test; $p = 0.8053$)

(F) When group housed, inhibition of $DRN^{TH}$ to $NAc^{sh}$ does not attenuate sociability. (eYFP, n=5; paired *t*-test; $p = 0.0803$; eNpHR, n=6; paired *t*-test; $p = 0.9370$)

(G, H) Inhibition of $DRN^{TH}$ neurons projecting to the $NAc^{sh}$ does not suppresses social interaction time in socially isolated female mice, both in three-chamber test (G) and juvenile interaction test (H). (Figure 9G; eYFP, n=10; paired *t*-test; $p = 0.7231$; eNpHR, n=9; paired *t*-test; $p = 0.9905$; Figure 9H; eYFP, n=10; paired *t*-test; $p = 0.9685$; eNpHR, n=7; paired *t*-test; $p = 0.7661$)

(I) Inhibition of $DRN^{TH}$ to NAc terminals does not alter the open filed test also in female mice. (eYFP, n=11; paired *t*-test; $p = 0.1435$; eNpHR, n=8; paired *t*-test; $p = 0.6868$)

(J) $DRN^{TH}$ to NAc terminal inhibition does not change social interaction time in group housed female mice. (eYFP, n=3; paired *t*-test; $p = 0.9740$; eNpHR, n=5; paired *t*-test; $p = 0.4471$)

## Optogenetically activating the $DRN^{TH}$ to $NAc^{sh}$ circuit has no effect on social isolation-induced sociability changes.

I previously found that inhibition of $DRN^{TH}$ to $NAc^{sh}$ circuit attenuated the social interaction time only after 24-hours of social isolation. Therefore, I wanted to check whether activating the same circuit may increase the sociability following social isolation. I hypothesized that if $DRN^{TH}$-$NAc^{sh}$ circuit is specific to social isolation, the sociability of group-housed mice will not show alteration even though it is optogenetically manipulated.

I injected AAV-DIO-eYFP or AAV-DIO-ChR2-eYFP into the DRN of TH-cre mice and implanted optic fibers bilaterally into the $NAc^{sh}$ (Figure 10A). When $DRN^{TH}$ to $NAc^{sh}$ circuit was activated, surprisingly, no changes in sociability were observed following 24-hours of social isolation or group housing (Figure 10C, 10D, and 10F), contrast to the inhibition of $DRN^{TH}$-$NAc^{sh}$ (Figure 9C and 9D). Moreover, activation of $DRN^{TH}$ terminals in the $NAc^{sh}$ did not affect the anxiety (Figure 10E). In female mice, sociability and anxiety were not affected by activation of $DRN^{TH}$ to $NAc^{sh}$ circuit, both social isolated or group housed state (Figure 10G, 10H, 10I, and 10J). These results imply that artificially activating $DRN^{TH}$ to $NAc^{sh}$ circuit does not affect the sociability and the anxiety level in both sexes.

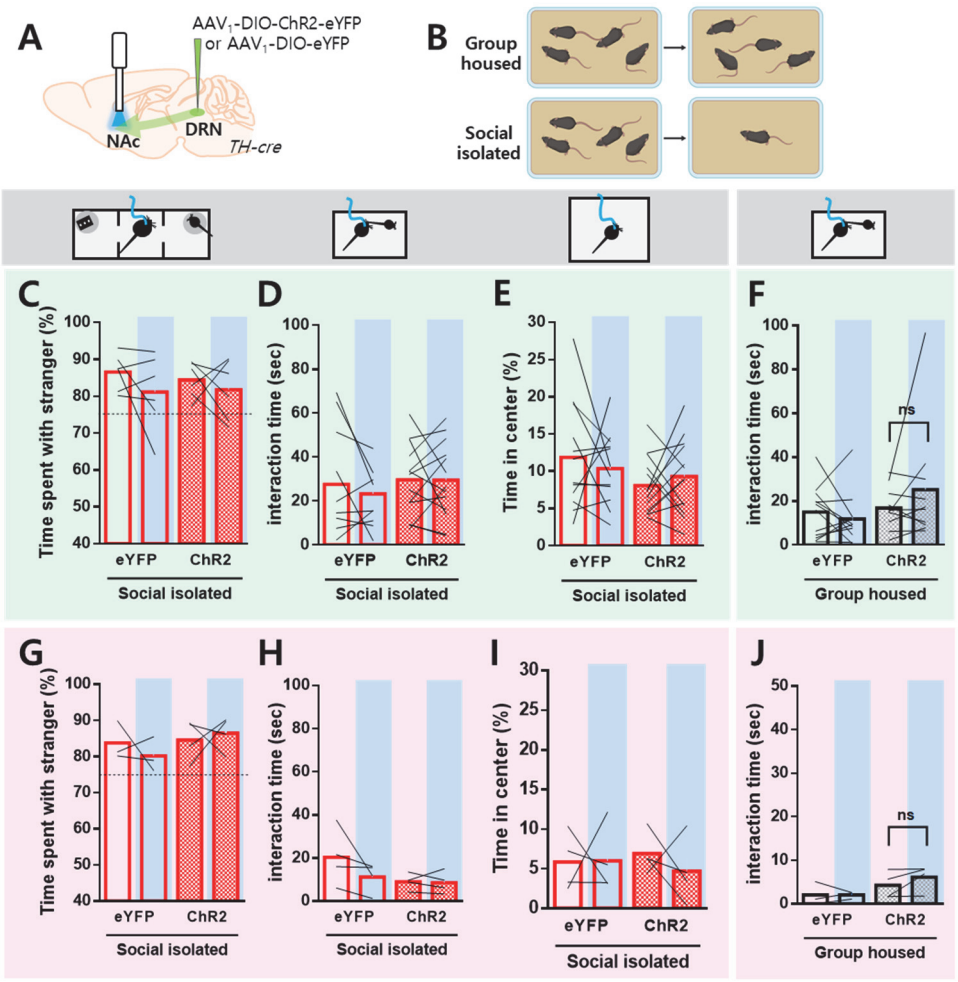


**Figure 10. Activation of DRN$^{TH}$ to NAc$^{sh}$ does not affect social interaction time.**

(A) Experimental schema for photo-activation of DRN$^{TH}$ neuron terminals in the NAc$^{sh}$.

(B) Schematic image of group housed and social isolated mice.

(C, D) In socially isolated male mice, activation of DRN$^{TH}$ neurons projecting to the NAc$^{sh}$ does not alter social interaction time in three-chamber test (C) and juvenile interaction test (D). (Figure 10C; eYFP n=6; paired *t*-test; $p$ = 0.2701; ChR2, n=6;

paired *t*-test; $p = 0.5647$; Figure 10D; eYFP n=9; paired *t*-test; $p = 0.1804$; ChR2, n=13; paired *t*-test; $p = 0.9730$)

(E) Activation of $DRN^{TH}$ to NAc terminals does not change time spent in center during open field test. (eYFP n=12; paired *t*-test; $p = 0.5659$; ChR2, n=13; paired *t*-test; $p = 0.4937$)

(F) In group-housed male mice, activation of $DRN^{TH}$ neurons projecting to the $NAc^{sh}$ does not affect sociability. (eYFP n=12; paired *t*-test; $p = 0.4309$; ChR2, n=10; paired *t*-test; $p = 0.2673$)

(G, H, I) In socially isolated female mice, activation of $DRN^{TH}$ to $NAc^{sh}$ circuit does not alter social interaction time in three-chamber test (G) and juvenile interaction test (H). Moreover, the anxiety was not change (I). (Figure 10G; eYFP n=3; paired *t*-test; $p = 0.5677$; ChR2, n=4; paired *t*-test; $p = 0.7286$; Figure 10H; eYFP n=4; paired *t*-test; $p = 0.2055$; ChR2, n=4; paired *t*-test; $p = 0.8370$; Figure 10I; eYFP n=4; paired *t*-test; $p = 0.9695$; ChR2, n=4; paired *t*-test; $p = 0.5059$)

(J) In group housed female mice, activation of $DRN^{TH}$ neurons projecting to the $NAc^{sh}$ does not alter social interaction time. (eYFP n=3; paired *t*-test; $p > 0.9999$; ChR2, n=4; paired *t*-test; $p = 0.2133$)

## Female sex hormones are not related with unchanged isolation-induced sociability in the female mice.

24-hour isolated female mice did not show alterations in sociability and were not further modulated by optogenetic-inhibition nor activation.

Sexual dimorphisms exist from brain anatomy (Ruigrok et al., 2014) to psychological processes and in various neurological disorders (Bálint et al., 2009; Gillberg et al., 2006; Wooten et al., 2004). One cause of sex differences has been explained by the actions of sex hormones in females (Gillies and McArthur, 2010; Riecher-Rössler et al., 1994). The estradiol, a major female sex hormone which is an estrogen steroid hormone, is known to affect dopaminergic function differently in brain regions of the female mice. For example, estradiol increases dopamine release in the striatum, inhibits dopaminergic activity in the NAc, modulates dopamine synthesis and inhibits dopaminergic effects in anterior pituitary (Becker, 1999; Bourque et al., 2012; Raymond et al., 1978). Due to these complexities and diversity of dopamine's regulation in the females, I wanted to check whether female sex hormones were the cause of unchanged isolation-induced sociability.

To further investigate sexual dimorphism in social isolation, I used ovariectomized (OVX) females to see whether female sex hormones may be a contributing factor to male-specific phenotypes in social isolation. Five to six-weeks old females were ovariectomized and three-chamber test was performed at least three weeks after (Figure 11A). The sociability level was comparable between isolated

OVX females and isolated sham-control females. Moreover, no effect was detected also in the group-housed females (Figure 11B). These findings demonstrate that sexual dimorphism following social isolation is not via female sex hormones.

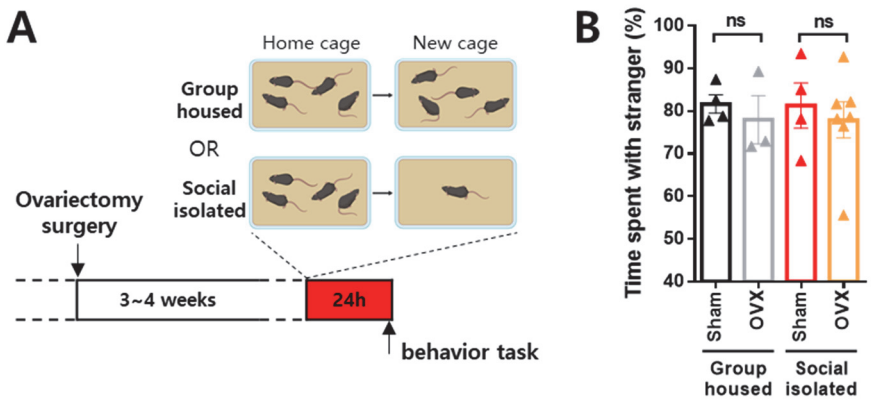


**Figure 11. Female sex hormones do not affect social-isolation-induced sociability.**

(A) Behavioral schematics for ovariectomized- and sham-females.

(B) Ovariectomized females did not show any sociability alterations with sham-control females, both in group-housed and social-isolated state. (Group housed sham, n=4, 81.65 ± 2.187; Group housed OVX, n=3, 77.98 ± 5.659; unpaired *t*-test; $p = 0.5257$; Social isolated sham, n=4, 81.29 ± 5.311; Social isolated OVX, n=7, 77.92 ± 4.230; unpaired *t*-test; $p = 0.6362$)

# DISCUSSION

It is widely accepted that social isolation is a serious issue for social animals. Despite its great significance, previous studies mainly focused on chronic effect of social isolation and did not perceive on the sexual differences. In this chapter, I observed sexual dimorphic alterations in social behaviors in response to 24-hour social isolation. Male-specific sociability increase was detected after 24-hours of social isolation. In contrast, isolated females showed an increase in anxiety level rather than increased sociability. By utilizing optogenetic tools, I found that isolation-induced sociability increase was modulated by $DRN^{TH}$ to $NAc^{sh}$ circuit in a sex dependent manner. Furthermore, I found that this sexual dimorphism following social isolation is not by way of female sex hormones. In sum, these results suggest that social isolation has different effects on sociability in male and female mice.

Sexual dimorphism occurred after being social isolated for 24 hours. It is reported that brain regions related with social behavior express various subtypes of estrogen receptor (Nelson and Trainor, 2007). DRN do not show sex difference in the number of estrogen receptor (Sagoshi et al., 2020).

Matthews et al. have shown that $DRN^{TH}$ neurons show calcium activity in response to social interaction in which is more heightened after 24-hour social isolation (Matthews et al., 2016). Thus, although $DRN^{TH}$ responses to social isolation, the precise downstream circuit and the underlying mechanisms remain unspecified. I found that social isolation triggers sociability changes differently between males and females and further narrowed down the mechanism to neural circuit level.

# CHAPTER III

## Social-isolation-activated neuronal ensembles of $DRN^{TH}$ and their synaptic connectivity are necessary for sociability changes by social isolation

# INTRODUCTION

In the previous chapter, I found male-specific isolation-induced sociability increase and the dopaminergic afferents from the DRN to the $NAc^{sh}$ are modulating isolation-induced sociability changes. By narrowing down the neural population from total population to the "isolation-activated" neuronal ensembles, I further investigated the sociability following social isolation. I hypothesized that the isolation-activated neurons will be necessary for the isolation-induced sociability increase. To test this possibility, I used IEG-based tagging tools combined with DREADD (designer receptors exclusively activated by designer drug) system to specifically manipulated the isolation-activated neurons.

In this chapter, I investigated the isolation-activated neurons through chemogenetics, patch clamp recording and dual-eGRASP. Inhibition of isolation-activated $DRN^{TH}$ neurons resulted in attenuation of sociability, which reversed the sociability down to the levels of group-housed. Interestingly, when I inhibited the group-house-activated $DRN^{TH}$ neurons, no changes in sociability was observed. Furthermore, I found a higher neural excitability in the isolation-activated $NAc^{sh}$ neurons. Finally, I used dual-eGRASP to examine the synapses between isolation-activated $DRN^{TH}$ cells and $NAc^{sh}$ cells and found an increase in spine density. In summary, these results imply that the isolation-activated neural ensembles in $DRN^{TH}$ and $NAc^{sh}$ are strengthened from the synaptic level during 24-hours of social

isolation, thus increasing the sociability. Therefore, I inhibited neural activation of $DRN^{TH}$ during 24-hours of being isolated and could attenuate isolation-induced sociability increase. Activity of $DRN^{TH}$ neurons during isolation is required for isolation-induced sociability increase.

Through all the data, I found that the activated neuronal ensembles and the synaptic strengthening between them are necessary for the sociability increase following social isolation.

# EXPERIMENTAL PROCEDURES

## Animals

TH-cre male and female mice were maintained in a C57BL/6J background. Animals were housed with food and water *ad libitum* on a 12-hour light-dark cycle. For labeling TH positive neurons in DRN, I used tdTomato reporter mice. All procedures were approved by the Institutional Animal Care and Use Committee (IACUC) of Seoul National University.

## AAVs

Adeno-Associated Viruses serotype 1/2 (AAV1/2; AAV particle that contains both serotype 1 and 2 capsids) were used in all the experiments of chapter three. For chemogenetic modulation of dopaminergic neurons, $pAAV_{1/2}$-TRE3G-DIO-hM4Di-mCherry ($1x10^9$ GC) or $pAAV_{1/2}$-Ef1a-DIO-hM4Di-mCherry ($1x10^9$ GC) were used. For patch clamp recording, the activated neurons were labeled with $pAAV_{1/2}$-TRE3G-mEmeraldNuc ($1x10^8$ GC). All dual-eGRASP virus cocktails were identical or slightly modified from previously described (Choi et al., 2018).

## Stereotaxic surgery

Both TH-cre males and females were anaesthetized with a ketamine/xylazine solution and positioned on a stereotaxic apparatus (Stoelting Co.). The virus was injected through 32gauge needle with Hamilton syringe at a rate of 0.1 μl/min and total injection volume was 1 μl. A tip of the needle was positioned 0.05 mm below the target coordinate right before the injection for 2 minutes. After the injection, the needle stayed in place for extra 7 minutes and was withdrawn slowly. Stereotaxic coordinates for each target sites were: Nucleus accumbens (AP: +1.5/ ML: ±0.65/ DV: -4.5), Dorsal raphe nuclei (AP: -4.2/ ML: 0/ DV: -3.3).

## Behavioral task

Both male and female mice were kept in homecage after AAV injection. Cagemates were moved to a new cage with new beddings at least two weeks before being group housed or social isolated. On the day of group housing or social isolating, 250 μl of 5 mg/ml doxycycline solution dissolved in saline was injected by intraperitoneal injection during brief anesthesia by isoflurane (Choi et al., 2018). All stranger mice were three to five weeks old with matched sex to the test mice.

For three-chamber test, habituation in the apparatus was performed for ten minutes, with laser off. After habituation period, an unfamiliar juvenile mouse was placed under one cup, and an object was placed under the other. Ten minutes of test period was performed.

For open field test, the test mouse was placed in the center and were left to

explore the chamber for 10 minutes.

## Chemogenetic manipulations

The designer drug clozapine-*N*-oxide (CNO, 10mg/kg, i.p. ; Sigma) was administered 40 minutes before behavioral tasks. For electrophysiology, 5uM of CNO was used and the effect was measured 10 minutes after CNO perfusion.

## Immunohistochemistry

Brains were post-fixed in 4% paraformaldehyde (PFA) at 4 °C overnight and transferred to 30% sucrose for 2 days at 4 °C. Brains were embedded in OCT mounting medium and sections were cut in 40 µ thick using a cryostat (Leica). For immunohistochemistry, primary antibodies rabbit anti-TH (AB152; Millipore) and rabbit anti-c-fos (sc-52; Santa Cruz, 226003; SySy) were diluted 1:500-1:1000 in blocking solution and incubated for 24h at 4 °C. Secondary antibodies in blocking solution were incubated for 2h at room temperature, and sections were mounted with vectashield. Images were viewed under a Zeiss LSM 700 confocal microscope.

## Electrophysiology

Adult mice of both sexes were anesthetized with isoflurane and brains were

quickly dissected. N-methyl-D-glucamine (NMDG) solution (93 mM NMDG, 2.5 mM KCl, 1.2 mM $NaH_2PO_4$, 30 mM, $NaHCO_3$, 20 mM HEPES, 25 mM Glucose, 5 mM sodium ascorbate, 2 mM Thiourea, 3mM sodium pyruvate, 10 mM $MgSO_4$, 0.5 mM $CaCl_2$) was used during brain slicing and recovery. Transverse slices of DRN (250 μm) or NAc (300μm) was prepared in ice-cold NMDG solution with vibratome then was recovered in 32℃ NMDG solution for 6~7 minutes. After at least 1h recovery in ACSF (124 mM NaCl, 2.5 mM KCl, 1 mM $NaH_2PO_4$, 25 mM $NaHCO_3$, 10 mM glucose, 2 mM $CaCl_2$, and 2 mM $MgSO_4$), slice was placed to the recording chamber perfused with 32℃ ACSF. To obtain reliable recordings, patched cells were stabilized for at least 3 minutes. Only cells with a change in access resistance <20% were included in the analysis. The recording pipettes (2~4 MΩ) were filled with an internal solution containing 145 mM K-gluconate, 5 mM NaCl, 10 mM HEPES, 1 mM $MgCl_2$, 0.2 mM EGTA, 2 mM MgATP, and 0.1 mM $Na_3GTP$ (280 ~ 300 mOsm, adjust to pH 7.2 with KOH). Current injections were performed in 25pA step with 500ms duration.

## Sample preparation and confocal imaging for dual-eGRASP

Perfused brains were fixed with 4% PFA in phosphate buffered saline (PBS) overnight at 4℃, and dehydrated in 30% sucrose in PBS for 2 days at 4℃. Brains were sliced by Cryostat into 50μm section for dual-eGRASP analysis. Sections were mounted in VECTASHIELD mounting medium (Vector Laboratories, H-1000). For dual-eGRASP analysis, NAc dendrites were imaged in Z-stack by Leica SP8

confocal microscope with 63x objective with distilled water immersion.

## Image analysis for dual-eGRASP

Processing of confocal image and 3D reconstruction of dendrites were performed using Imaris (Bitplane, Zurich, Switzerland) software. Before analysis all image samples were blinded for exclude any bias. Each mScarlet-I-positive or iRFP670-positive dendrite was marked as a filament manually while hiding other fluorescent signals, and each cyan or yellow eGRASP signal was marked as cyan or yellow sphere through IMARIS automatic detection. Cyan eGRASP and yellow eGRASP puncta on dendrites were manually counted and overlapped cyan and yellow eGRASP signals was considered as yellow signal since the presynaptic neuron of the synapse is c-fos-positive dopaminergic neuron during social isolation. Dendrites without any cyan eGRASP or mScarlet-I, iRFP670-overlapping dendrites were ruled out for more precise analysis.

# RESULTS (Collaborated with Dong Il Choi)

## Social-isolation-activated DRN$^{TH}$ neurons are necessary for sociability increase by isolation.

To assess the necessity of DRN$^{TH}$ activity for social-isolation driven sociability increase, I wanted to specifically manipulate the activated dopaminergic neurons. Thus, I combined chemogenetics with IEG-based tagging system.

I used reverse tetracycline-controlled transactivator (rtTA) under Fos promoter to express hM4Di in the activated dopaminergic neurons in doxycycline-dependent manner (Haasteren et al., 2000; Loew et al., 2010; Reijmers et al., 2007; Zhou et al., 2006). Cre-dependent hM4Di-mCherry was injected into the DRN of TH-cre mice. After 4 weeks of virus expression, the mice underwent 24-hours of social isolation with doxycycline injected (Figure 12A). Then I confirmed the function of hM4Di by patch clamp recording the hM4Di-mCherry expressing neurons. As expected, the neural firing was inhibited by CNO treatment (Figure 12B). Therefore, I could conclude that 24-hour was enough to express functional hM4Di.

Then, I used this chemogenetics and IEG-based labeling system to specifically manipulate the isolation-activated DRN$^{TH}$ neurons. Mice were socially isolated and doxycycline injected simultaneously. After 24-hours, I injected CNO or saline and three-chamber test was performed 40 minutes after (Figure 13A). Inhibition of social-isolation-activated DRN$^{TH}$ neurons attenuated the sociability to

the baseline levels of interaction (Figure 13B) with no changes in velocity and total distance moved (Figure 13C and 13D). Furthermore, I analyzed the activation ratio by labeling tyrosine hydroxylase in the hM4Di-mCherry expressed DRN slice. About 15% of $DRN^{TH}$ neurons were expressed with hM4Di (Figure 13E), indicating that this activated population of $DRN^{TH}$ neurons are necessary for mediating the increase in social isolation.

In order to confirm that this result drawn out from isolation-activated neurons, I performed the same experiment with group-house-activated neurons (Figure 14A). If it is specific to social isolation, inhibiting the group-house-activated neurons will have no effect on sociability. Strikingly, I found no alterations in sociability and anxiety when group-house-activated $DRN^{TH}$ neurons were inhibited (Figure 14B, 14C, 14D and 14E). Therefore, I concluded that DRN dopaminergic neural ensembles which are activated by social isolation is critical for the sociability increase.

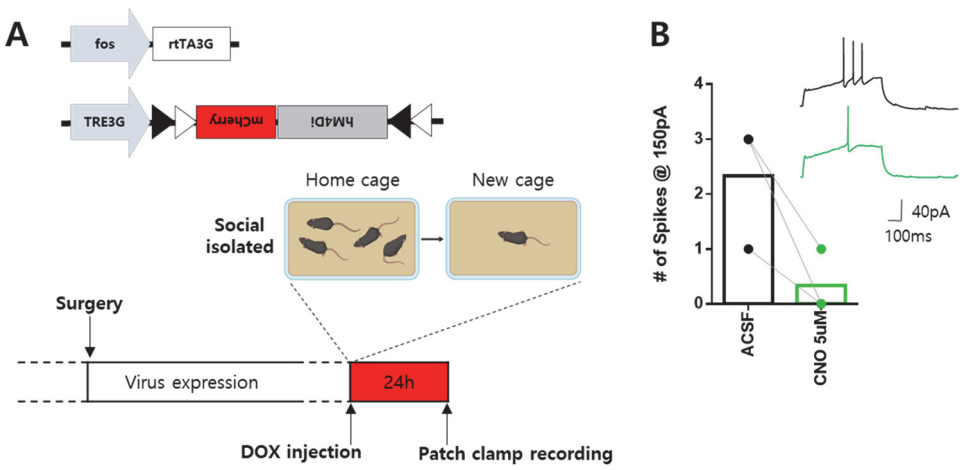


**Figure 12. 24-hour induction of hM4Di is functional.**

(A) Experimental scheme for labeling the isolation-activated $DRN^{TH}$ neurons.

(B) When perfused with CNO, hM4Di expressing neurons showed decreased excitability.

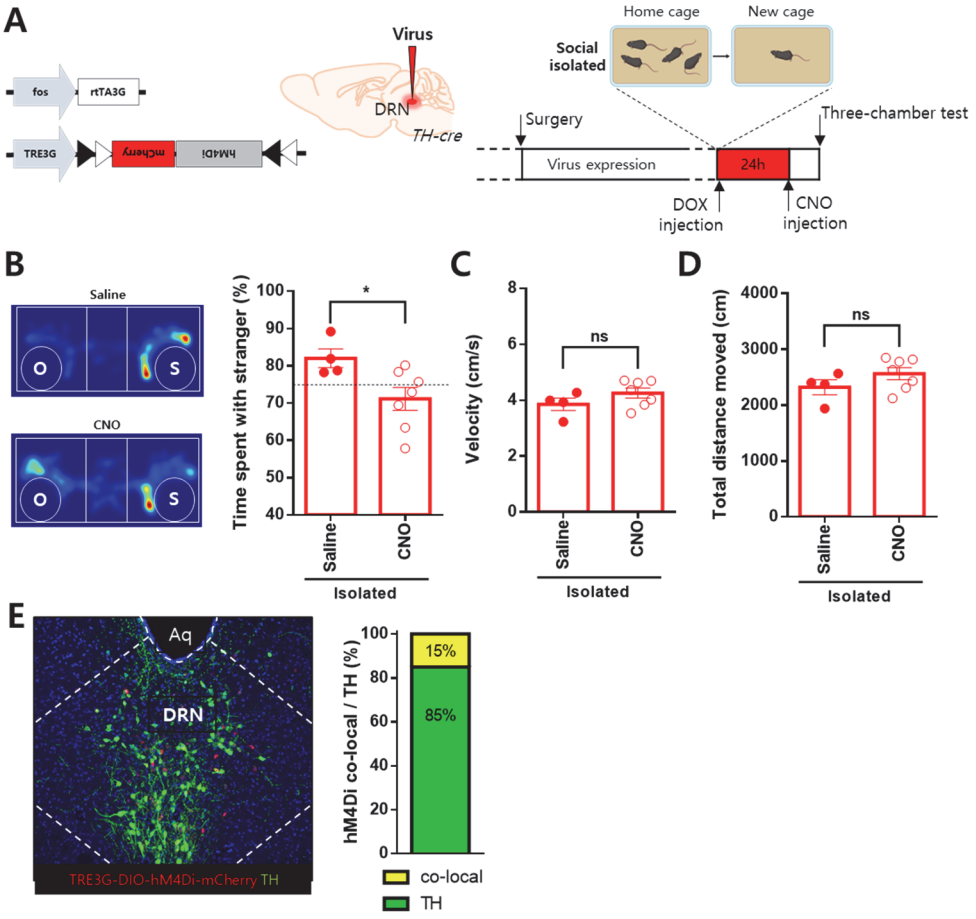


**Figure 13. Isolation-activated dopaminergic neurons in the DRN are essential for increase in isolation-induced sociability.**

(A) Schematic image of virus injection and behavior scheme.

(B) Heat maps illustrating the three-chamber test that underwent inhibition of isolation-activated population through CNO (left, upper) or saline-treated control (left, bottom). The effect of chemogenetically inhibiting isolation-activated $DRN^{TH}$ neurons. CNO treated isolated male mice showed significant decrease in sociability. (Saline, N=4; 82.01 ± 2.515; CNO, N=7; 71.13 ± 3.071; unpaired *t*-test; $*p = 0.0400$)

(C, D) Inhibition of isolation-activated $DRN^{TH}$ neurons did not change the velocity (C) and the total distance moved (D). (Figure 13D; Saline, N=4; 3.855 ± 0.2220; CNO, N=7; 4.256 ± 0.1755; unpaired *t*-test; $p = 0.1958$; Figure 13E; Saline, N=4; 2321 ± 133.8; CNO, N=7; 2563 ± 106.1; unpaired *t*-test; $p = 0.1959$)

(E) Representative image of hM4Di-mCherry expression in dopaminergic neurons of the DRN. Among the $DRN^{TH}$ neurons, 15% were activated by social isolation. 5 slices from each mouse, data from 3 mice.

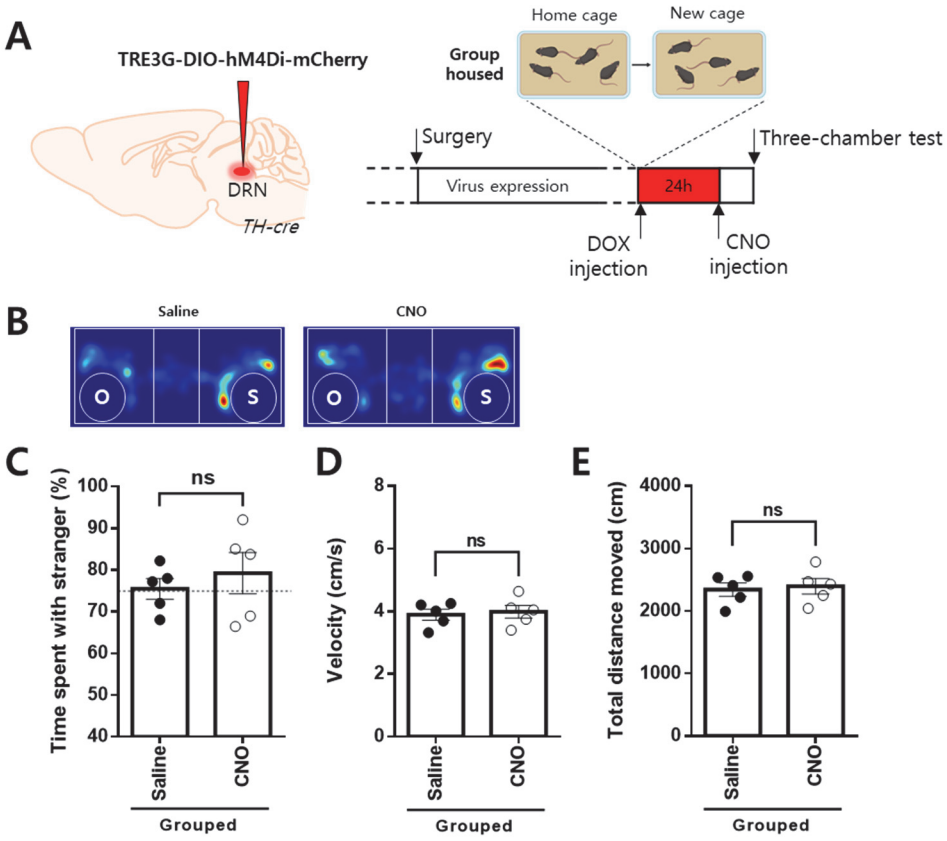


**Figure 14. Inhibition of group-house-activated dopaminergic neurons in the DRN do not alter the sociability.**

(A) Schematic image of virus injection and behavior scheme.

(B) Heat maps illustrating the three-chamber test that underwent inhibition of group-house-activated population through CNO (right) or saline-treated control (left).

(C) No changes in sociability was detected when group-housed-activated $DRN^{TH}$ neurons were chemogenetically inhibited. (Saline, n=5; 75.48 ± 2.473; CNO, n=5; 79.23 ± 4.934; unpaired *t*-test; $p = 0.5160$)

(D, E) Inhibiting the group-house-activated $DRN^{TH}$ neurons did not change the velocity (D) and the total distance moved (E). (Figure 14D; Saline, n=5; 3.896 ± 0.1748; CNO, n=5; 3.989 ± 0.2052; unpaired *t*-test; $p = 0.7389$; Figure 14E; Saline, n=5; 2343 ± 106.1; CNO, n=5; 2396 ± 123.3; unpaired *t*-test; $p = 0.7503$)

## Isolation-activated NAc$^{sh}$ neurons show higher excitability.

I investigated whether sexual differences are detected in the neuronal excitability of the isolation-induced fos positive neurons. Excitability is one of intrinsic properties of neurons, in which sets the threshold for action potential firing and modulates synaptic transmission (Hille, 1978). By using Fos-rtTA system, I selectively labeled the activated neurons with nucleus-targeted mEmerald (mEmeraldNuc), in which the fluorescence protein was driven by the TRE3G promoter controlled by Fos promoter-driven rtTA3G (Figure 15A). In the isolated male, mEmeraldNuc positive neurons were significantly more excitable compared with mEmeraldNuc negative neurons (Figure 15B). However, although isolation-induced fos expression was also observed in the isolated female mice, the excitability of mEmeraldNuc positive cells was comparable to the mEmeraldNuc negative cells' excitability (Figure 15C). I again detected sexual dimorphism, in which the increased excitability was shown only in the socially isolated male mice. Another interesting point is that the relationship between the fos-expressing neurons and their excitability do not always correlate, since the isolation-activated neurons in the females did not show an increase in excitability.

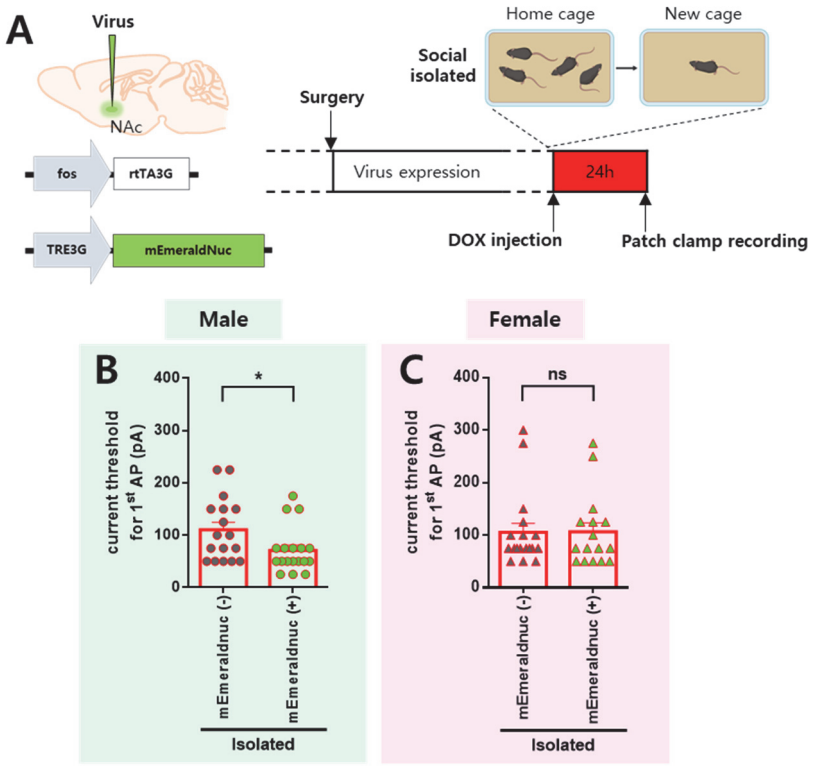


**Figure 15. Only in the male mice, the neuronal excitability of isolation-activated NAc$^{sh}$ neurons are more excitable than the non-activated NAc$^{sh}$ neurons.**

(A) Experimental scheme of labeling the isolation-activated NAc$^{sh}$ neurons.

(B) In the isolated male mice, the current threshold for the 1$^{st}$ action potential to appear is significantly lower in the mEmeraldNuc positive neurons. (mEmeraldNuc negative neurons, n=17 from 3 mice; mEmeraldNuc positive neurons, n=18 from 3 mice; mEmeraldNuc negative neurons, 110.3 ± 14.55; mEmeraldNuc positive neurons, 70.83 ± 10.36; unpaired *t*-test; *$p$ = 0.0327)

(C) In the isolated female mice, mEmeraldNuc positive and negative neurons

showed comparable current threshold for the 1st action potential. (mEmeraldNuc negative neurons, n=18 from 3 mice; mEmeraldNuc positive neurons, n=16 from 3 mice; mEmeraldNuc negative neurons, 105.6 ± 16.73; mEmeraldNuc positive neurons, 106.3 ± 17.31; unpaired *t*-test; $p = 0.9772$)

## Optimization of Dual-eGRASP in $DRN^{TH}$ to $NAc^{sh}$ circuit.

Through previous results in this chapter, Fos-rTA system was confirmed to capture the activated neurons in group housed or social isolated mice. Therefore, I further applied this system to study the synaptic connectivity between the activated neuronal ensembles. I hypothesized that social isolation will alter DRN dopaminergic circuitry to the $NAc^{sh}$ for driving isolation-induced sociability increase. In order to capture the synapses of activated $DRN^{TH}$ neurons to activated $NAc^{sh}$ neurons, I modified the previous virus strategy of dual-eGRASP (Choi et al., 2018).

Since the dopaminergic neurons, a specific cell type, in the DRN should be labeled, I used TH-cre mice. Pre-eGRASP was expressed Cre-dependently in the DRN, with yellow pre-eGRASP in activated dopaminergic neurons and cyan pre-eGRASP in non-activated dopaminergic neurons (Figure 16A and 16B). Yellow pre-eGRASP was driven by the TRE3G promoter controlled by Fos promoter-driven rtTA3G and cyan pre-eGRASP was driven by the EF1α promoter. Post-eGRASP was expressed bilaterally in $NAc^{sh}$, with myristoylated mScarlet-I in activated cells and myristoylated iRFP670 in non-activated cells (Figure 16A and 16B). Myristoylated mScarlet-I was driven by the TRE3G promoter controlled by Fos promoter-driven rtTA3G. Myristoylated iRFP670 was driven by the human synapsin (hSyn) promoter further with CaMKIIα promoter-driven FLPO in order to achieve the cre-out system (Jung et al., 2019). Consequently, I could specifically label the isolation-activated synapses in yellow eGRASP and isolation-non-activated synapses in cyan eGRASP, in which are on isolation-activated $NAc^{sh}$ neurons and isolation-non-activated $NAc^{sh}$

neurons (Figure 16C and 16D).

To validate the expression specificity of yellow pre-eGRASP in Fos-rTA system, I checked the yellow eGRASP expression in a doxycycline-dependent manner. Yellow eGRASP puncta were only observed in doxycycline injected mice which implicates a precise control of expression (Figure 17A and 17B).

Based on the optimized conditions, I performed quantitative analysis by reconstructing 3D models through IMARIS program (Figure 18A). $NAc^{sh}$ dendrites were represented as filaments; myristoylated mScarlet-I dendrites as red filaments and myristoylated iRFP670 dendrites as gray filaments. Yellow eGRASP and cyan eGRASP puncta were marked as yellow sphere and cyan sphere, respectively. Thus, yellow sphere on red dendrite means a synapse between activated $DRN^{TH}$ and activated $NAc^{sh}$ neurons. Analyzing methods were identical to the previous research (Choi et al., 2018).

Therefore, all conditions, from virus constructs to imaging analysis, were optimized for combination with social isolation.

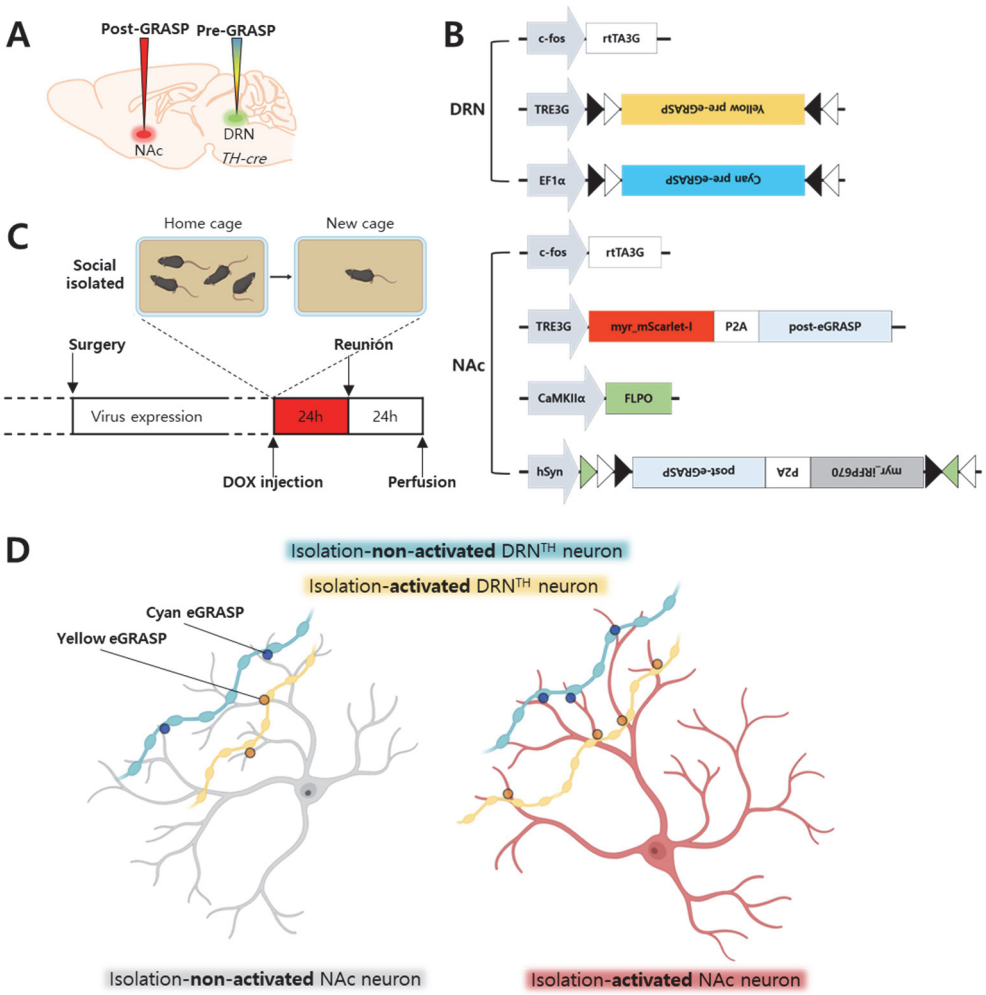


**Figure 16. Strategy to compare the synapses between isolation-activated DRN$^{TH}$ and NAc$^{sh}$ neurons using dual-eGRASP.**

*(in collaboration with Dong Il Choi)*

(A) Experimental scheme for virus injection sites.

(B) Illustration of AAV constructs and the combinations used for DRN and NAc.

(C) Timeline of experimental protocol to label synapses with dual-eGRASP.

(D) Illustration of four types of synapses between $DRN^{TH}$ and $NAc^{sh}$ neurons. Isolation-non-activated NAc neurons are drawn in gray and isolation-activated NAc neurons are drawn in red. The cyan eGRASP signals are represented in cyan circles, in which the synapses are from isolation-non-activated $DRN^{TH}$ neurons. The yellow eGRASP signals are pictured in yellow circles, in which the synapses are from isolation-activated $DRN^{TH}$ neurons.

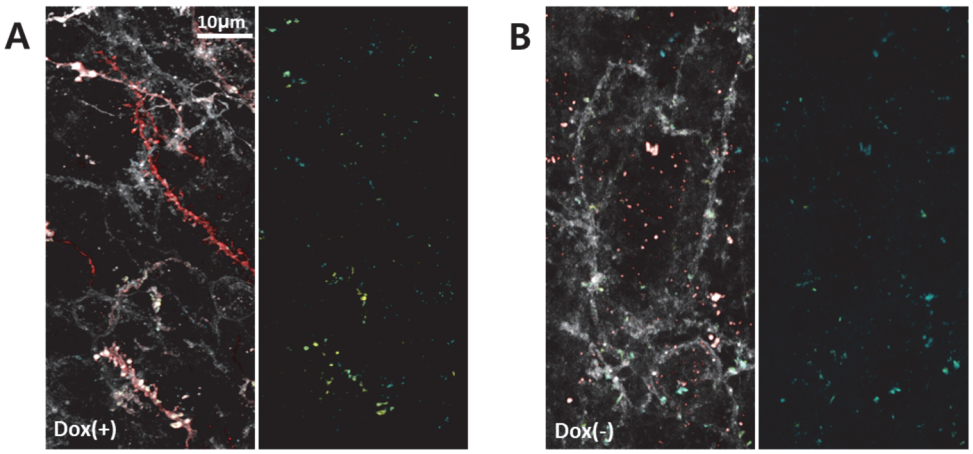


**Figure 17. Validation of Fos-rtTA induced dual-eGRASP system through doxycycline.**

*(in collaboration with Dong Il Choi)*

(A, B) Representative images of cyan eGRASP and yellow eGRASP signals with doxycycline i.p. (A) and without doxycycline i.p. (B).

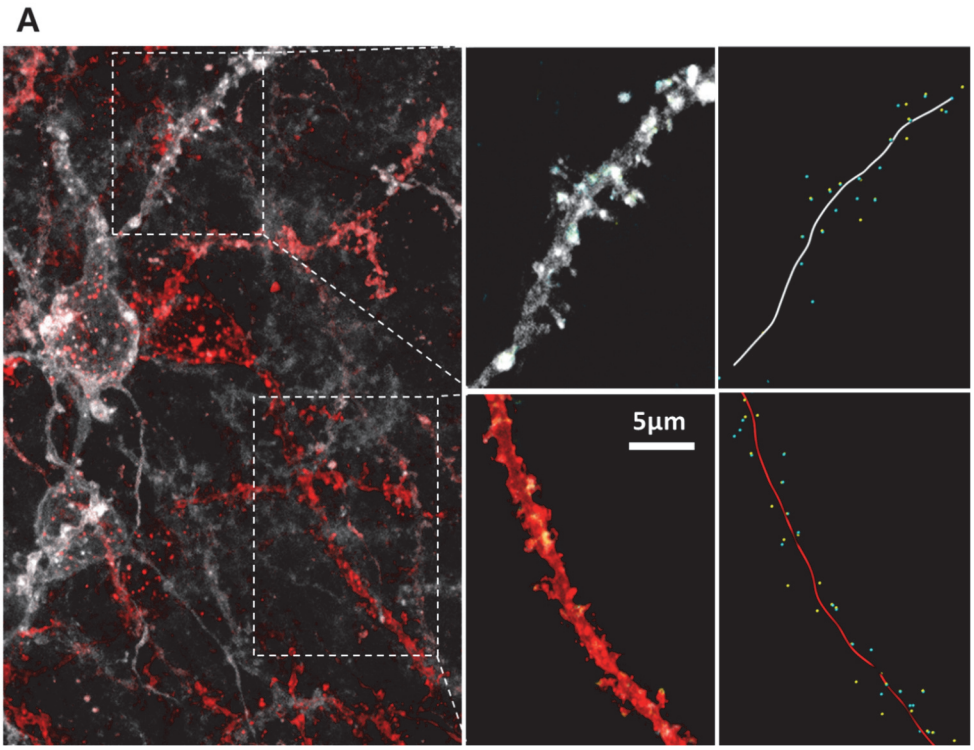


**Figure 18. Representative images of 3D modeling for analysis.**

*(in collaboration with Dong Il Choi)*

(A) All reconstructions were produced through IMARIS. $NAc^{sh}$ dendrites were reconstructed as filaments, myristoylated mScarlet-I dendrites into red filaments and myristoylated iRFP670 dendrites into gray filaments. Yellow eGRASP and cyan eGRASP puncta were marked as yellow sphere and cyan sphere, respectively.

## Male-specific increase of synaptic density between isolation-activated $DRN^{TH}$ and $NAc^{sh}$ neurons.

First, I checked whether the number of isolation-activated neurons were increased compared to the number of group-housed-activated neurons. Interestingly, social isolation did not induce an increase in the number of activated neurons in $DRN^{TH}$ and $NAc^{sh}$ of both sexes (Figure 19A and 19B).

Next, I investigated whether synaptic changes were observed when mice were socially isolated for 24 hours. I injected pre-eGRASP virus cocktails into the DRN of TH-cre mice and post-eGRASP virus cocktails bilaterally into the $NAc^{sh}$ (Figure 16A, 16B, 16C and 20A). Surprisingly, the spine density was significantly increased by social isolation in the male mice (Figure 20D). In contrast, strikingly, the isolated female mice did not show any increased spine density (Figure 20E). These synapse-level results were consistent with all the previous data in this study, suggesting the synaptic involvement of $DRN^{TH}$-$NAc^{sh}$ circuit in sexual dimorphism following social isolation. Importantly, this dual-eGRASP data go together with the electrophysiological results (Figure 15B and 15C) in which the excitability of the neuron is critical for synaptic strengthening and further more implicating the sexual dimorphism in $DRN^{TH}$ to $NAc^{sh}$ circuit.

Here, I show that 24-hours of social isolation facilitates synaptic strengthening between $DRN^{TH}$ and $NAc^{sh}$, in which further affects male-specific social-isolation-induced sociability increase. Whereas no synaptic strengthening has

occurred in the isolated female, isolation did not induce sociability increase.

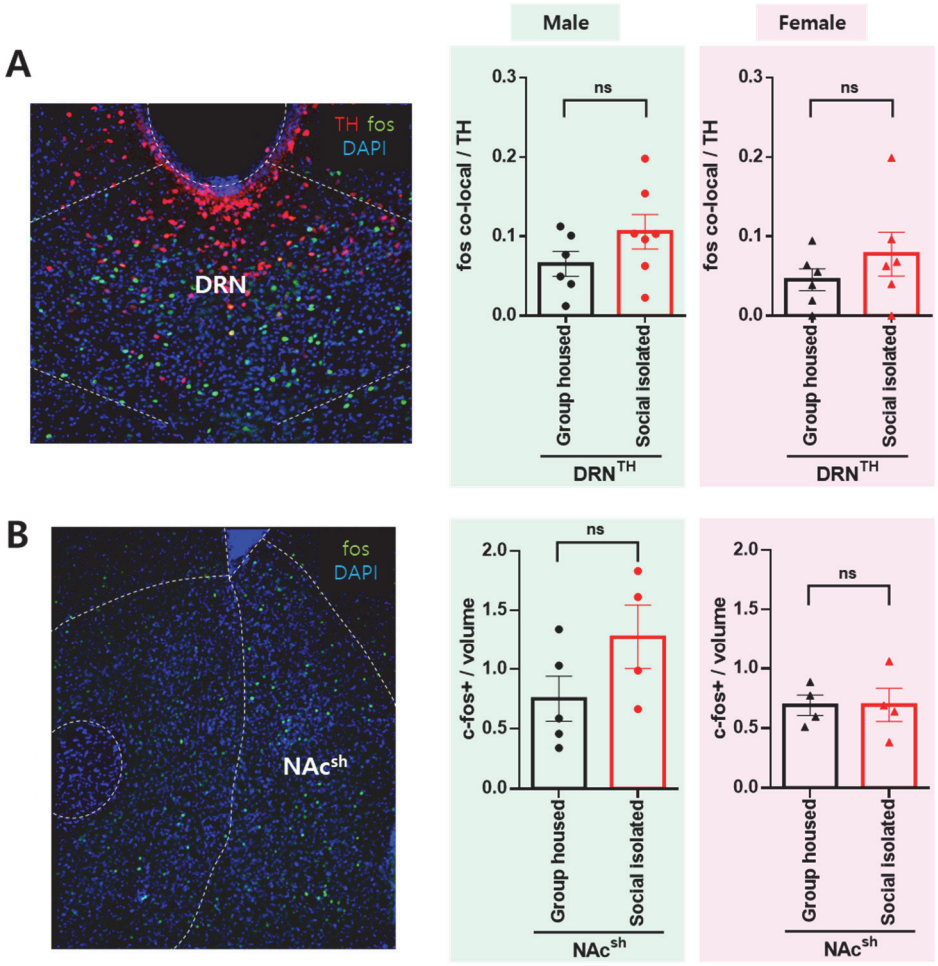


**Figure 19. The number of activated neurons in DRN$^{TH}$ and NAc$^{sh}$ are comparable between group housed and social isolated state.**

(A) Both male and females, social isolation did not affect the number of c-fos positive cells in the DRN$^{TH}$. (male in green, female in pink; group housed male, 0.06543 ± 0.01563, n=6; social isolated male, 0.1058 ± 0.02163, n=7; unpaired *t*-test; $p = 0.1711$; group housed female, 0.04536 ± 0.01372, n=6; social isolated female, 0.07771 ± 0.02759, n=6; unpaired *t*-test; $p = 0.3186$)

(B) Both male and females, social isolation did not affect the number of c-fos positive cells in the $NAc^{sh}$. (male in green, female in pink; group housed male, 0.7514 ± 0.1878, n=5; social isolated male, 1.274 ± 0.2706, n=4; unpaired *t*-test; $p = 0.1454$; group housed female, 0.6913 ± 0.08466, n=4; social isolated female, 0.6930 ± 0.1396, n=4; unpaired *t*-test; $p = 0.9918$)

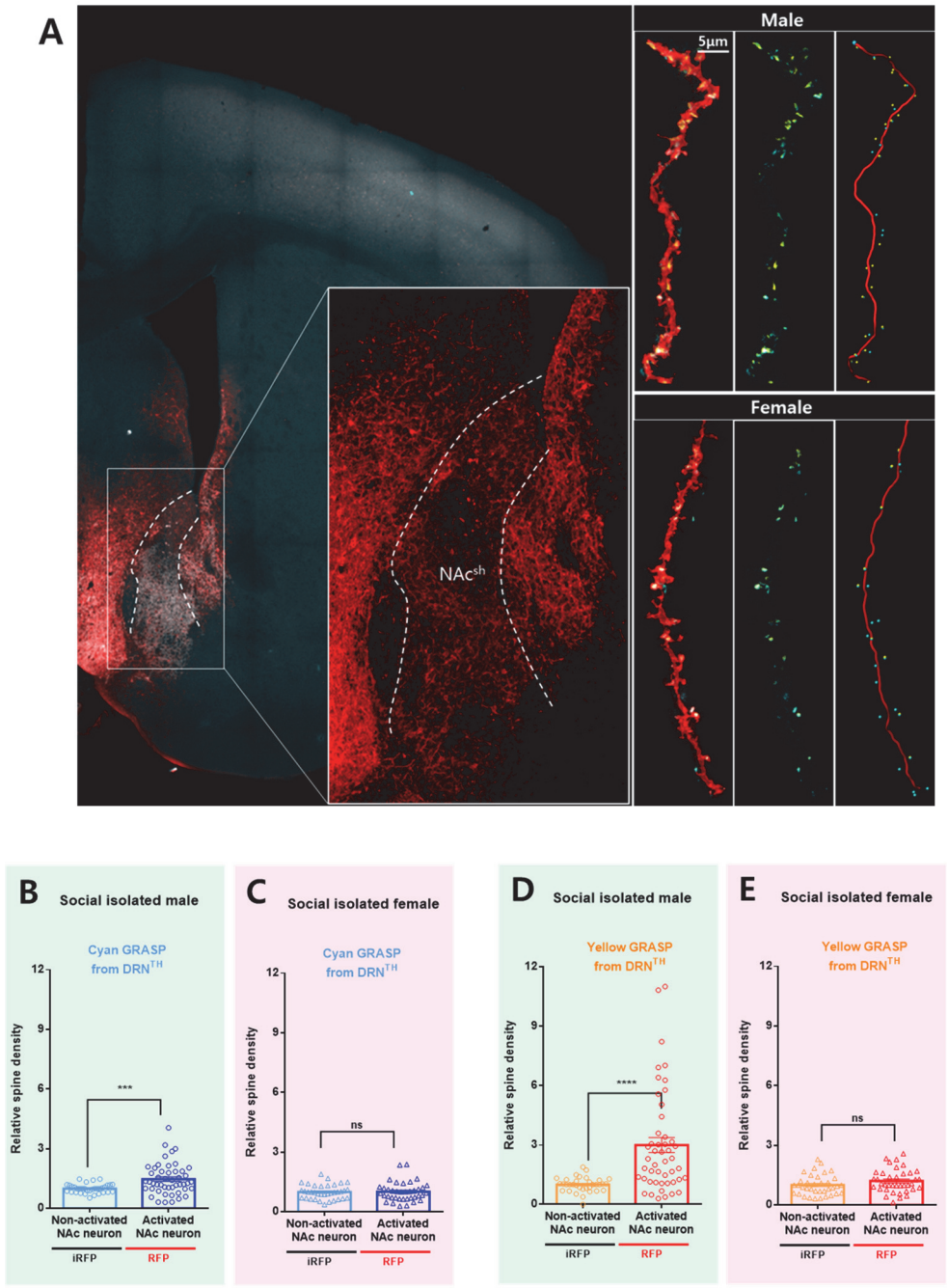


**Figure 20. Sexual dimorphism is observed between synaptic connections of isolation-activated DRN$^{TH}$ and NAc$^{sh}$ neurons.**

*(in collaboration with Dong Il Choi)*

(A) Representative image of $NAc^{sh}$ expressing dual-eGRASP.

(B, C, D and E) Isolation-induced spine density changes. The densities of cyan eGRASP (B and C) or yellow eGRASP (D and E) on mScarlet-I positive dendrites are normalized to the corresponding cyan eGRASP or yellow eGRASP on iRFP670 positive dendrites from the same images. Each data point represents a dendrite.

(B) (n = 36 for NAc non-activated dendrites, n = 59 for NAc activated dendrites, from 18 mice; Mann Whitney two-tailed test; ***$p = 0.0008$)

(C) (n = 36 for NAc non-activated dendrites, n = 38 for NAc activated dendrites, from 6 mice; Mann Whitney two-tailed test; $p = 0.9165$)

(D) (n = 36 for NAc non-activated dendrites, n = 59 for NAc activated dendrites, from 18 mice; Mann Whitney two-tailed test; ****$p < 0.0001$)

(E) (n = 36 for NAc non-activated dendrites, n = 38 for NAc activated dendrites, from 6 mice; Mann Whitney two-tailed test; $p = 0.1231$).

## $DRN^{TH}$ neurons showed a sharp increase in excitability following social isolation.

I found that the increased sociability reflects the strength of neural connectivity between $DRN^{TH}$ and $NAc^{sh}$ cells. This result can be further suggested that the activated synapses between the activated neurons indicate the degree of social interaction after 24-hours of social isolation. Therefore, I hypothesized that increased sociability will not be detected if the synaptic connectivity was blocked during social isolation.

To inhibit the $DRN^{TH}$ neurons from being isolated, I used the DREADD system. Since the plasma CNO levels peak with the maximum concentration at 30 minutes and fall to the baseline within 360 minutes (MacLaren et al., 2016), I needed to examined the excitability of $DRN^{TH}$ neurons after different time points during social isolation (Figure 21A). Thus, I performed whole-cell patch-clamp recording for measuring neuronal excitability in social isolated mice, at 2 hours, 4 hours, and 24 hours after social isolation. Interestingly, a robust increase in excitability was observed in 2 hours after social isolation and sharply decreased from 4 hours which continued to 24 hours (Figure 21B and 21C). Since the excitability peak by social isolation was during the working time of CNO, I could perform experiments to block the synaptic potentiation.

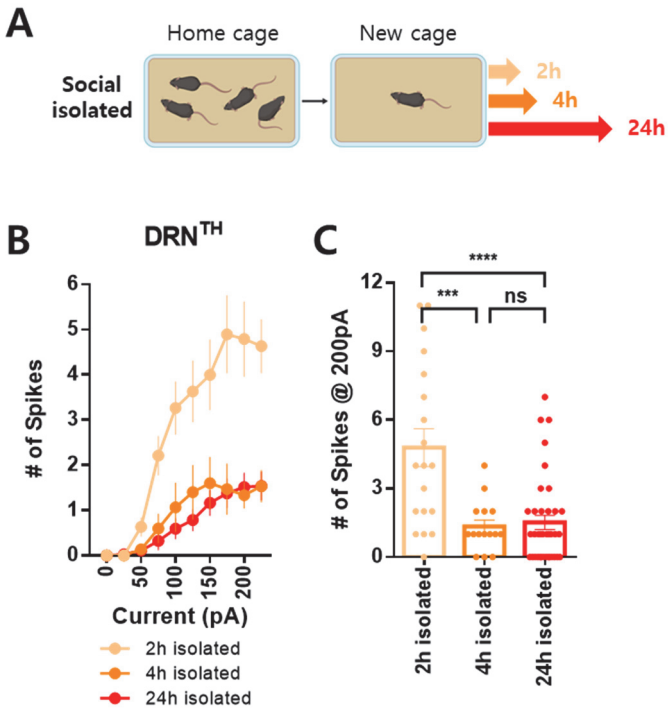


**Figure 21. The neuronal excitability of DRN$^{TH}$ neurons peak at 2 hours of social isolation.**

(A) Schematic image of social isolated male mice at three different time points.

(B) When male mice were social isolated for 2 hours, the DRN$^{TH}$ neurons showed a robust increase in excitability, in which the effect was disappeared from 4 hours and maintained to 24 hours.

(C) The number of spikes at 200pA showed a significant increase at 2-hour isolated males, compared with 4-hour and 24-hour. (2h isolated, n=19; 4h isolated, n=15; 24h isolated, n=37; one-way ANOVA Bonferroni's multiple comparisons test; ***$p$ = 0.0002; ****$p < 0.0001$; $p > 0.9999$)

## Activity of $DRN^{TH}$ neurons during isolation is necessary for isolation-induced sociability increase.

I expressed hM4Di in dopaminergic neurons of the DRN and the neural activity was inhibited by CNO injection when being social isolated (Figure 22A). Surprisingly, isolation-induced sociability increase disappeared when $DRN^{TH}$ neurons were inhibited during isolation (Figure 22B). This change was not due to the change in anxiety, as inhibition of $DRN^{TH}$ had no influence on velocity and total distance moved in three-chamber test (Figure 22C). I further performed open field test to examine the anxiety level more precisely. Even though $DRN^{TH}$ neurons were inhibited during 24-hours of social isolation, the time spent in center, velocity and total distance moved were unchanged (Figure 22D and 22E), in which means that the alterations were specific to sociability. Therefore, these results imply that the activation of $DRN^{TH}$ neurons are needed during isolation in order to increase the sociability.

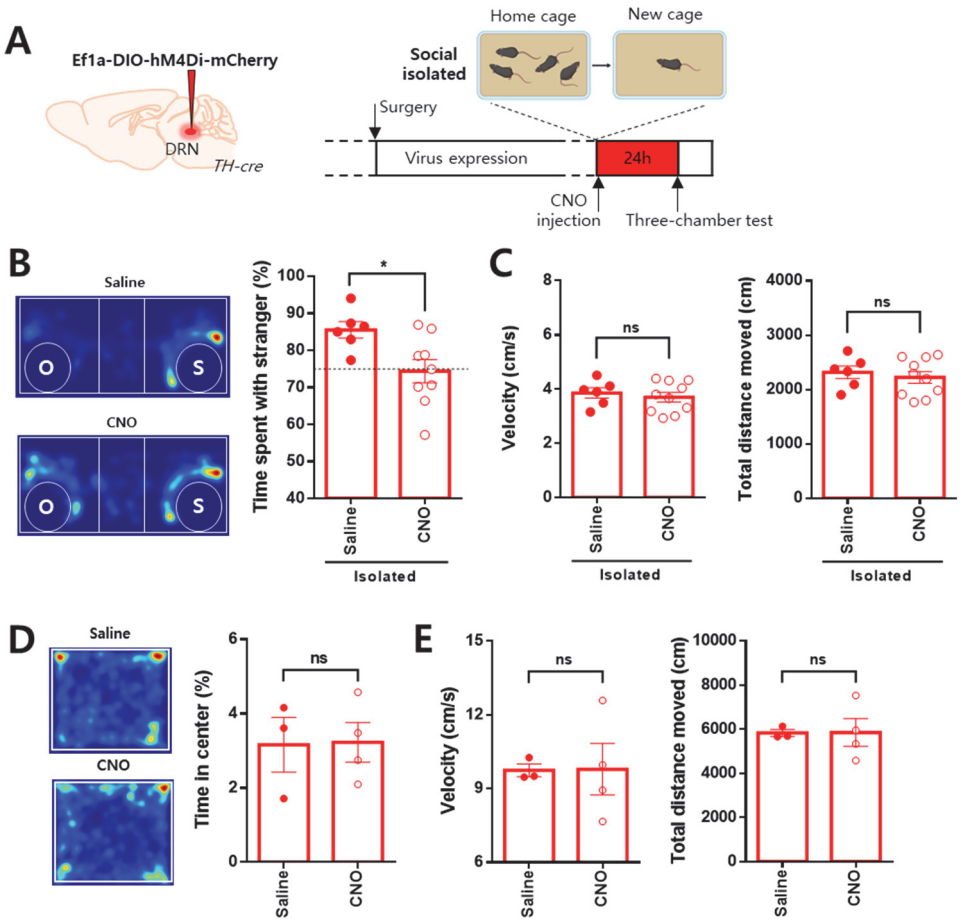


**Figure 22. Activity of DRN$^{TH}$ neurons during isolation is necessary for isolation-induced sociability increase.**

(A) Experimental scheme for virus injection site and timeline of behavioral tasks.

(B) Inhibition of DRN$^{TH}$ neurons during social isolation decreases isolation-induced sociability increase. When same DRN$^{TH}$ neurons were inhibited during group housing, it had no effect on sociability. (Saline, n=6, 85.51 ± 2.237; CNO, n=9, 74.35 ± 3.157; unpaired *t*-test; **p* = 0.0224)

(C) Velocity and total distance moved were not affected when inhibiting $DRN^{TH}$ neurons during social isolation. (Velocity; saline, n=6, 3.860 ± 0.1942; CNO, n=10, 3.700 ± 0.1787; unpaired *t*-test; $p = 0.5718$; Total distance moved; saline, n=6, 2316 ± 116.5; CNO, n=10, 2222 ± 108.1; unpaired *t*-test; $p = 0.5816$)

(D) No effect in anxiety level through open field test. (saline, n=3, 3.161 ± 0.7410; CNO, n=4, 3.224 ± 0.5310; unpaired *t*-test; $p = 0.9458$)

(E) Velocity and total distance moved were not affected by inhibition of $DRN^{TH}$ during 24-hours of social isolation. (Velocity; saline, n=3, 9.740 ± 0.2586; CNO, n=4, 9.784 ± 1.045; unpaired *t*-test; $p = 0.9735$; Total distance moved; saline, n=3, 5829 ± 152.9; CNO, n=4, 5853 ± 625.4; unpaired *t*-test; $p = 0.9757$)

# DISCUSSION

This chapter demonstrates that social isolation recruit isolation-activated neurons in $DRN^{TH}$ and $NAc^{sh}$. By strengthening the synaptic connections between these neuronal ensembles, increase in social interaction occurs.

After labeling isolation-activated or group-house-activated $DRN^{TH}$ neurons, I inhibited these neuronal ensembles when examining the sociability. Even though the number of activated neurons in both states are comparable, strikingly, only inhibiting the isolation-activated neurons could attenuate the isolation-induced sociability increase. These results strongly indicate that isolation-induced sociability increase requires the activated neuronal ensembles of $DRN^{TH}$ to be intact. Furthermore, the isolation-activated neuronal ensembles of the isolated male mice exhibited higher excitability. However, even though isolation induced the fos expression in female mice, no increase in neuronal excitability was detected. This sexual dimorphism results indicate that the fos and excitability do not always correlate. The neuronal excitability is one of the well revealed neuronal properties in the memory field, that the increased neuronal excitability has the necessity and sufficiency for memory expression (Han et al., 2009; Yiu et al., 2014). Whereas CREB is the mechanism of excitability in the field of memory, isolation-activated neurons may share the basis but further experiments are needed to clarify.

Based on chemogenetic modulation and electrophysiological data, I far

narrowed down to the synaptic level. Interestingly, the synaptic density between the activated neuronal ensembles were significantly increased only in the isolated male mice. This increase occurred by just being social isolated for just 24-hours. In addition, this synaptic strengthening was not detected in the isolated females, which also correlates with the unchanged sociability after being social isolated. This is the first study to visualize the isolation-activated synapses, in which correlates with the sociability degree.

Many researchers now focus down to the synaptic level to reveal the underlying mechanisms of various phenotypes. One paper from Medendorp et al. has reported that 3-month social isolated mice shows abnormal social behaviors with immature spine morphology in the prefrontal cortex (Medendorp et al., 2018). Despite the interesting results, we do not know whether the changes are circuit-specific nor activated-neuron-specific. The approach using dual-eGRASP will guide future studies in further narrowing down their previous results.

# CHAPTER IV

# CONCLUSION

# CONCLUSION

This study answered to where and how isolation-induced sociability changes occur in a sex-dependent manner. Through optogenetics, chemogenetics, patch clamp recording and dual-eGRASP technique, I could narrow down the underlying mechanism to the synaptic level. Sexual dimorphism following 24-hours of social isolation starts by activation of $DRN^{TH}$ neurons, in which then triggers synaptic strengthening with $NAc^{sh}$ neurons during the 24-hours. Thus, these modulations generate increased sociability. In contrast, in isolated females, since synaptic strengthening did not occur, isolation-induced sociability was not triggered.

In Chapter II, I detected sex-dependent isolation-induced sociability increase. Then I further manipulated $DRN^{TH}$-$NAc^{sh}$ circuit to examine whether this circuit is modulating the sociability, both in males and females. When I inhibited the circuit, the increased sociability by isolation was attenuated only in the males. To examine female's resilience to social isolation, I performed ovariectomy to see if female sex hormones are the cause. However, ovariectomized females did not show any isolation-induced sociability increase, which indicates that the resilient phenotype was not from sex hormones.

In Chapter III, I narrowed down the neuronal population of manipulation, from total to "isolation-activated" neurons. By combining fos-based labeling system with chemogenetics, I could modulate the activated neuronal ensembles.

Surprisingly, inhibition of isolation-activated neurons lowered the interaction time, whereas inhibition of group-house-activated neurons did not alter the sociability. Furthermore, 24-hours of social isolation facilitated the synaptic strengthening between the isolation-activated neurons. When $DRN^{TH}$ neurons' activity was blocked during isolation, sociability increase was not detected. This result implies that $DRN^{TH}$ neurons should be triggered in order to induce synaptic strengthening and sociability increase.

In human studies, sexual dimorphism in sociability is also observed. Sexual dimorphisms exist from brain anatomy (Ruigrok et al., 2014) to psychological processes and in various neurological disorders (Bálint et al., 2009; Gillberg et al., 2006; Wooten et al., 2004). It is reported that social isolation affects men and women differently (McLean et al., 2011). Moreover, a research by Vandervoort observed that men are more isolated than women (Vandervoort, 2000). It is further known that evidence from animal models reproduce the sex differences observed in humans (Leranth et al., 2000). According to previous studies and this thesis, social isolation mediates sociability changes in human and in mice. However due to the extensive differences in biology and social system, it is hard to classify into one basis. Even though the dissimilarities, it is known that neuromodulatory systems have coevolved to modulate social behaviors. Therefore, I expect this study will provide valuable set of data for future sociability studies with gender factor. The final aim of this study is to help develop therapeutics for sociability disorders such as autism spectrum disease.

This study, for the first time, revealed that one of the intrinsic mechanisms

in sociability, moreover the sex differences in sociability, is on the synapse. By applying dual-eGRASP technique to neuromodulatory system of the mouse brain, I further provided the visualization of neuromodulatory synapses that are activated during social isolation. I hope that the findings will provide us with groundwork for the synaptic manipulation of sociability. This approach can be modified by applying to different types of social behavior and to various brain regions.

# REFERENCES

Asher, M., and Aderka, I.M. (2018). Gender differences in social anxiety disorder. *74*, 1730-1741.

Badiani, A., Oates, M.M., Day, H.E., Watson, S.J., Akil, H., and Robinson, T.E. (1998). Amphetamine-induced behavior, dopamine release, and c-fos mRNA expression: modulation by environmental novelty. J Neurosci *18*, 10579-10593.

Bálint, S., Czobor, P., Komlósi, S., Mészáros, Á., Simon, V., and Bitter, I. (2009). Attention deficit hyperactivity disorder (ADHD): gender- and age-related differences in neurocognition. Psychological Medicine *39*, 1337-1345.

Barik, J., Marti, F., Morel, C., Fernandez, S.P., Lanteri, C., Godeheu, G., Tassin, J.-P., Mombereau, C., Faure, P., and Tronche, F. (2013). Chronic Stress Triggers Social Aversion via Glucocorticoid Receptor in Dopaminoceptive Neurons. Science *339*, 332.

Baumeister, R.F., and Leary, M.R. (1995). The Need to Belong: Desire for Interpersonal Attachments as a Fundamental Human Motivation. Psychological Bulletin *117*, 497-529.

Becker, J.B. (1999). Gender Differences in Dopaminergic Function in Striatum and Nucleus Accumbens. Pharmacology Biochemistry and Behavior *64*, 803-812.

Berkman, L.F., Vaccarino, V., and Seeman, T.J.A.o.B.M. (1993). Gender differences in cardiovascular morbidity and mortality: The contribution of social networks and support.

Bertran-Gonzalez, J., Bosch, C., Maroteaux, M., Matamales, M., Herve, D., Valjent, E., and Girault, J.A. (2008). Opposing patterns of signaling activation in dopamine D1 and D2 receptor-expressing striatal neurons in response to cocaine and haloperidol. J Neurosci *28*, 5671-5685.

Borland, J.M., Aiani, L.M., Norvelle, A., Grantham, K.N., O'Laughlin, K., Terranova, J.I., Frantz, K.J., and Albers, H.E. (2019). Sex-dependent regulation of social reward by oxytocin receptors in the ventral tegmental area. Neuropsychopharmacology *44*, 785-792.

Bourque, M., Dluzen, D.E., and Di Paolo, T.J.F.i.n. (2012). Signaling pathways mediating the neuroprotective effects of sex steroids and SERMs in Parkinson's disease. *33*, 169-178.

Brancato, A., Bregman, D., Ahn, H.F., Pfau, M.L., Menard, C., Cannizzaro, C., Russo, S.J., and Hodes, G.E. (2017). Sub-chronic variable stress induces sex-specific effects on glutamatergic synapses in the nucleus accumbens. Neuroscience *350*, 180-189.

Calipari, E.S., Juarez, B., Morel, C., Walker, D.M., Cahill, M.E., Ribeiro, E., Roman-Ortiz, C., Ramakrishnan, C., Deisseroth, K., Han, M.H.*, et al.* (2017). Dopaminergic dynamics underlying sex-specific cocaine reward. Nat Commun *8*, 13877.

Calizo, L.H., Akanwa, A., Ma, X., Pan, Y.-z., Lemos, J.C., Craige, C., Heemstra, L.A., and Beck, S.G. (2011). Raphe serotonin neurons are not homogenous: Electrophysiological, morphological and neurochemical evidence. Neuropharmacology *61*, 524-543.

Chandra, R., Francis, T.C., Konkalmatt, P., Amgalan, A., Gancarz, A.M., Dietz, D.M., and Lobo, M.K. (2015). Opposing role for Egr3 in nucleus accumbens cell subtypes in cocaine action. J Neurosci *35*, 7927-7937.

Choi, J.-H., Sim, S.-E., Kim, J.-i., Choi, D.I., Oh, J., Ye, S., Lee, J., Kim, T., Ko, H.-G., and Lim, C.-S.J.S. (2018). Interregional synaptic maps among engram cells underlie memory formation. *360*, 430-435.

Di Ciano, P., Robbins, T.W., and Everitt, B.J. (2008). Differential effects of nucleus accumbens core, shell, or dorsal striatal inactivations on the persistence, reacquisition, or reinstatement of responding for a drug-paired conditioned reinforcer. Neuropsychopharmacology *33*, 1413-1425.

Dolen, G., Darvishzadeh, A., Huang, K.W., and Malenka, R.C. (2013). Social reward requires coordinated activity of nucleus accumbens oxytocin and serotonin. Nature *501*, 179-184.

Eisenberger, N.I. (2012). The pain of social disconnection: examining the shared neural underpinnings of physical and social pain. Nat Rev Neurosci *13*, 421-434.

Ekstrand, M.I., Nectow, A.R., Knight, Z.A., Latcha, K.N., Pomeranz, L.E., and Friedman, J.M. (2014). Molecular profiling of neurons based on connectivity. Cell *157*, 1230-1242.

Ferguson, S.M., and Robinson, T.E. (2004). Amphetamine-evoked gene expression in striatopallidal neurons: regulation by corticostriatal afferents and the ERK/MAPK signaling cascade. Journal of neurochemistry *91*, 337-348.

Fernandez, S.P., Cauli, B., Cabezas, C., Muzerelle, A., Poncer, J.C., and Gaspar, P. (2016). Multiscale single-cell analysis reveals unique phenotypes of raphe 5-HT

neurons projecting to the forebrain. Brain Struct Funct *221*, 4007-4025.

Gillberg, C., Cederlund, M., Lamberg, K., and Zeijlon, L. (2006). Brief Report: "The Autism Epidemic". The Registered Prevalence of Autism in a Swedish Urban Area. Journal of Autism and Developmental Disorders *36*, 429.

Gillies, G.E., and McArthur, S. (2010). Estrogen Actions in the Brain and the Basis for Differential Action in Men and Women: A Case for Sex-Specific Medicines. Pharmacological Reviews *62*, 155-198.

Greenberg, G.D., Laman-Maharg, A., Campi, K.L., Voigt, H., Orr, V.N., Schaal, L., and Trainor, B.C. (2013). Sex differences in stress-induced social withdrawal: role of brain derived neurotrophic factor in the bed nucleus of the stria terminalis. Front Behav Neurosci *7*, 223.

Grueter, B.A., Robison, A.J., Neve, R.L., Nestler, E.J., and Malenka, R.C. (2013). FosB differentially modulates nucleus accumbens direct and indirect pathway function. Proc Natl Acad Sci U S A *110*, 1923-1928.

Gunaydin, L.A., Grosenick, L., Finkelstein, J.C., Kauvar, I.V., Fenno, L.E., Adhikari, A., Lammel, S., Mirzabekov, J.J., Airan, R.D., Zalocusky, K.A.*, et al.* (2014). Natural neural projection dynamics underlying social behavior. Cell *157*, 1535-1551.

Haasteren, G.v., Li, S., Ryser, S., and Schlegel, W. (2000). Essential Contribution of Intron Sequences to Ca2+-Dependent Activation of c-fos Transcription in Pituitary Cells. NEN *72*, 368-378.

Han, J.-H., Kushner, S., Yiu, A., Hsiang, H.-L., Buch, T., Waisman, A., Bontempi, B., Neve, R., Frankland, P., and Josselyn, S. (2009). Selective Erasure of a Fear

Memory. Science (New York, NY) *323*, 1492-1496.

Hasbi, A., Nguyen, T., Rahal, H., Manduca, J.D., Miksys, S., Tyndale, R.F., Madras, B.K., Perreault, M.L., and George, S.R. (2020). Sex difference in dopamine D1-D2 receptor complex expression and signaling affects depression- and anxiety-like behaviors. Biol Sex Differ *11*, 8.

Hille, B. (1978). Ionic channels in excitable membranes. Current problems and biophysical approaches. Biophys J *22*, 283-294.

Huang, K.W., Ochandarena, N.E., Philson, A.C., Hyun, M., Birnbaum, J.E., Cicconet, M., and Sabatini, B.L. (2019). Molecular and anatomical organization of the dorsal raphe nucleus. Elife *8*.

Huang, Q., Zhou, Y., and Liu, L.Y. (2017). Effect of post-weaning isolation on anxiety- and depressive-like behaviors of C57BL/6J mice. Exp Brain Res *235*, 2893-2899.

Ishimura, K., Takeuchi, Y., Fujiwara, K., Tominaga, M., Yoshioka, H., and Sawada, T. (1988). Quantitative analysis of the distribution of serotonin-immunoreactive cell bodies in the mouse brain. Neuroscience Letters *91*, 265-270.

Jung, H., Kim, S.W., Kim, M., Hong, J., Yu, D., Kim, J.H., Lee, Y., Kim, S., Woo, D., Shin, H.S.*, et al.* (2019). Noninvasive optical activation of Flp recombinase for genetic manipulation in deep mouse brain regions. Nat Commun *10*, 314.

Kang, S.J., Kwak, C., Lee, J., Sim, S.E., Shim, J., Choi, T., Collingridge, G.L., Zhuo, M., and Kaang, B.K. (2015). Bidirectional modulation of hyperalgesia via the specific control of excitatory and inhibitory neuronal activity in the ACC. Mol Brain *8*, 81.

Karkhanis, A.N., Locke, J.L., McCool, B.A., Weiner, J.L., and Jones, S.R. (2014). Social isolation rearing increases nucleus accumbens dopamine and norepinephrine responses to acute ethanol in adulthood. Alcohol Clin Exp Res *38*, 2770-2779.

Ke, M.T., Nakai, Y., Fujimoto, S., Takayama, R., Yoshida, S., Kitajima, T.S., Sato, M., and Imai, T. (2016). Super-Resolution Mapping of Neuronal Circuitry With an Index-Optimized Clearing Agent. Cell Rep *14*, 2718-2732.

Krishnan, V., Han, M.H., Graham, D.L., Berton, O., Renthal, W., Russo, S.J., Laplant, Q., Graham, A., Lutter, M., Lagace, D.C*., et al.* (2007). Molecular adaptations underlying susceptibility and resistance to social defeat in brain reward regions. Cell *131*, 391-404.

Kronman, H., Richter, F., Labonte, B., Chandra, R., Zhao, S., Hoffman, G., Lobo, M.K., Schadt, E.E., and Nestler, E.J. (2019). Biology and Bias in Cell Type-Specific RNAseq of Nucleus Accumbens Medium Spiny Neurons. Sci Rep *9*, 8350.

Krupina, N.A., Khlebnikova, N.N., Narkevich, V.B., Naplekova, P.L., and Kudrin, V.S. (2020). The Levels of Monoamines and Their Metabolites in the Brain Structures of Rats Subjected to Two- and Three-Month-Long Social Isolation. Bull Exp Biol Med *168*, 605-609.

Leranth, C., Roth, R.H., Elsworth, J.D., Naftolin, F., Horvath, T.L., and Redmond, D.E. (2000). Estrogen Is Essential for Maintaining Nigrostriatal Dopamine Neurons in Primates: Implications for Parkinson's Disease and Memory. The Journal of Neuroscience *20*, 8604.

Li, B.J., Liu, P., Chu, Z., Shang, Y., Huan, M.X., Dang, Y.H., and Gao, C.G.

(2017). Social isolation induces schizophrenia-like behavior potentially associated with HINT1, NMDA receptor 1, and dopamine receptor 2. Neuroreport *28*, 462-469.

Lin, R., Liang, J., Wang, R., Yan, T., Zhou, Y., Liu, Y., Feng, Q., Sun, F., Li, Y., Li, A.*, et al.* (2020). The Raphe Dopamine System Controls the Expression of Incentive Memory. Neuron.

Loew, R., Heinz, N., Hampf, M., Bujard, H., and Gossen, M. (2010). Improved Tet-responsive promoters with minimized background expression. BMC Biotechnol *10*, 81.

MacLaren, D., Browne, R., Shaw, J., Radhakrishnan, S., Khare, P., España, R., and Clark, S. (2016). Clozapine N-Oxide Administration Produces Behavioral Effects in Long–Evans Rats: Implications for Designing DREADD Experiments. eNeuro *3*.

Matthews, G.A., Nieh, E.H., Vander Weele, C.M., Halbert, S.A., Pradhan, R.V., Yosafat, A.S., Glober, G.F., Izadmehr, E.M., Thomas, R.E., Lacy, G.D.*, et al.* (2016). Dorsal Raphe Dopamine Neurons Represent the Experience of Social Isolation. Cell *164*, 617-631.

McLean, C.P., Asnaani, A., Litz, B.T., and Hofmann, S.G. (2011). Gender differences in anxiety disorders: prevalence, course of illness, comorbidity and burden of illness. J Psychiatr Res *45*, 1027-1035.

Medendorp, W.E., Petersen, E.D., Pal, A., Wagner, L.M., Myers, A.R., Hochgeschwender, U., and Jenrow, K.A. (2018). Altered Behavior in Mice Socially Isolated During Adolescence Corresponds With Immature Dendritic Spine

Morphology and Impaired Plasticity in the Prefrontal Cortex. Front Behav Neurosci *12*, 87.

Nelson, R.J., and Trainor, B.C. (2007). Neural mechanisms of aggression. Nature Reviews Neuroscience *8*, 536-546.

Newmann, J.P.J.J.o.H., and Behavior, S. (1986). Gender, life strains, and depression. 161-178.

Oliver, D.K., Intson, K., Sargin, D., Power, S.K., McNabb, J., Ramsey, A.J., and Lambe, E.K. (2020). Chronic social isolation exerts opposing sex-specific consequences on serotonin neuronal excitability and behaviour. Neuropharmacology *168*, 108015.

Raymond, V., Beaulieu, M., Labrie, F., and Boissier, J.J.S. (1978). Potent antidopaminergic activity of estradiol at the pituitary level on prolactin release. *200*, 1173-1175.

Reijmers, L.G., Perkins, B.L., Matsuo, N., and Mayford, M. (2007). Localization of a stable neural correlate of associative memory. Science *317*, 1230-1233.

Ren, J., Friedmann, D., Xiong, J., Liu, C.D., Ferguson, B.R., Weerakkody, T., DeLoach, K.E., Ran, C., Pun, A., Sun, Y.*, et al.* (2018). Anatomically Defined and Functionally Distinct Dorsal Raphe Serotonin Sub-systems. Cell *175*, 472-487 e420.

Riecher-Rössler, A., Häfner, H., Stumbaum, M., Maurer, K., and Schmidt, R. (1994). Can Estradiol Modulate Schizophrenic Symptomatology? Schizophrenia Bulletin *20*, 203-214.

Ruigrok, A.N.V., Salimi-Khorshidi, G., Lai, M.-C., Baron-Cohen, S., Lombardo,

M.V., Tait, R.J., and Suckling, J. (2014). A meta-analysis of sex differences in human brain structure. Neuroscience & Biobehavioral Reviews *39*, 34-50.

Sagoshi, S., Maejima, S., Morishita, M., Takenawa, S., Otubo, A., Takanami, K., Sakamoto, T., Sakamoto, H., Tsukahara, S., and Ogawa, S. (2020). Detection and characterization of estrogen receptor beta expression in the brain with newly developed transgenic mice. Neuroscience.

Seo, C., Guru, A., Jin, M., Ito, B., Sleezer, B.J., Ho, Y.-Y., Wang, E., Boada, C., Krupa, N.A., Kullakanda, D.S.*, et al.* (2019). Intense threat switches dorsal raphe serotonin neurons to a paradoxical operational mode. Science *363*, 538.

Smith, R.J., Lobo, M.K., Spencer, S., and Kalivas, P.W. (2013). Cocaine-induced adaptations in D1 and D2 accumbens projection neurons (a dichotomy not necessarily synonymous with direct and indirect pathways). Curr Opin Neurobiol *23*, 546-552.

Stratford, T.R., and Wirtshafter, D.J.B.r. (1990). Ascending dopaminergic projections from the dorsal raphe nucleus in the rat. *511*, 173-176.

Trainor, B.C. (2011). Stress responses and the mesolimbic dopamine system: social contexts and sex differences. Horm Behav *60*, 457-469.

Trulson, M.E., Cannon, M.S., and Raese, J.D.J.B.r.b. (1985). Identification of dopamine-containing cell bodies in the dorsal and median raphe nuclei of the rat brain using tyrosine hydroxylase immunochemistry. *15*, 229-234.

Vandervoort, D. (2000). Social isolation and gender. Current Psychology *19*, 229-236.

Wallace, D.L., Han, M.H., Graham, D.L., Green, T.A., Vialou, V., Iniguez, S.D.,

Cao, J.L., Kirk, A., Chakravarty, S., Kumar, A.*, et al.* (2009). CREB regulation of nucleus accumbens excitability mediates social isolation-induced behavioral deficits. Nat Neurosci *12*, 200-209.

Walsh, J.J., Christoffel, D.J., Heifets, B.D., Ben-Dor, G.A., Selimbeyoglu, A., Hung, L.W., Deisseroth, K., and Malenka, R.C. (2018). 5-HT release in nucleus accumbens rescues social deficits in mouse autism model. Nature *560*, 589-594.

Wooten, G.F., Currie, L.J., Bovbjerg, V.E., Lee, J.K., and Patrie, J. (2004). Are men at greater risk for Parkinson's disease than women? Journal of Neurology, Neurosurgery & Psychiatry *75*, 637-639.

Yiu, A.P., Mercaldo, V., Yan, C., Richards, B., Rashid, A.J., Hsiang, H.L., Pressey, J., Mahadevan, V., Tran, M.M., Kushner, S.A.*, et al.* (2014). Neurons are recruited to a memory trace based on relative neuronal excitability immediately before training. Neuron *83*, 722-735.

Zelikowsky, M., Hui, M., Karigo, T., Choe, A., Yang, B., Blanco, M.R., Beadle, K., Gradinaru, V., Deverman, B.E., and Anderson, D.J. (2018). The Neuropeptide Tac2 Controls a Distributed Brain State Induced by Chronic Social Isolation Stress. Cell *173*, 1265-1279 e1219.

Zhang, J., Zhang, L., Jiao, H., Zhang, Q., Zhang, D., Lou, D., Katz, J.L., and Xu, M. (2006). c-Fos facilitates the acquisition and extinction of cocaine-induced persistent changes. J Neurosci *26*, 13287-13296.

Zhou, X., Vink, M., Klaver, B., Berkhout, B., and Das, A.T. (2006). Optimization of the Tet-On system for regulated gene expression through viral evolution. Gene Ther *13*, 1382-1390.

# 국문초록

사회적 동물에서의 사회성은 매우 중요한 부분이며, 따라서 사회적 연결을 유지하기 위해 많은 노력을 한다. 사회적으로 단절이 되면 사회적 고통을 느끼게 되며, “사회적 고립”은 사회적 연결 고리가 끊어지는 종류 중 하나에 속한다. 사회적 고립에 의한 사회성 변화와 불안 수준에 대한 연구는 오랜 기간 동안 다양한 분야에서 연구가 진행되어 왔다. 주로 사회적 고립 상태를 몇 달 이상 유지하는 장기적인 영향에 대한 연구들이 이루어져왔지만, 하루 동안 사회적 고립이 되었을 때의 사회성 변화와 이러한 변화가 어떠한 메커니즘으로 이루어지는지에 대한 연구가 필요하였다.

본 연구는, 사회적 고립 시 성별에 따라 사회성이 다르게 변한다는 것을 발견하였으며, 수컷 생쥐에서만 사회적 고립에 의한 사회성 증가를 관찰하였다. 이러한 행동학적 변화가 나타나는 메커니즘을 밝히기 위해, 배측봉선핵에 존재하는 도파민 신경세포와 측좌핵에 초점을 맞춰 연구를 진행하였다. 광유전학을 활용하여 두 부위 간의 신경회로를 조절하였으며, 억제 시켰을 때 사회적 고립에 의한 사회성 증가가 나타나지 않는다는 것을 확인하였다. 더 나아가 사회적 고립에 의해 활성화를 보이는 신경세포만을 표지 하여 화학유전체학을 통해 신경세포의 활성 상

태를 조절하였다. 이를 통해, 사회적 고립에 의한 사회성 증가는 사회적 고립에 의해 활성화된 신경세포를 필요로 한다는 것을 밝혔다. 더 나아가 활성화된 신경세포 사이의 시냅스 변화를 시각화하여, 배측봉선핵의 도파민 신경세포와 측좌핵 신경세포 간의 시냅스 밀도가 증가했다는 것을 발견하였다. 이는 행동학적으로 관찰하고 조절한 실험 결과와 일치한다.

따라서, 성별에 따른 사회적 고립에 의한 사회성 변화의 원인을 시냅스 수준부터 행동학적 수준까지 밝혀, 사회적 고립에 의한 사회성 증가의 메커니즘을 밝혀내었다.

.....

주요어 : 사회적 고립, 사회성, 배측봉선핵, 측좌핵, 시냅스

학번 : 2015-20451

이학박사학위논문

# 성별에 따른 사회적 고립의 영향과 시냅스 변화에 대한 연구

Studies on sexual dimorphism in social isolation and synaptic changes

2020년 8월


서울대학교 대학원

생명과학부

최 자 은

# ABSTRACT

## Studies on sexual dimorphism in social isolation and synaptic changes

Ja Eun Choi

School of Biological Sciences

The Graduate School

Seoul National University

Social animals prefer socially connected state and consume considerable energy to maintain the social bonds. To study social connections, many researchers have used the concept of social pain. Disconnection of social bond, which is social isolation, is one type of social pain (Eisenberger, 2012). When socially isolated, a strong motivation to seek social interactions occur in humans (Baumeister and Leary, 1995) as well as in rodents (Matthews et al., 2016). Numerous social isolation studies have been performed by modulating the duration of isolation in accordance with the

objectives, from as short as one day to as long as several months (Matthews et al., 2016; Zelikowsky et al., 2018). It is observed that sociability itself shows a sex-dependent phenotype (Borland et al., 2019; Brancato et al., 2017), which the sexual dimorphism is also detected in the isolated mice (Oliver et al., 2020). In human studies, it is reported that social isolation affects men and women differently (McLean et al., 2011; Vandervoort, 2000). Even though numerous researches have observed the sexual dimorphism in sociability, the underlying mechanism of "why and how" still remains largely unclear. Moreover, it is not investigated about the circuit-specific and synapse-specific perspective on how sociability is differently modulated by isolation in sex dependent manner.

The dopamine system in the brain is known to be related with reward, including rewards linked with sociability (Gunaydin et al., 2014). Extensive studies on the function of ventral tegmental area (VTA), a traditional brain region in the mesolimbic dopamine system, is being researched. Recently, the dorsal raphe nucleus (DRN), which is a distinct brain region containing the dopaminergic neurons, is receiving attention for the independent role of dopamine neurons (Lin et al., 2020; Matthews et al., 2016). However, the role of DRN dopaminergic neuron ($DRN^{TH}$) on circuit level and the consequences on sex-specific sociability remain largely unknown.

I observed that only the male mice showed increased sociability after 24 hours of social isolation. Using optogenetics and chemogenetics combined with immediate early gene (IEG)-based tagging system, I further manipulated the total

population and the isolation-activated neuronal ensembles of $DRN^{TH}$ and NAc shell ($NAc^{sh}$) and modulated isolation-induced sociability. I also found that synaptic strengthening between the isolation-activated neurons in $DRN^{TH}$ and $NAc^{sh}$ has occurred and this strengthening is needed for sociability increase. These findings will provide information on how isolation-induced sociability changes are modulated from synaptic level in sexual dimorphic way.

.....

Keywords : Social isolation, Sociability, Dorsal raphe nucleus, Nucleus accumbens, synapse

*Student Number : 2015-20451*

# CONTENTS

# LIST OF FIGURES

# CHAPTER I

# INTRODUCTION

# BACKGROUND

Maintaining social connections in socially innate animals is important throughout the life time. Thus, social disconnection is a powerful social pain and one type of social pain is the social isolation. Furthermore, sex differences in sociability are also seen in nature. Despite the various phenotypes revealed related to social isolation, remarkably little is known about the circuit-specific details and the neurobiological role of DRN dopaminergic neurons in social isolation and its sexual dimorphic outputs. This study presents the first evidence on how social isolation is regulated from synaptic level to behavioral level.

## Social isolation

Mice are highly social species that participate in social behaviors. Social isolation is a paradigm which separates the cagemates into individuals (Figure 1). Mice kept in the isolated state can be as short as 24 hours to as long as several months. Also, the age of the mice being isolated is known to be critical for the various effect. Therefore, researchers choose the duration of social isolation and the age of the mice being isolated by their experimental objectives.

Manipulation of social environment such as isolation leads to disruptions in various behavioral phenotypes; anxiety (Huang et al., 2017; Karkhanis et al., 2014;

Zelikowsky et al., 2018), depression (Oliver et al., 2020), cognition (Li et al., 2017) and sociability (Matthews et al., 2016; Zelikowsky et al., 2018). In molecular level, social isolation leads to changes in the level of NMDA receptor, monoamines and Tac2 expression in various brain regions (Krupina et al., 2020; Li et al., 2017; Zelikowsky et al., 2018). Sexual dimorphism is one of the phenotypes observed is the sociability, which is reported from human (Asher and Aderka, 2018) to mice (Greenberg et al., 2013; Oliver et al., 2020).

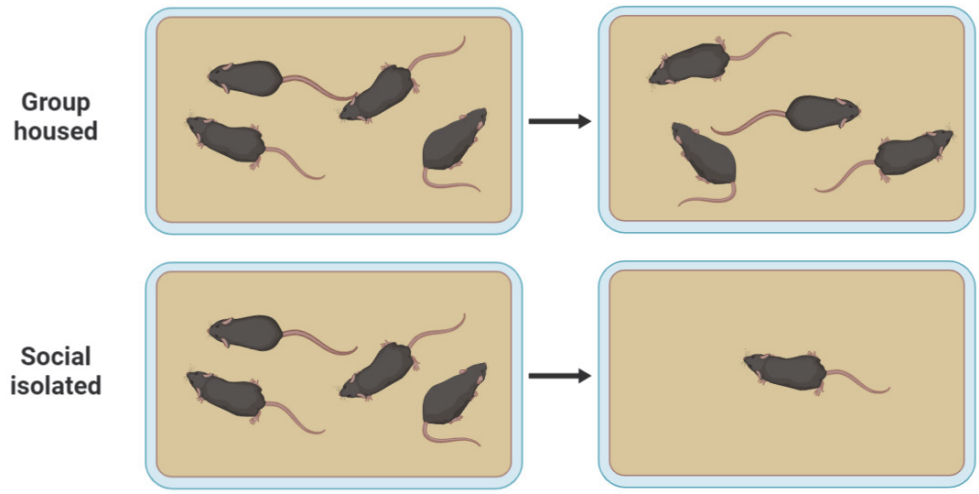


**Figure 1. Schematic image of group housed and social isolated mice**

Illustration of group housing and social isolation. Before moving the mice to a new cage, they were kept in the homecage for at least two weeks for adaptation. Group housing were performed by moving all the littermates to a new cage for 24 hours. Social isolation was performed by moving one mouse to each new cages for 24 hours.

## Dorsal raphe nucleus (DRN)

The DRN is a heterogeneous structure which is consisted with several cell types (Calizo et al., 2011; Huang et al., 2019; Seo et al., 2019). Serotonergic neurons are the most abundant cell type and provide majority of the serotonergic projections throughout the brain (Fernandez et al., 2016; Ishimura et al., 1988; Ren et al., 2018). Related to serotonergic neurons and sociability, a recent research from Malenka's lab has revealed that serotonergic projections from DRN to nucleus accumbens modifies social interaction (Walsh et al., 2018).

Even though the most well-known brain region in the mesolimbic dopamine system is the ventral tegmental area (VTA), distinct brain region containing the dopaminergic neurons exists in the DRN. The existence of dopaminergic neuronal population in the DRN has been described from several decades (Stratford and Wirtshafter, 1990; Trulson et al., 1985). Recently, the role of dopamine neurons in DRN ($DRN^{TH}$) have been receiving attention (Lin et al., 2020; Matthews et al., 2016), but is still a field of the unknown.

The DRN is one of the region related with social isolation. In 2016, Matthews and colleagues reported that the dopaminergic neurons of DRN represents the state of loneliness by 24-hours of isolation (Matthews et al., 2016). Four years after, another research group reported that the serotonergic neurons of DRN are affected in a chronic isolated state (Oliver et al., 2020).

## Nucleus accumbens (NAc)

The NAc can be divided into two sub-regions by structure with distinct projections, the NAc core and the NAc shell ($NAc^{sh}$) (Di Ciano et al., 2008). The neuronal cell type can also be classified into sub-populations according to the expression of dopamine receptors; D1-type and D2-type medium spiny neurons (MSNs). Since D1-MSNs and D2-MSNs have distinguished projections throughout the brain (Smith et al., 2013), various functions are related with the NAc. The NAc is studied to be related with motivation, addiction, reward, and reinforcement learning. In addition, it is also known to regulate social behaviors (Dolen et al., 2013; Gunaydin et al., 2014; Wallace et al., 2009). Moreover, a recent study from Eric J. Nestler's lab revealed the transcriptomes of NAc cell types and found sex differences in the molecule level (Kronman et al., 2019).

## Immediate early genes (IEGs)

Immediate early genes (IEGs) are used as neuronal activity markers. Even though FosB is the most well studied IEGs in striatal circuits (Grueter et al., 2013), there are studies revealing the role of c-fos (Badiani et al., 1998; Bertran-Gonzalez et al., 2008; Chandra et al., 2015; Ferguson and Robinson, 2004). Several researches have reported that cocaine induces a change in c-fos expression in the striatum (Bertran-Gonzalez et al., 2008) or c-fos expression modulation can change the response to cocaine (Zhang et al., 2006).

## Description of behavioral tests

The most widely used behavioral task to examine sociability is the three-chamber test. Therefore, in this study, three-chamber test was mainly used (Figure 2). Test mouse is allowed to freely move in the apparatus for 10 minutes, which is the habituation session. After the habituation, an unfamiliar juvenile mouse is placed under one cup, and an object is placed under the other cup. Then the test mouse is tested for the preference to the unfamiliar juvenile mouse for 10 minutes, which is the test session. The time of sniffing to each cup is analyzed and regarded as sociability. The velocity and the distance moved of test mouse can also be analyzed for anxiety index.

Juvenile interaction test is another behavioral task for examining sociability (Figure 3). Test mouse is placed in a new cage with new beddings for one minute to explore the context. Then, an unfamiliar juvenile stranger mouse is gently introduced into the apparatus. The interaction time of the test mouse is analyzed for 5 minutes.

This study used open field test to measure the anxiety level of the test mouse (Figure 4). The test mouse is placed in the center of the apparatus for 10 minutes of exploration. The total distance moved and time spent in the center is analyzed and regarded as the anxiety level.

**Figure 2. Schematic image of three-chamber test.**

Illustration of test mouse undergoing three-chamber test. An object is placed under one side of the chamber and an unfamiliar juvenile mouse in placed under other side of the chamber. Sociability was represented by counting the sniffing time to the stranger mouse by the total interaction time to each sides.

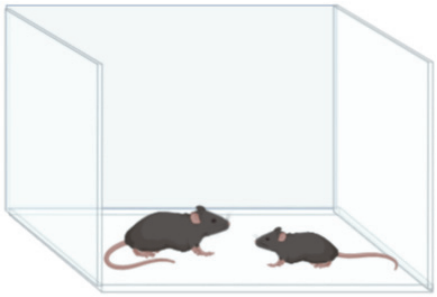

**Figure 3. Schematic image of juvenile interaction test.**

Illustration of test mouse interacting with unfamiliar juvenile mouse. The test mouse is exposed to the stranger mouse and the interaction time was presented as sociability.

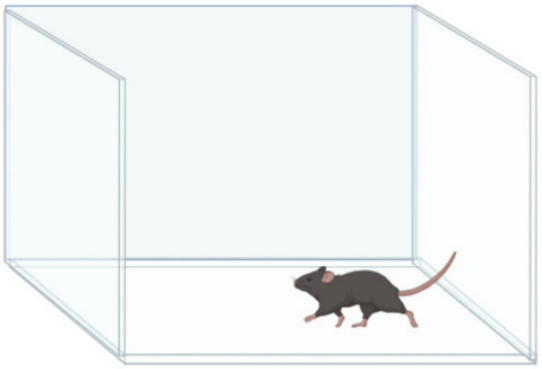

**Figure 4. Schematic image of open field test (OFT).**

Illustration of test mouse undergoing open field test. The test mouse in put in a chamber and was allowed to move freely. The time spent in the center was calculated with the total time spent in the chamber, which represented the anxiety of the mouse.

# PURPOSE OF THIS STUDY

Maintaining social connections in social creatures are important. Therefore, socially innate animals prefer socially connected state. Evidence from human studies and animal studies mention the action of dopamine on behaviors (Calipari et al., 2017; Hasbi et al., 2020), especially on sociability (Berkman et al., 1993; Newmann and Behavior, 1986; Trainor, 2011; Vandervoort, 2000). In addition, sexual dimorphism in sociability is observed in humans (McLean et al., 2011; Vandervoort, 2000), as in mice. However, the basic questions about how and where the sex-dependent social-isolation-induced phenotypes exist have not been pursued. In this thesis, I present for the first time on how social isolation is regulated from synaptic level to behavioral level.

In chapter II, I begin by observing sexual dimorphism in sociability after 24-hours of social isolation. I focused on the dopaminergic neurons in DRN and its monosynaptic connections with the $NAc^{sh}$ to reveal the underlying mechanism. I utilized optogenetic tools to activate or inhibit the $DRN^{TH}$-$NAc^{sh}$ circuit after social isolation to see whether this neural circuit modulates social-isolation-induced sociability.

In chapter III, I narrowed down the neural ensembles from total population to the isolation-activated cells and further manipulated these neurons. I tested whether inhibiting only the isolation-activated neurons can attenuate the isolation-

induced sociability. Then, I observed neuronal excitability, one of electrophysiological properties, and compared the isolation-activated with isolation-non-activated cells. Next, I further narrowed down to the synaptic level. I applied the dual-eGRASP technique and examined the synaptic density between isolation-activated $DRN^{TH}$ and $NAc^{sh}$ after social isolation. Finally, I inhibited the $DRN^{TH}$ neurons when being social isolated for 24-hours to see whether the activation of $DRN^{TH}$ neurons are necessary for the induction of isolation-induced sociability changes.

In this thesis, I address the underlying mechanism of social isolation and its sex-dependent phenotypes from synaptic level to behavioral level. Furthermore, I propose that the activated neuronal ensembles by social isolation are necessary for isolation-induced sociability, as engrams' role in memory.

# CHAPTER II

# Sexual dimorphism in 24-hours of social isolation is regulated by $DRN^{TH}$ and $NAc^{sh}$ neurons

# INTRODUCTION

Social animals, both human and mice, spend substantial amount of time to be socially connected. Thus, disconnecting the social bond raise social pain and one type of social disconnection is the “social isolation”. Moreover, sex may play a role in the responsiveness to social isolation, as previous study has reported that men were more isolated than women (Vandervoort, 2000). Rodents, also, prefer housing in a group rather than housing in an isolated state. However, less is revealed about the “where” and “how” the brain is regulating the social isolation induced changes, especially related with sociability. Moreover, the basic questions about sexual dimorphisms underlying social isolation have not been pursued.

In this chapter, I observed sex-dependent phenotypes in sociability changes after 24-hours of social isolation. Only the isolated male mice showed an increase in sociability following social isolation. In addition, I characterized the dopaminergic neurons projecting from DRN to $NAc^{sh}$ by screening the axonal projections, performing patch clamp recordings, and tracing monosynaptic connections in retrograde way. Finally, I optogenetically manipulated $DRN^{TH}$ to $NAc^{sh}$ circuit and confirmed that this neural circuit modulates isolation-induced sociability increase only in the male mice.

# EXPERIMENTAL PROCEDURES

## Animals

TH-cre male and female mice were maintained in a C57BL/6J background. Animals were housed with food and water *ad libitum* on a 12-hour light-dark cycle. For labeling TH positive neurons in DRN, I used tdTomato reporter mice. All procedures were approved by the Institutional Animal Care and Use Committee (IACUC) of Seoul National University.

## AAVs

Adeno-Associated Viruses serotype 1 were used in all the experiments of chapter 2. For optogenetic modulation of dopaminergic neurons, $pAAV_1$-Ef1a-DIO-eYFP ($1x10^9$ GC) or $pAAV_1$-Ef1a-DIO-ChR2-eYFP ($1x10^9$ GC) or $pAAV_1$-Ef1a-DIO-eNpHR-eYFP ($1x10^9$ GC) were used (Kang et al., 2015).

## Stereotaxic surgery

Both TH-cre males and females were anaesthetized with a ketamine/xylazine solution and positioned on a stereotaxic apparatus (Stoelting Co.). The virus was injected into DRN through 32gauge needle with Hamilton syringe at a rate of 0.1 μl/min and total injection volume was 1 μl. A tip of the needle was

positioned 0.05 mm below the target coordinate right before the injection for 2 minutes. After the injection, the needle stayed in place for extra 7 minutes and was withdrawn slowly (AP: -4.2/ ML: 0/ DV: -3.3). For bilateral optic cannula implantations, cannula (custom and Newdoon) was implanted 0.5mm above $NAc^{sh}$ and was held in place with dental cement (AP: +1.5/ ML: ±0.65/ DV: -4.5). Coordinates for virus injection in $NAc^{sh}$ (AP: +1.5/ ML: ±0.65/ DV-4.5).

## Behavioral task

Both male and female mice were kept in homecage after AAV injection. Each cage was moved to a new cage with new beddings at least two weeks before being group housed or social isolated. For every behavior task using optogenetics, mice were quickly put into the anesthesia chamber with isoflurane and the patch cord was connected to the optic cannula. All stranger mice were three to five weeks old with matched sex to the test mice.

For three-chamber test, habituation in the apparatus was performed for ten minutes, with laser off. After habituation period, an unfamiliar juvenile mouse was placed under one cup, and an object was placed under the other. Ten minutes of test period was performed with laser on or off.

For juvenile interaction test, the test mouse was placed in a cage with new beddings for one minute, with laser off. Then, an unfamiliar juvenile stranger mouse was introduced into the apparatus. Test period for interaction was performed for five

minutes with laser on or off.

For open field test, the test mouse was placed in the center and were left to explore the chamber for 10 minutes, with laser on or off.

## Brain clearing

SeeDB2 was followed published protocols (Ke et al., 2016). The brain sample was perfused with 4'C chilled 1x PBS and 4% paraformaldehyde in 1x PBS. Perfused brains were fixed in 4% PFA for 12 hours. Sample were sliced by vibratome into 1mm thickness for clearing. All SeeDB2 incubation procedures were performed at room temperature.

## Immunohistochemistry

Brains were post-fixed in 4% paraformaldehyde (PFA) at 4 °C overnight and transferred to 30% sucrose for 2 days at 4 °C. Brains were embedded in OCT mounting medium and sections were cut in 40 μ thick using a cryostat (Leica). For immunohistochemistry, primary antibodies rabbit anti-TH (AB152; Millipore) were diluted 1:500 in blocking solution and incubated for 24h at 4 °C. Secondary antibodies in blocking solution were incubated for 2h at room temperature, and sections were mounted with vectashield. Images were viewed under a Zeiss LSM 700 confocal microscope.

## Electrophysiology

Adult mice of both sexes were anesthetized with isoflurane and brains were quickly dissected. N-methyl-D-glucamine (NMDG) solution (93 mM NMDG, 2.5 mM KCl, 1.2 mM $NaH_2PO_4$, 30 mM, $NaHCO_3$, 20 mM HEPES, 25 mM Glucose, 5 mM sodium ascorbate, 2 mM Thiourea, 3mM sodium pyruvate, 10 mM $MgSO_4$, 0.5 mM $CaCl_2$) was used during brain slicing and recovery. Transverse slices of DRN (250 μm) or NAc (300μm) was prepared in ice-cold NMDG solution with vibratome then was recovered in 32℃ NMDG solution for 6~7 minutes. After at least 1h recovery in ACSF (124 mM NaCl, 2.5 mM KCl, 1 mM $NaH_2PO_4$, 25 mM $NaHCO_3$, 10 mM glucose, 2 mM $CaCl_2$, and 2 mM $MgSO_4$), slice was placed to the recording chamber perfused with 32℃ ACSF. To obtain reliable recordings, patched cells were stabilized for at least 3 minutes. Only cells with a change in access resistance <20% were included in the analysis. The recording pipettes (2~4 MΩ) were filled with an internal solution containing 145 mM K-gluconate, 5 mM NaCl, 10 mM HEPES, 1 mM $MgCl_2$, 0.2 mM EGTA, 2 mM MgATP, and 0.1 mM $Na_3GTP$ (280 ~ 300 mOsm, adjust to pH 7.2 with KOH). Current injections were performed in 25pA step with 500ms duration.

## Ovariectomy

Juvenile female mice (5~7 weeks of age) were ovariectomized under

subcutaneous injections of ketamine. Fallopian tubes were traced and both ovaries were removed, then the skin was sutured. For the control group, the cagemates of ovariectomized mice were selected and were performed with sham surgery. After 3 to 4 weeks of recovery in the homecage, ovariectomized group and sham group went under behavior tasks.

# RESULTS

## Sexual dimorphism in sociability is observed after 24-hours of social isolation

To examine whether 24-hours of social isolation affects sociability and to check the immediate effect of social isolation, I performed three-chamber test in two different time points; 2-hour and 24-hour. I hypothesized that if sociability is changed by 24-hour social isolation with specific circuit and synapses strengthened, the 2-hour time point will have no behavioral phenotypes since it is not yet strengthened. Moreover, I tested with male and female mice to see whether sexual differences are observed by social isolation.

When the male mice were isolated for 24-hours, significant increase in sociability was detected compared to 2-hour isolated males (Figure 5B). In contrast, the group housed males showed no changes in sociability both in 2-hour and 24-hour (Figure 5A). Strikingly, the sociability of female mice was tolerant to social isolation, both at 2-hour and 24-hour (Figure 5C and 5D).

Interestingly, in case of anxiety, social isolation induced higher anxiety only in the female mice (Figure 6A and 6C) without changes in total distance moved (Figure 6B and 6D). This results can be interpreted as sexual dimorphic effect of 24-hour social isolation, which goes together with the sex-specific effect of chronic social isolation (Huang et al., 2017).

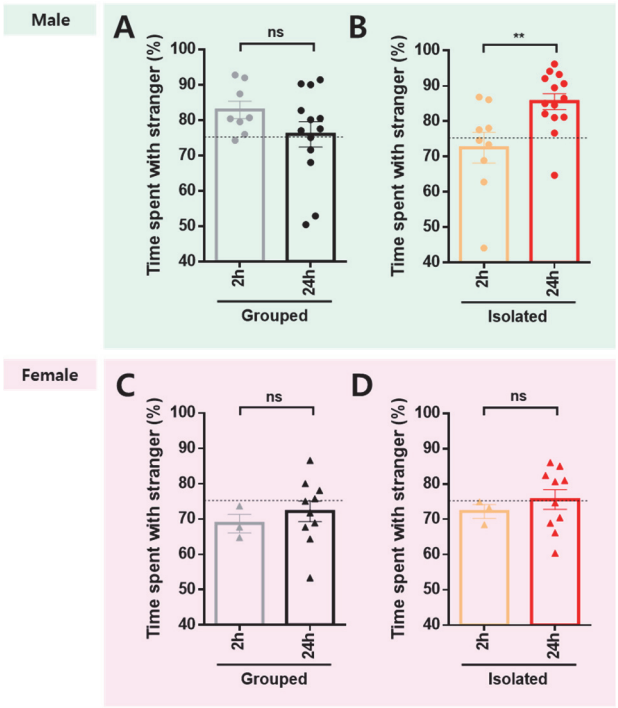


**Figure 5. Sociability changes after 2-hours or 24-hours of social isolation in male and female mice.**

(A, B) In male mice, sociability does not differ between the time of group housed. However, social interaction time was significantly increased in 24-hour isolated males than 2-hour isolated male. (Figure 5A; 2h, n=8; 24h, n=13; 2h, 82.90 ± 2.482; 24h, 75.99 ± 3.575; unpaired *t*-test; $p = 0.1818$; Figure 5B; 2h, n=9; 24h, n=14; 2h, 72.49 ± 4.351; 24h, 85.53 ± 2.221; unpaired *t*-test; $^{**}p = 0.0078$)

(C, D) In female mice, group housing nor social isolation does not alter the sociability. (Figure 5C; 2h, n=3; 24h, n=10; 2h, 68.73 ± 2.625; 24h, 72.16 ± 2.927; unpaired *t*-test; $p = 0.5570$; Figure 5D; 2h, n=3; 24h, n=10; 2h, 72.19 ± 1.938; 24h, 75.56 ± 2.776; unpaired *t*-test; $p = 0.5391$)

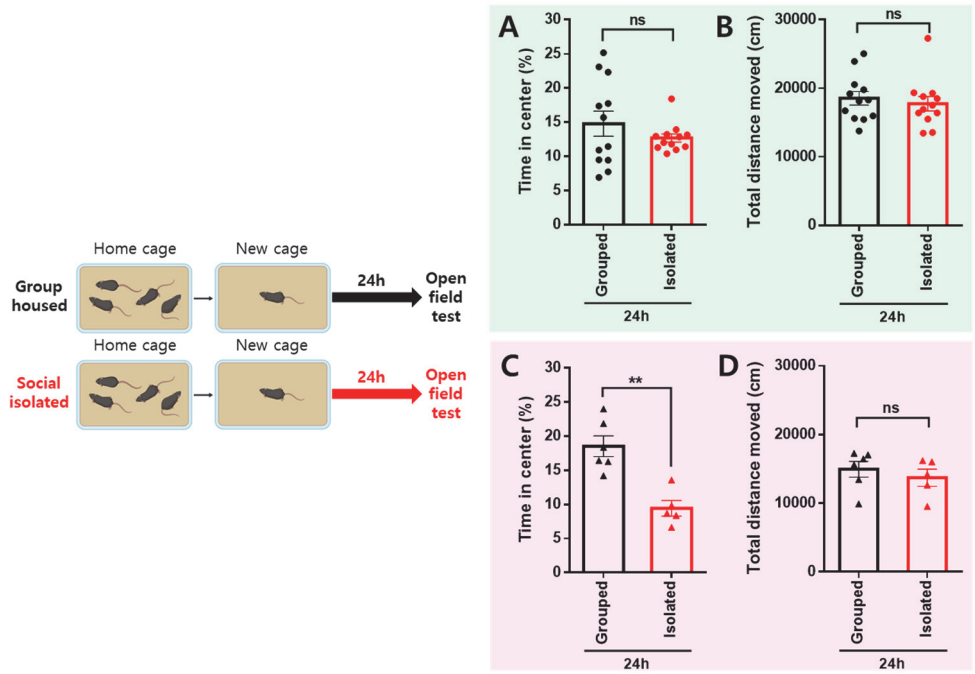


**Figure 6. The anxiety level after 24-hours of social isolation.**

(A, B) In male mice, social isolation for 24-hours did not alter the anxiety level nor the total distance moved. (Figure 6A; grouped, n=12; isolated, n=12; grouped, 14.79 ± 1.832; isolated, 12.71 ± 0.6035; unpaired *t*-test; $p = 0.2927$; Figure 6B; grouped, n=12; isolated, n=12; grouped, 18537 ± 985.6; isolated, 17745 ± 1041; unpaired *t*-test; $p = 0.5858$)

(C, D) In female mice, 24-hours after social isolation significantly increased the anxiety level with no changes in the total distance moved. (Figure 6C; grouped, n=6; isolated, n=5; grouped, 18.52 ± 1.519; isolated, 9.427 ± 1.159; unpaired *t*-test; $^{**}p = 0.0013$; Figure 6D; grouped, n=6; isolated, n=5; grouped, 14952 ± 1159; isolated, 13713 ± 1231; unpaired *t*-test; $p = 0.4836$)

## Characterization of $DRN^{TH}$ to $NAc^{sh}$ circuit.

Alterations to the dopamine system may underlie the observed male-specific sociability increase following 24-hours of social isolation. This hypothesis has been provided through various studies reporting that social isolation modulates dopaminergic neurons (Barik et al., 2013; Krishnan et al., 2007; Matthews et al., 2016). The ventral tegmental area (VTA), one of the most well-known brain region in the mesolimbic dopamine system, is intensely investigated and various functions of the VTA are being revealed. However, distinct brain region containing the dopaminergic neurons, the dorsal raphe nucleus (DRN), is yet to be discovered. Recently, the role of dopamine neurons in DRN ($DRN^{TH}$) have been receiving attention (Matthews et al., 2016), but is still a field of the unknown.

Therefore, I labeled the $DRN^{TH}$ neurons by injecting AAV-DIO-eYFP in TH-cre mouse to observe the axonal projections. Interestingly, I could detect a strong projection to the NAc (Figure 7A). Next, I examined the functional connections between $DRN^{TH}$ and $NAc^{sh}$ by performing patch clamp recording (Figure 7B). 36 out of 39 $NAc^{sh}$ neurons showed laser-induced EPSC (Figure 7C) and had an average of 50pA response (Figure 7D).

I further performed retrograde tracing to characterize the circuit. Bilateral injection of CAV-cre into the $NAc^{sh}$ in tdTomato reporter mice allowed to label the monosynaptic-connected cells from the $NAc^{sh}$ (Figure 8A). Combination with immunohistochemistry, I could discriminate the dopaminergic monosynaptic neurons with the other connections. Co-labeling of DRN slices for tyrosine

hydroxylase (TH) revealed that neurons projecting from the DRN to $NAc^{sh}$ are 42% dopaminergic (Figure 8B). The connection between DRN and $NAc^{sh}$ was similar to previous study (Ekstrand et al., 2014).

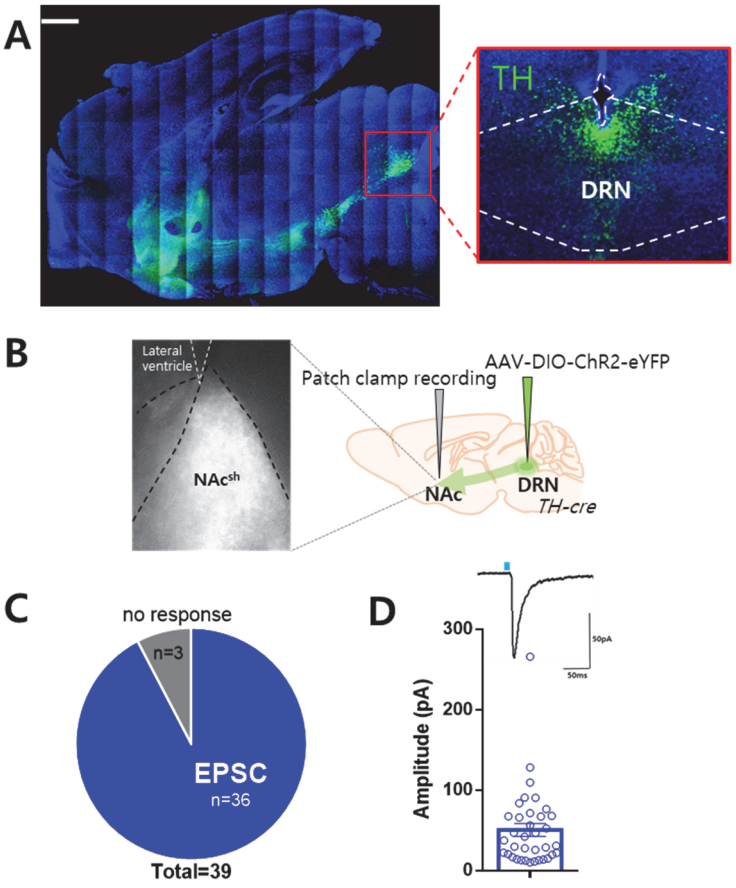


**Figure 7. Whole brain projection of DRN$^{TH}$ and the functional connection with NAc$^{sh}$ neurons.**

(A) Whole brain projection of DRN$^{TH}$ neurons and their distribution in the DRN.

(B) Experimental schema for patch clamp recording and representative image of DRN$^{TH}$ neurons labeled with ChR2-eYFP.

(C) 36 out of 39 neurons in the NAc$^{sh}$ showed light-induced EPSC responses.

(D) Example trace of light-induced peak in DRN$^{TH}$ neuron and the average amplitude. (36 cells from 7 mice)

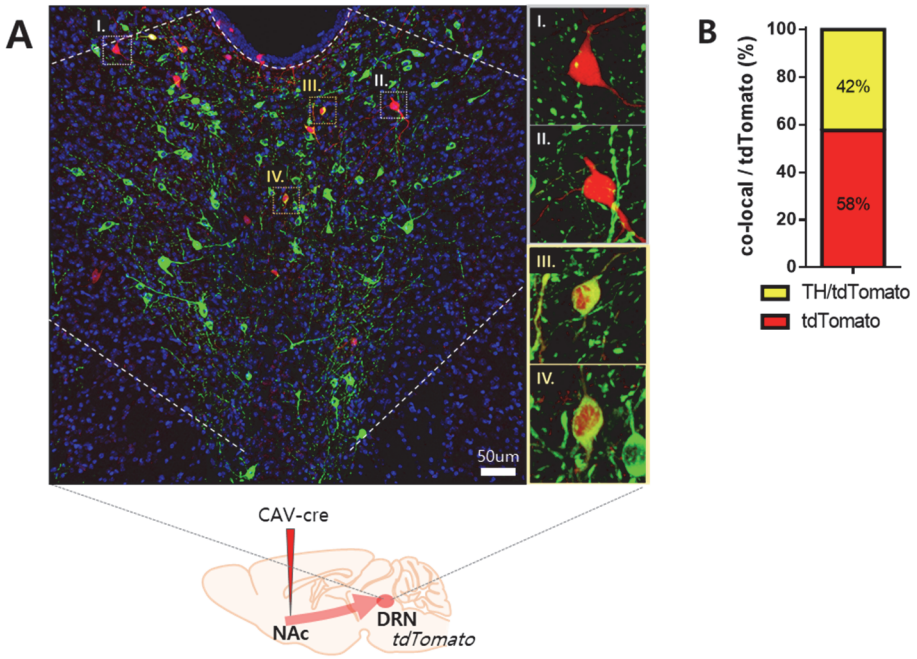


**Figure 8. Cell type characterization of DRN$^{TH}$ to NAc$^{sh}$ circuit.**

(A) Experimental scheme for labeling monosynaptic pre-connections of the NAc$^{sh}$ and the representative image of TH immunostaining in DRN slice

(B) Among the tdTomato cells that were monosynaptially labeled in the DRN, about 42% of the cells were TH positive

## Optogenetic inhibition of $DRN^{TH}$ to $NAc^{sh}$ circuit attenuates social isolation-induced sociability increase.

Socially isolated male mice showed significant increase in sociability. Therefore, I wanted to test whether modulation of the $DRN^{TH}$ to $NAc^{sh}$ circuit could change the sociability induced by isolation. To do so, I injected AAV-DIO-eYFP or AAV-DIO-eNpHR-eYFP into the DRN of TH-cre mice and implanted optic fibres bilaterally into the $NAc^{sh}$ (Figure 9A). In the male mice, terminal inhibition of $DRN^{TH}$ neurons significantly decreased the sociability increase by social isolation (Figure 9C and 9D). This behavioral change was not due to the anxiety level changes (Figure 9E). Interestingly, no changes in sociability were observed in female mice (Figure 9G and 9H). To confirm whether this optogenetic manipulation was specific to social isolation, I performed the same experiment in the group house mice. Surprisingly, the group housed male mice with $DRN^{TH}$ terminals inhibited in the $NAc^{sh}$, did not spend less time interacting with the stranger mouse (Figure 9F), by comparison to social isolated male mice in which exhibited reduced sociability (Figure 9C). Photo-inhibition of $DRN^{TH}$ neuron terminals in the $NAc^{sh}$ did not elicit alterations in the social interaction time in the female mice that were group house also (Figure 9J). Collectively, the sociability decreases by optogenetically inhibiting $DRN^{TH}$ to $NAc^{sh}$ was unique to male mice and only after social isolation. These findings suggest that social isolation-induced sociability increase and the sociability decrease by inhibition of $DRN^{TH}$ to $NAc^{sh}$ circuit show sexual dimorphism.

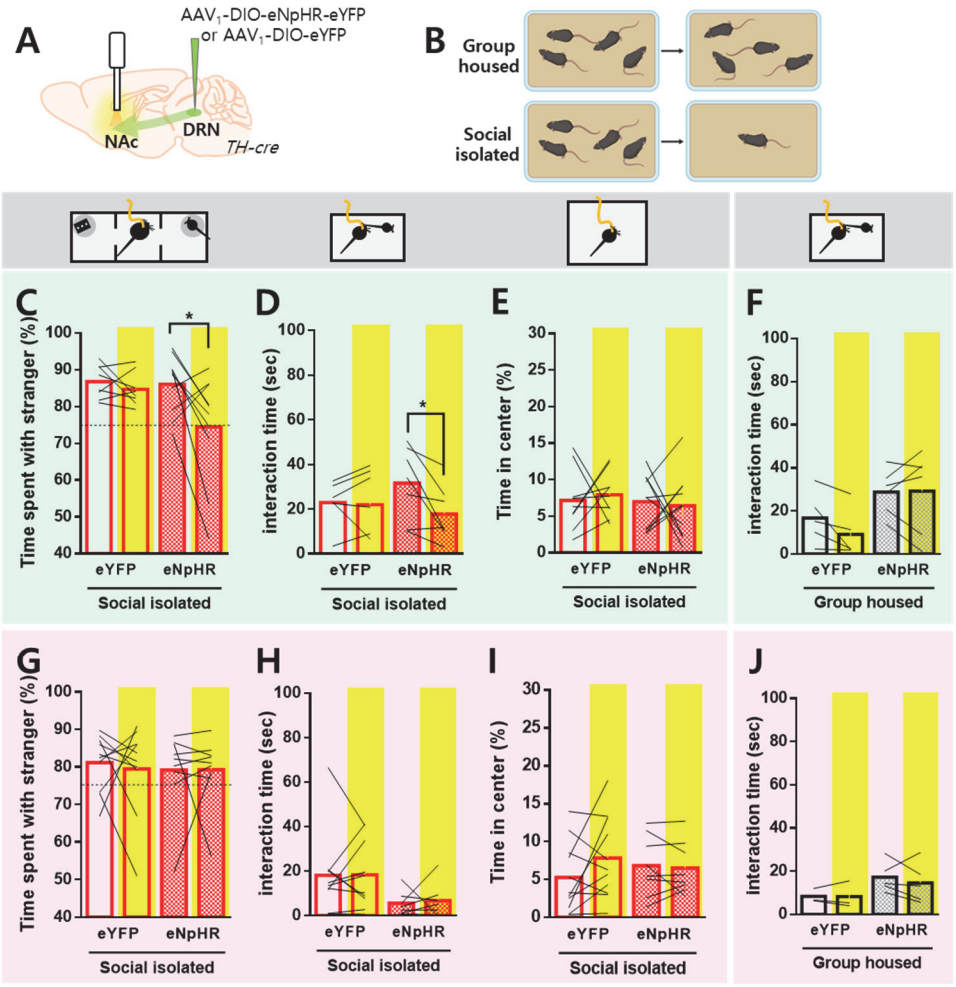


**Figure 9. Inhibition of DRN$^{TH}$ to NAc$^{sh}$ after social isolation decreases interaction time only in male mice.**

(A) Experimental schema for photo-inhibition of DRN$^{TH}$ terminals in NAc$^{sh}$.

(B) Schematic image of group housed and social isolated mice

(C, D) In socially isolated male mice, inhibition of DRN$^{TH}$ neurons projecting to the NAc$^{sh}$ significantly suppresses social interaction time in three-chamber test (C) and

juvenile interaction test (D) (Figure 9C; eYFP, n=8; paired *t*-test; $p = 0.3424$; eNpHR, n=10; paired *t*-test; $*p = 0.0410$; Figure 9D; eYFP, n=6; paired *t*-test; $p = 0.6937$; eNpHR, n=7; paired *t*-test; $*p = 0.0265$)

(E) Inhibition of $DRN^{TH}$ to NAc terminals does not alter the open field test. (eYFP, n=9; paired *t*-test; $p = 0.7110$; eNpHR, n=10; paired *t*-test; $p = 0.8053$)

(F) When group housed, inhibition of $DRN^{TH}$ to $NAc^{sh}$ does not attenuate sociability. (eYFP, n=5; paired *t*-test; $p = 0.0803$; eNpHR, n=6; paired *t*-test; $p = 0.9370$)

(G, H) Inhibition of $DRN^{TH}$ neurons projecting to the $NAc^{sh}$ does not suppresses social interaction time in socially isolated female mice, both in three-chamber test (G) and juvenile interaction test (H). (Figure 9G; eYFP, n=10; paired *t*-test; $p = 0.7231$; eNpHR, n=9; paired *t*-test; $p = 0.9905$; Figure 9H; eYFP, n=10; paired *t*-test; $p = 0.9685$; eNpHR, n=7; paired *t*-test; $p = 0.7661$)

(I) Inhibition of $DRN^{TH}$ to NAc terminals does not alter the open filed test also in female mice. (eYFP, n=11; paired *t*-test; $p = 0.1435$; eNpHR, n=8; paired *t*-test; $p = 0.6868$)

(J) $DRN^{TH}$ to NAc terminal inhibition does not change social interaction time in group housed female mice. (eYFP, n=3; paired *t*-test; $p = 0.9740$; eNpHR, n=5; paired *t*-test; $p = 0.4471$)

## Optogenetically activating the $DRN^{TH}$ to $NAc^{sh}$ circuit has no effect on social isolation-induced sociability changes.

I previously found that inhibition of $DRN^{TH}$ to $NAc^{sh}$ circuit attenuated the social interaction time only after 24-hours of social isolation. Therefore, I wanted to check whether activating the same circuit may increase the sociability following social isolation. I hypothesized that if $DRN^{TH}$-$NAc^{sh}$ circuit is specific to social isolation, the sociability of group-housed mice will not show alteration even though it is optogenetically manipulated.

I injected AAV-DIO-eYFP or AAV-DIO-ChR2-eYFP into the DRN of TH-cre mice and implanted optic fibers bilaterally into the $NAc^{sh}$ (Figure 10A). When $DRN^{TH}$ to $NAc^{sh}$ circuit was activated, surprisingly, no changes in sociability were observed following 24-hours of social isolation or group housing (Figure 10C, 10D, and 10F), contrast to the inhibition of $DRN^{TH}$-$NAc^{sh}$ (Figure 9C and 9D). Moreover, activation of $DRN^{TH}$ terminals in the $NAc^{sh}$ did not affect the anxiety (Figure 10E). In female mice, sociability and anxiety were not affected by activation of $DRN^{TH}$ to $NAc^{sh}$ circuit, both social isolated or group housed state (Figure 10G, 10H, 10I, and 10J). These results imply that artificially activating $DRN^{TH}$ to $NAc^{sh}$ circuit does not affect the sociability and the anxiety level in both sexes.

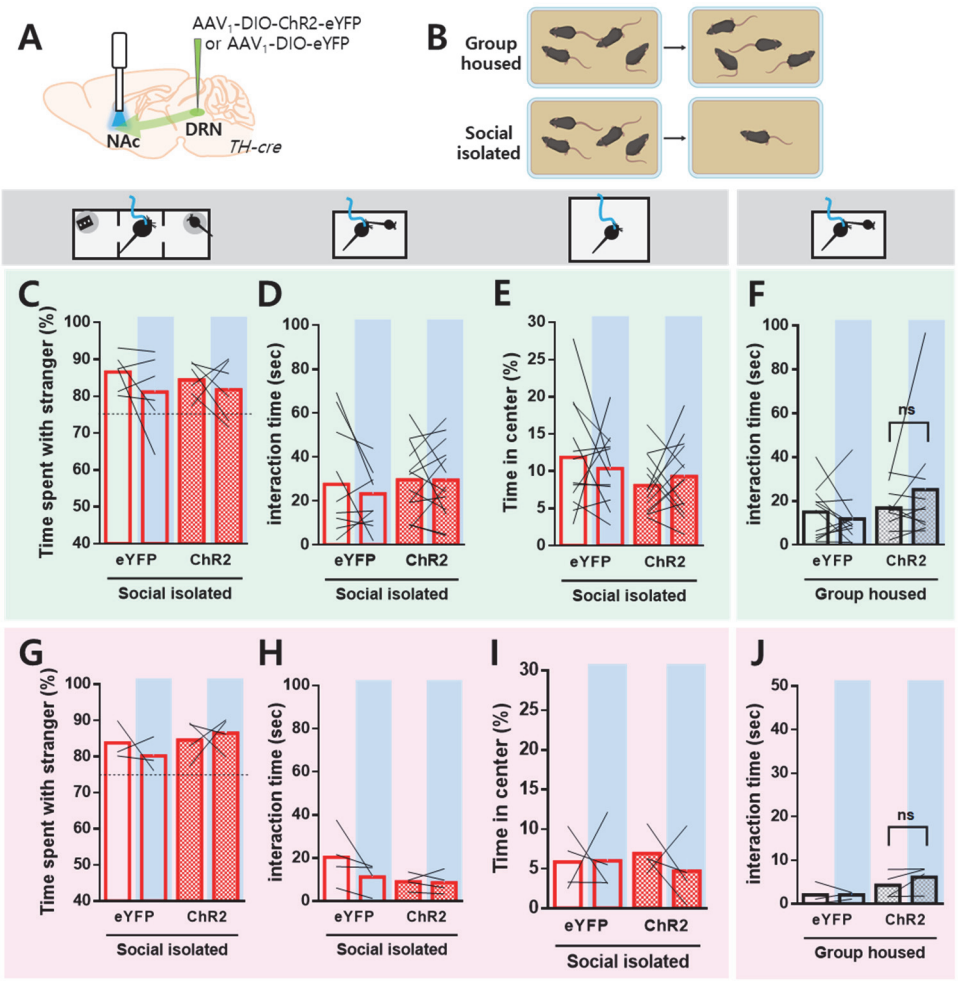


**Figure 10. Activation of DRN$^{TH}$ to NAc$^{sh}$ does not affect social interaction time.**

(A) Experimental schema for photo-activation of DRN$^{TH}$ neuron terminals in the NAc$^{sh}$.

(B) Schematic image of group housed and social isolated mice.

(C, D) In socially isolated male mice, activation of DRN$^{TH}$ neurons projecting to the NAc$^{sh}$ does not alter social interaction time in three-chamber test (C) and juvenile interaction test (D). (Figure 10C; eYFP n=6; paired *t*-test; $p$ = 0.2701; ChR2, n=6;

paired *t*-test; $p = 0.5647$; Figure 10D; eYFP n=9; paired *t*-test; $p = 0.1804$; ChR2, n=13; paired *t*-test; $p = 0.9730$)

(E) Activation of $DRN^{TH}$ to NAc terminals does not change time spent in center during open field test. (eYFP n=12; paired *t*-test; $p = 0.5659$; ChR2, n=13; paired *t*-test; $p = 0.4937$)

(F) In group-housed male mice, activation of $DRN^{TH}$ neurons projecting to the $NAc^{sh}$ does not affect sociability. (eYFP n=12; paired *t*-test; $p = 0.4309$; ChR2, n=10; paired *t*-test; $p = 0.2673$)

(G, H, I) In socially isolated female mice, activation of $DRN^{TH}$ to $NAc^{sh}$ circuit does not alter social interaction time in three-chamber test (G) and juvenile interaction test (H). Moreover, the anxiety was not change (I). (Figure 10G; eYFP n=3; paired *t*-test; $p = 0.5677$; ChR2, n=4; paired *t*-test; $p = 0.7286$; Figure 10H; eYFP n=4; paired *t*-test; $p = 0.2055$; ChR2, n=4; paired *t*-test; $p = 0.8370$; Figure 10I; eYFP n=4; paired *t*-test; $p = 0.9695$; ChR2, n=4; paired *t*-test; $p = 0.5059$)

(J) In group housed female mice, activation of $DRN^{TH}$ neurons projecting to the $NAc^{sh}$ does not alter social interaction time. (eYFP n=3; paired *t*-test; $p > 0.9999$; ChR2, n=4; paired *t*-test; $p = 0.2133$)

## Female sex hormones are not related with unchanged isolation-induced sociability in the female mice.

24-hour isolated female mice did not show alterations in sociability and were not further modulated by optogenetic-inhibition nor activation.

Sexual dimorphisms exist from brain anatomy (Ruigrok et al., 2014) to psychological processes and in various neurological disorders (Bálint et al., 2009; Gillberg et al., 2006; Wooten et al., 2004). One cause of sex differences has been explained by the actions of sex hormones in females (Gillies and McArthur, 2010; Riecher-Rössler et al., 1994). The estradiol, a major female sex hormone which is an estrogen steroid hormone, is known to affect dopaminergic function differently in brain regions of the female mice. For example, estradiol increases dopamine release in the striatum, inhibits dopaminergic activity in the NAc, modulates dopamine synthesis and inhibits dopaminergic effects in anterior pituitary (Becker, 1999; Bourque et al., 2012; Raymond et al., 1978). Due to these complexities and diversity of dopamine's regulation in the females, I wanted to check whether female sex hormones were the cause of unchanged isolation-induced sociability.

To further investigate sexual dimorphism in social isolation, I used ovariectomized (OVX) females to see whether female sex hormones may be a contributing factor to male-specific phenotypes in social isolation. Five to six-weeks old females were ovariectomized and three-chamber test was performed at least three weeks after (Figure 11A). The sociability level was comparable between isolated

OVX females and isolated sham-control females. Moreover, no effect was detected also in the group-housed females (Figure 11B). These findings demonstrate that sexual dimorphism following social isolation is not via female sex hormones.

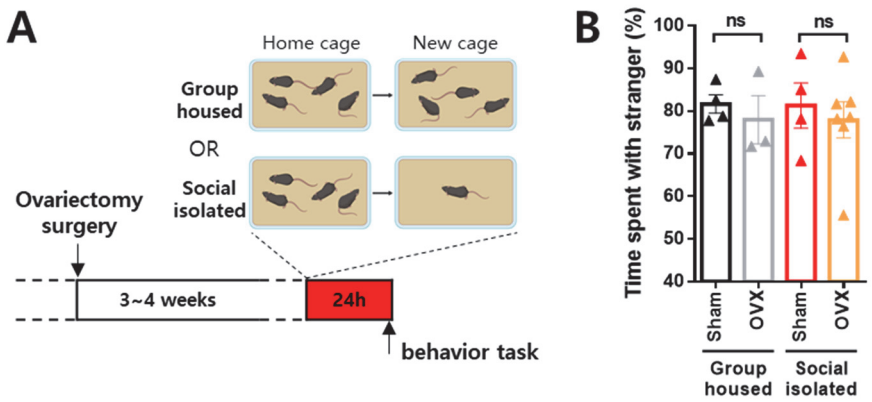


**Figure 11. Female sex hormones do not affect social-isolation-induced sociability.**

(A) Behavioral schematics for ovariectomized- and sham-females.

(B) Ovariectomized females did not show any sociability alterations with sham-control females, both in group-housed and social-isolated state. (Group housed sham, n=4, 81.65 ± 2.187; Group housed OVX, n=3, 77.98 ± 5.659; unpaired *t*-test; $p = 0.5257$; Social isolated sham, n=4, 81.29 ± 5.311; Social isolated OVX, n=7, 77.92 ± 4.230; unpaired *t*-test; $p = 0.6362$)

# DISCUSSION

It is widely accepted that social isolation is a serious issue for social animals. Despite its great significance, previous studies mainly focused on chronic effect of social isolation and did not perceive on the sexual differences. In this chapter, I observed sexual dimorphic alterations in social behaviors in response to 24-hour social isolation. Male-specific sociability increase was detected after 24-hours of social isolation. In contrast, isolated females showed an increase in anxiety level rather than increased sociability. By utilizing optogenetic tools, I found that isolation-induced sociability increase was modulated by $DRN^{TH}$ to $NAc^{sh}$ circuit in a sex dependent manner. Furthermore, I found that this sexual dimorphism following social isolation is not by way of female sex hormones. In sum, these results suggest that social isolation has different effects on sociability in male and female mice.

Sexual dimorphism occurred after being social isolated for 24 hours. It is reported that brain regions related with social behavior express various subtypes of estrogen receptor (Nelson and Trainor, 2007). DRN do not show sex difference in the number of estrogen receptor (Sagoshi et al., 2020).

Matthews et al. have shown that $DRN^{TH}$ neurons show calcium activity in response to social interaction in which is more heightened after 24-hour social isolation (Matthews et al., 2016). Thus, although $DRN^{TH}$ responses to social isolation, the precise downstream circuit and the underlying mechanisms remain unspecified. I found that social isolation triggers sociability changes differently between males and females and further narrowed down the mechanism to neural circuit level.

# CHAPTER III

## Social-isolation-activated neuronal ensembles of $DRN^{TH}$ and their synaptic connectivity are necessary for sociability changes by social isolation

# INTRODUCTION

In the previous chapter, I found male-specific isolation-induced sociability increase and the dopaminergic afferents from the DRN to the $NAc^{sh}$ are modulating isolation-induced sociability changes. By narrowing down the neural population from total population to the "isolation-activated" neuronal ensembles, I further investigated the sociability following social isolation. I hypothesized that the isolation-activated neurons will be necessary for the isolation-induced sociability increase. To test this possibility, I used IEG-based tagging tools combined with DREADD (designer receptors exclusively activated by designer drug) system to specifically manipulated the isolation-activated neurons.

In this chapter, I investigated the isolation-activated neurons through chemogenetics, patch clamp recording and dual-eGRASP. Inhibition of isolation-activated $DRN^{TH}$ neurons resulted in attenuation of sociability, which reversed the sociability down to the levels of group-housed. Interestingly, when I inhibited the group-house-activated $DRN^{TH}$ neurons, no changes in sociability was observed. Furthermore, I found a higher neural excitability in the isolation-activated $NAc^{sh}$ neurons. Finally, I used dual-eGRASP to examine the synapses between isolation-activated $DRN^{TH}$ cells and $NAc^{sh}$ cells and found an increase in spine density. In summary, these results imply that the isolation-activated neural ensembles in $DRN^{TH}$ and $NAc^{sh}$ are strengthened from the synaptic level during 24-hours of social

isolation, thus increasing the sociability. Therefore, I inhibited neural activation of $DRN^{TH}$ during 24-hours of being isolated and could attenuate isolation-induced sociability increase. Activity of $DRN^{TH}$ neurons during isolation is required for isolation-induced sociability increase.

Through all the data, I found that the activated neuronal ensembles and the synaptic strengthening between them are necessary for the sociability increase following social isolation.

# EXPERIMENTAL PROCEDURES

## Animals

TH-cre male and female mice were maintained in a C57BL/6J background. Animals were housed with food and water *ad libitum* on a 12-hour light-dark cycle. For labeling TH positive neurons in DRN, I used tdTomato reporter mice. All procedures were approved by the Institutional Animal Care and Use Committee (IACUC) of Seoul National University.

## AAVs

Adeno-Associated Viruses serotype 1/2 (AAV1/2; AAV particle that contains both serotype 1 and 2 capsids) were used in all the experiments of chapter three. For chemogenetic modulation of dopaminergic neurons, $pAAV_{1/2}$-TRE3G-DIO-hM4Di-mCherry ($1x10^9$ GC) or $pAAV_{1/2}$-Ef1a-DIO-hM4Di-mCherry ($1x10^9$ GC) were used. For patch clamp recording, the activated neurons were labeled with $pAAV_{1/2}$-TRE3G-mEmeraldNuc ($1x10^8$ GC). All dual-eGRASP virus cocktails were identical or slightly modified from previously described (Choi et al., 2018).

## Stereotaxic surgery

Both TH-cre males and females were anaesthetized with a ketamine/xylazine solution and positioned on a stereotaxic apparatus (Stoelting Co.). The virus was injected through 32gauge needle with Hamilton syringe at a rate of 0.1 μl/min and total injection volume was 1 μl. A tip of the needle was positioned 0.05 mm below the target coordinate right before the injection for 2 minutes. After the injection, the needle stayed in place for extra 7 minutes and was withdrawn slowly. Stereotaxic coordinates for each target sites were: Nucleus accumbens (AP: +1.5/ ML: ±0.65/ DV: -4.5), Dorsal raphe nuclei (AP: -4.2/ ML: 0/ DV: -3.3).

## Behavioral task

Both male and female mice were kept in homecage after AAV injection. Cagemates were moved to a new cage with new beddings at least two weeks before being group housed or social isolated. On the day of group housing or social isolating, 250 μl of 5 mg/ml doxycycline solution dissolved in saline was injected by intraperitoneal injection during brief anesthesia by isoflurane (Choi et al., 2018). All stranger mice were three to five weeks old with matched sex to the test mice.

For three-chamber test, habituation in the apparatus was performed for ten minutes, with laser off. After habituation period, an unfamiliar juvenile mouse was placed under one cup, and an object was placed under the other. Ten minutes of test period was performed.

For open field test, the test mouse was placed in the center and were left to

explore the chamber for 10 minutes.

## Chemogenetic manipulations

The designer drug clozapine-*N*-oxide (CNO, 10mg/kg, i.p. ; Sigma) was administered 40 minutes before behavioral tasks. For electrophysiology, 5uM of CNO was used and the effect was measured 10 minutes after CNO perfusion.

## Immunohistochemistry

Brains were post-fixed in 4% paraformaldehyde (PFA) at 4 °C overnight and transferred to 30% sucrose for 2 days at 4 °C. Brains were embedded in OCT mounting medium and sections were cut in 40 µ thick using a cryostat (Leica). For immunohistochemistry, primary antibodies rabbit anti-TH (AB152; Millipore) and rabbit anti-c-fos (sc-52; Santa Cruz, 226003; SySy) were diluted 1:500-1:1000 in blocking solution and incubated for 24h at 4 °C. Secondary antibodies in blocking solution were incubated for 2h at room temperature, and sections were mounted with vectashield. Images were viewed under a Zeiss LSM 700 confocal microscope.

## Electrophysiology

Adult mice of both sexes were anesthetized with isoflurane and brains were

quickly dissected. N-methyl-D-glucamine (NMDG) solution (93 mM NMDG, 2.5 mM KCl, 1.2 mM $NaH_2PO_4$, 30 mM, $NaHCO_3$, 20 mM HEPES, 25 mM Glucose, 5 mM sodium ascorbate, 2 mM Thiourea, 3mM sodium pyruvate, 10 mM $MgSO_4$, 0.5 mM $CaCl_2$) was used during brain slicing and recovery. Transverse slices of DRN (250 μm) or NAc (300μm) was prepared in ice-cold NMDG solution with vibratome then was recovered in 32℃ NMDG solution for 6~7 minutes. After at least 1h recovery in ACSF (124 mM NaCl, 2.5 mM KCl, 1 mM $NaH_2PO_4$, 25 mM $NaHCO_3$, 10 mM glucose, 2 mM $CaCl_2$, and 2 mM $MgSO_4$), slice was placed to the recording chamber perfused with 32℃ ACSF. To obtain reliable recordings, patched cells were stabilized for at least 3 minutes. Only cells with a change in access resistance <20% were included in the analysis. The recording pipettes (2~4 MΩ) were filled with an internal solution containing 145 mM K-gluconate, 5 mM NaCl, 10 mM HEPES, 1 mM $MgCl_2$, 0.2 mM EGTA, 2 mM MgATP, and 0.1 mM $Na_3GTP$ (280 ~ 300 mOsm, adjust to pH 7.2 with KOH). Current injections were performed in 25pA step with 500ms duration.

## Sample preparation and confocal imaging for dual-eGRASP

Perfused brains were fixed with 4% PFA in phosphate buffered saline (PBS) overnight at 4℃, and dehydrated in 30% sucrose in PBS for 2 days at 4℃. Brains were sliced by Cryostat into 50μm section for dual-eGRASP analysis. Sections were mounted in VECTASHIELD mounting medium (Vector Laboratories, H-1000). For dual-eGRASP analysis, NAc dendrites were imaged in Z-stack by Leica SP8

confocal microscope with 63x objective with distilled water immersion.

## Image analysis for dual-eGRASP

Processing of confocal image and 3D reconstruction of dendrites were performed using Imaris (Bitplane, Zurich, Switzerland) software. Before analysis all image samples were blinded for exclude any bias. Each mScarlet-I-positive or iRFP670-positive dendrite was marked as a filament manually while hiding other fluorescent signals, and each cyan or yellow eGRASP signal was marked as cyan or yellow sphere through IMARIS automatic detection. Cyan eGRASP and yellow eGRASP puncta on dendrites were manually counted and overlapped cyan and yellow eGRASP signals was considered as yellow signal since the presynaptic neuron of the synapse is c-fos-positive dopaminergic neuron during social isolation. Dendrites without any cyan eGRASP or mScarlet-I, iRFP670-overlapping dendrites were ruled out for more precise analysis.

# RESULTS (Collaborated with Dong Il Choi)

## Social-isolation-activated DRN$^{TH}$ neurons are necessary for sociability increase by isolation.

To assess the necessity of DRN$^{TH}$ activity for social-isolation driven sociability increase, I wanted to specifically manipulate the activated dopaminergic neurons. Thus, I combined chemogenetics with IEG-based tagging system.

I used reverse tetracycline-controlled transactivator (rtTA) under Fos promoter to express hM4Di in the activated dopaminergic neurons in doxycycline-dependent manner (Haasteren et al., 2000; Loew et al., 2010; Reijmers et al., 2007; Zhou et al., 2006). Cre-dependent hM4Di-mCherry was injected into the DRN of TH-cre mice. After 4 weeks of virus expression, the mice underwent 24-hours of social isolation with doxycycline injected (Figure 12A). Then I confirmed the function of hM4Di by patch clamp recording the hM4Di-mCherry expressing neurons. As expected, the neural firing was inhibited by CNO treatment (Figure 12B). Therefore, I could conclude that 24-hour was enough to express functional hM4Di.

Then, I used this chemogenetics and IEG-based labeling system to specifically manipulate the isolation-activated DRN$^{TH}$ neurons. Mice were socially isolated and doxycycline injected simultaneously. After 24-hours, I injected CNO or saline and three-chamber test was performed 40 minutes after (Figure 13A). Inhibition of social-isolation-activated DRN$^{TH}$ neurons attenuated the sociability to

the baseline levels of interaction (Figure 13B) with no changes in velocity and total distance moved (Figure 13C and 13D). Furthermore, I analyzed the activation ratio by labeling tyrosine hydroxylase in the hM4Di-mCherry expressed DRN slice. About 15% of $DRN^{TH}$ neurons were expressed with hM4Di (Figure 13E), indicating that this activated population of $DRN^{TH}$ neurons are necessary for mediating the increase in social isolation.

In order to confirm that this result drawn out from isolation-activated neurons, I performed the same experiment with group-house-activated neurons (Figure 14A). If it is specific to social isolation, inhibiting the group-house-activated neurons will have no effect on sociability. Strikingly, I found no alterations in sociability and anxiety when group-house-activated $DRN^{TH}$ neurons were inhibited (Figure 14B, 14C, 14D and 14E). Therefore, I concluded that DRN dopaminergic neural ensembles which are activated by social isolation is critical for the sociability increase.

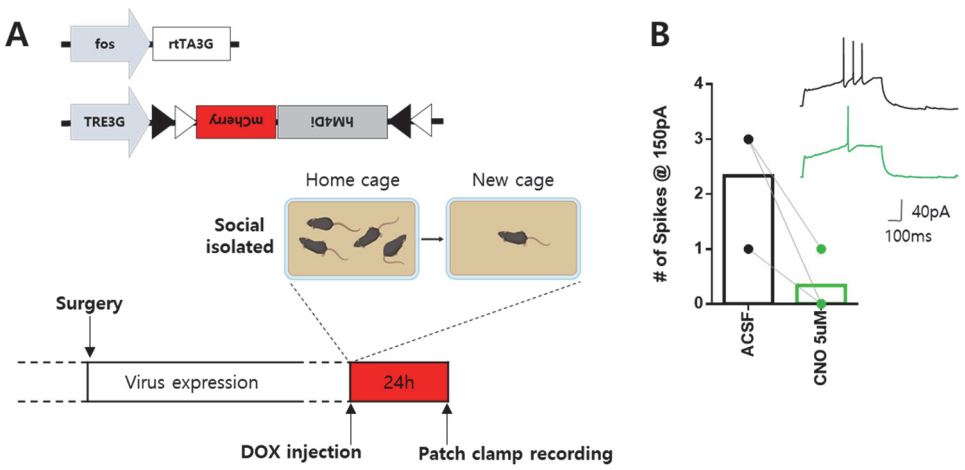


**Figure 12. 24-hour induction of hM4Di is functional.**

(A) Experimental scheme for labeling the isolation-activated $DRN^{TH}$ neurons.

(B) When perfused with CNO, hM4Di expressing neurons showed decreased excitability.

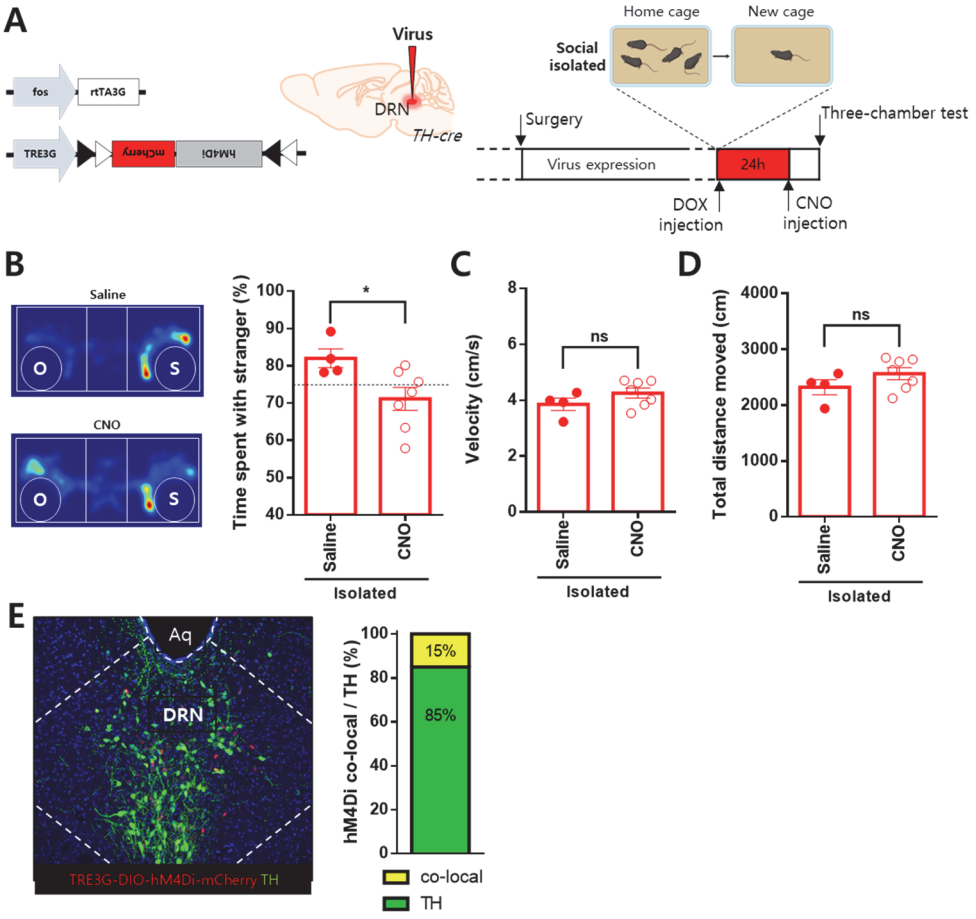


**Figure 13. Isolation-activated dopaminergic neurons in the DRN are essential for increase in isolation-induced sociability.**

(A) Schematic image of virus injection and behavior scheme.

(B) Heat maps illustrating the three-chamber test that underwent inhibition of isolation-activated population through CNO (left, upper) or saline-treated control (left, bottom). The effect of chemogenetically inhibiting isolation-activated $DRN^{TH}$ neurons. CNO treated isolated male mice showed significant decrease in sociability. (Saline, N=4; 82.01 ± 2.515; CNO, N=7; 71.13 ± 3.071; unpaired *t*-test; $*p = 0.0400$)

(C, D) Inhibition of isolation-activated $DRN^{TH}$ neurons did not change the velocity (C) and the total distance moved (D). (Figure 13D; Saline, N=4; 3.855 ± 0.2220; CNO, N=7; 4.256 ± 0.1755; unpaired *t*-test; $p = 0.1958$; Figure 13E; Saline, N=4; 2321 ± 133.8; CNO, N=7; 2563 ± 106.1; unpaired *t*-test; $p = 0.1959$)

(E) Representative image of hM4Di-mCherry expression in dopaminergic neurons of the DRN. Among the $DRN^{TH}$ neurons, 15% were activated by social isolation. 5 slices from each mouse, data from 3 mice.

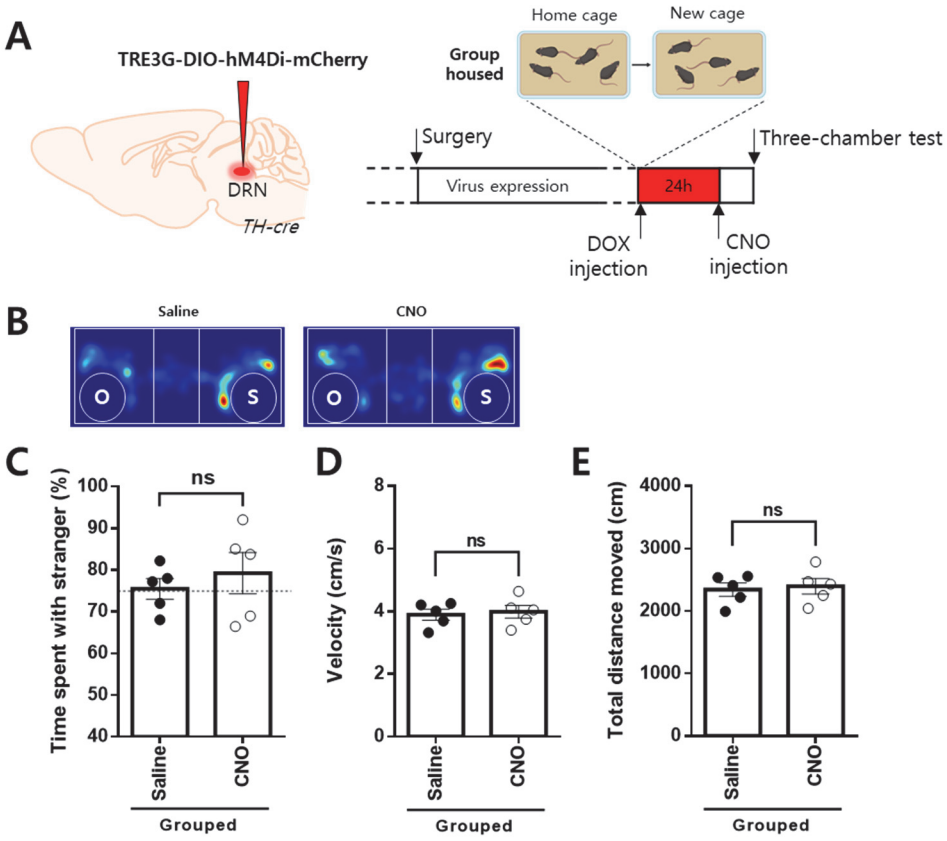


**Figure 14. Inhibition of group-house-activated dopaminergic neurons in the DRN do not alter the sociability.**

(A) Schematic image of virus injection and behavior scheme.

(B) Heat maps illustrating the three-chamber test that underwent inhibition of group-house-activated population through CNO (right) or saline-treated control (left).

(C) No changes in sociability was detected when group-housed-activated $DRN^{TH}$ neurons were chemogenetically inhibited. (Saline, n=5; 75.48 ± 2.473; CNO, n=5; 79.23 ± 4.934; unpaired *t*-test; $p = 0.5160$)

(D, E) Inhibiting the group-house-activated $DRN^{TH}$ neurons did not change the velocity (D) and the total distance moved (E). (Figure 14D; Saline, n=5; 3.896 ± 0.1748; CNO, n=5; 3.989 ± 0.2052; unpaired *t*-test; $p = 0.7389$; Figure 14E; Saline, n=5; 2343 ± 106.1; CNO, n=5; 2396 ± 123.3; unpaired *t*-test; $p = 0.7503$)

## Isolation-activated NAc$^{sh}$ neurons show higher excitability.

I investigated whether sexual differences are detected in the neuronal excitability of the isolation-induced fos positive neurons. Excitability is one of intrinsic properties of neurons, in which sets the threshold for action potential firing and modulates synaptic transmission (Hille, 1978). By using Fos-rtTA system, I selectively labeled the activated neurons with nucleus-targeted mEmerald (mEmeraldNuc), in which the fluorescence protein was driven by the TRE3G promoter controlled by Fos promoter-driven rtTA3G (Figure 15A). In the isolated male, mEmeraldNuc positive neurons were significantly more excitable compared with mEmeraldNuc negative neurons (Figure 15B). However, although isolation-induced fos expression was also observed in the isolated female mice, the excitability of mEmeraldNuc positive cells was comparable to the mEmeraldNuc negative cells' excitability (Figure 15C). I again detected sexual dimorphism, in which the increased excitability was shown only in the socially isolated male mice. Another interesting point is that the relationship between the fos-expressing neurons and their excitability do not always correlate, since the isolation-activated neurons in the females did not show an increase in excitability.

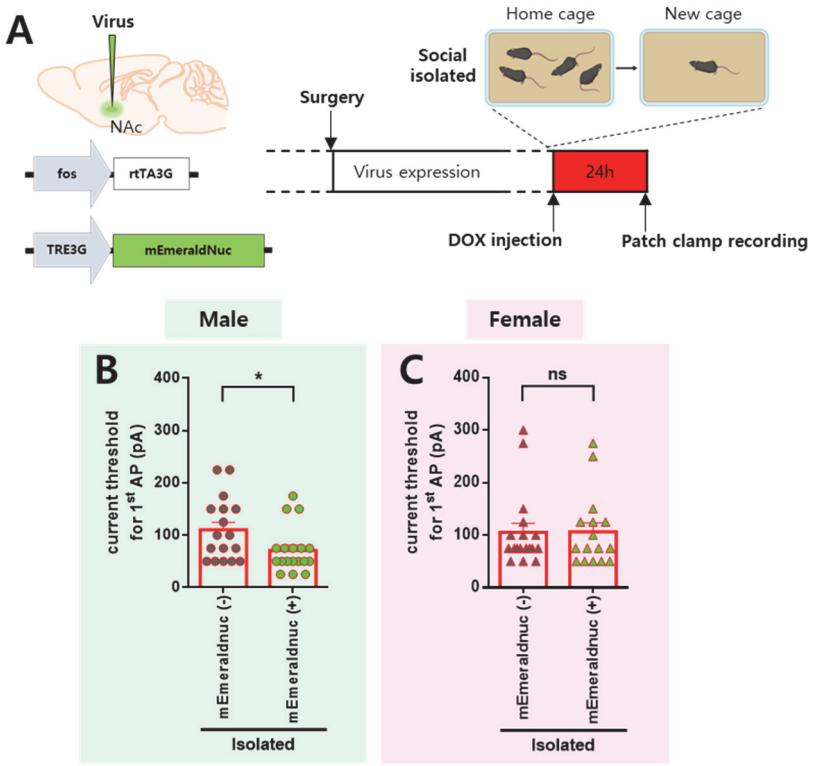


**Figure 15. Only in the male mice, the neuronal excitability of isolation-activated NAc$^{sh}$ neurons are more excitable than the non-activated NAc$^{sh}$ neurons.**

(A) Experimental scheme of labeling the isolation-activated NAc$^{sh}$ neurons.

(B) In the isolated male mice, the current threshold for the 1$^{st}$ action potential to appear is significantly lower in the mEmeraldNuc positive neurons. (mEmeraldNuc negative neurons, n=17 from 3 mice; mEmeraldNuc positive neurons, n=18 from 3 mice; mEmeraldNuc negative neurons, 110.3 ± 14.55; mEmeraldNuc positive neurons, 70.83 ± 10.36; unpaired *t*-test; *$p$ = 0.0327)

(C) In the isolated female mice, mEmeraldNuc positive and negative neurons

showed comparable current threshold for the 1st action potential. (mEmeraldNuc negative neurons, n=18 from 3 mice; mEmeraldNuc positive neurons, n=16 from 3 mice; mEmeraldNuc negative neurons, 105.6 ± 16.73; mEmeraldNuc positive neurons, 106.3 ± 17.31; unpaired *t*-test; $p = 0.9772$)

## Optimization of Dual-eGRASP in $DRN^{TH}$ to $NAc^{sh}$ circuit.

Through previous results in this chapter, Fos-rTA system was confirmed to capture the activated neurons in group housed or social isolated mice. Therefore, I further applied this system to study the synaptic connectivity between the activated neuronal ensembles. I hypothesized that social isolation will alter DRN dopaminergic circuitry to the $NAc^{sh}$ for driving isolation-induced sociability increase. In order to capture the synapses of activated $DRN^{TH}$ neurons to activated $NAc^{sh}$ neurons, I modified the previous virus strategy of dual-eGRASP (Choi et al., 2018).

Since the dopaminergic neurons, a specific cell type, in the DRN should be labeled, I used TH-cre mice. Pre-eGRASP was expressed Cre-dependently in the DRN, with yellow pre-eGRASP in activated dopaminergic neurons and cyan pre-eGRASP in non-activated dopaminergic neurons (Figure 16A and 16B). Yellow pre-eGRASP was driven by the TRE3G promoter controlled by Fos promoter-driven rtTA3G and cyan pre-eGRASP was driven by the EF1α promoter. Post-eGRASP was expressed bilaterally in $NAc^{sh}$, with myristoylated mScarlet-I in activated cells and myristoylated iRFP670 in non-activated cells (Figure 16A and 16B). Myristoylated mScarlet-I was driven by the TRE3G promoter controlled by Fos promoter-driven rtTA3G. Myristoylated iRFP670 was driven by the human synapsin (hSyn) promoter further with CaMKIIα promoter-driven FLPO in order to achieve the cre-out system (Jung et al., 2019). Consequently, I could specifically label the isolation-activated synapses in yellow eGRASP and isolation-non-activated synapses in cyan eGRASP, in which are on isolation-activated $NAc^{sh}$ neurons and isolation-non-activated $NAc^{sh}$

neurons (Figure 16C and 16D).

To validate the expression specificity of yellow pre-eGRASP in Fos-rTA system, I checked the yellow eGRASP expression in a doxycycline-dependent manner. Yellow eGRASP puncta were only observed in doxycycline injected mice which implicates a precise control of expression (Figure 17A and 17B).

Based on the optimized conditions, I performed quantitative analysis by reconstructing 3D models through IMARIS program (Figure 18A). $NAc^{sh}$ dendrites were represented as filaments; myristoylated mScarlet-I dendrites as red filaments and myristoylated iRFP670 dendrites as gray filaments. Yellow eGRASP and cyan eGRASP puncta were marked as yellow sphere and cyan sphere, respectively. Thus, yellow sphere on red dendrite means a synapse between activated $DRN^{TH}$ and activated $NAc^{sh}$ neurons. Analyzing methods were identical to the previous research (Choi et al., 2018).

Therefore, all conditions, from virus constructs to imaging analysis, were optimized for combination with social isolation.

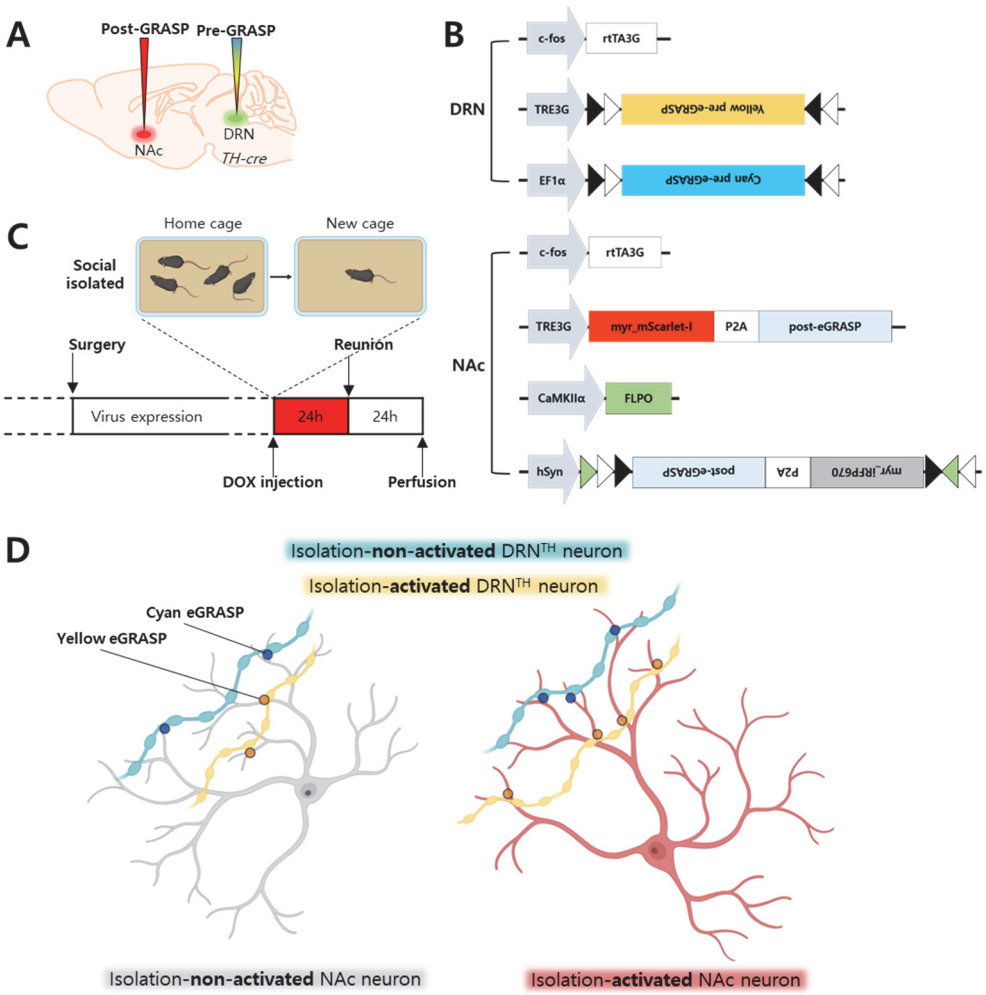


**Figure 16. Strategy to compare the synapses between isolation-activated DRN$^{TH}$ and NAc$^{sh}$ neurons using dual-eGRASP.**

*(in collaboration with Dong Il Choi)*

(A) Experimental scheme for virus injection sites.

(B) Illustration of AAV constructs and the combinations used for DRN and NAc.

(C) Timeline of experimental protocol to label synapses with dual-eGRASP.

(D) Illustration of four types of synapses between $DRN^{TH}$ and $NAc^{sh}$ neurons. Isolation-non-activated NAc neurons are drawn in gray and isolation-activated NAc neurons are drawn in red. The cyan eGRASP signals are represented in cyan circles, in which the synapses are from isolation-non-activated $DRN^{TH}$ neurons. The yellow eGRASP signals are pictured in yellow circles, in which the synapses are from isolation-activated $DRN^{TH}$ neurons.

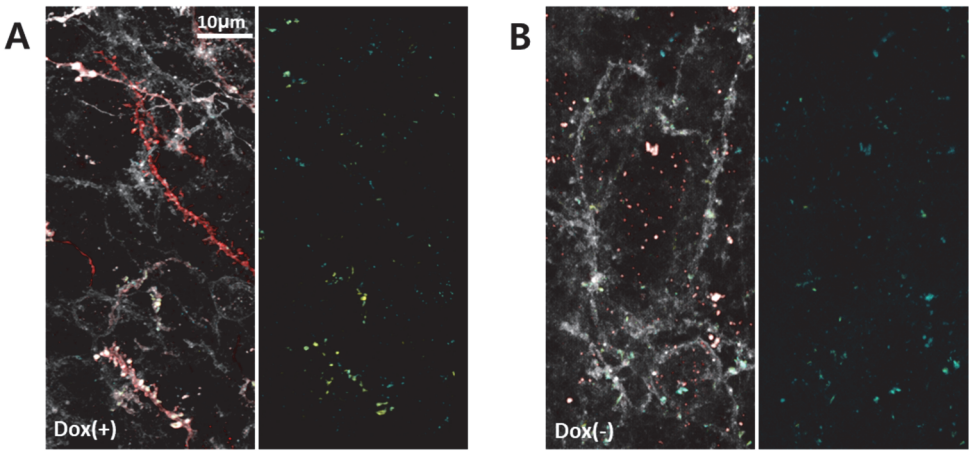


**Figure 17. Validation of Fos-rtTA induced dual-eGRASP system through doxycycline.**

*(in collaboration with Dong Il Choi)*

(A, B) Representative images of cyan eGRASP and yellow eGRASP signals with doxycycline i.p. (A) and without doxycycline i.p. (B).

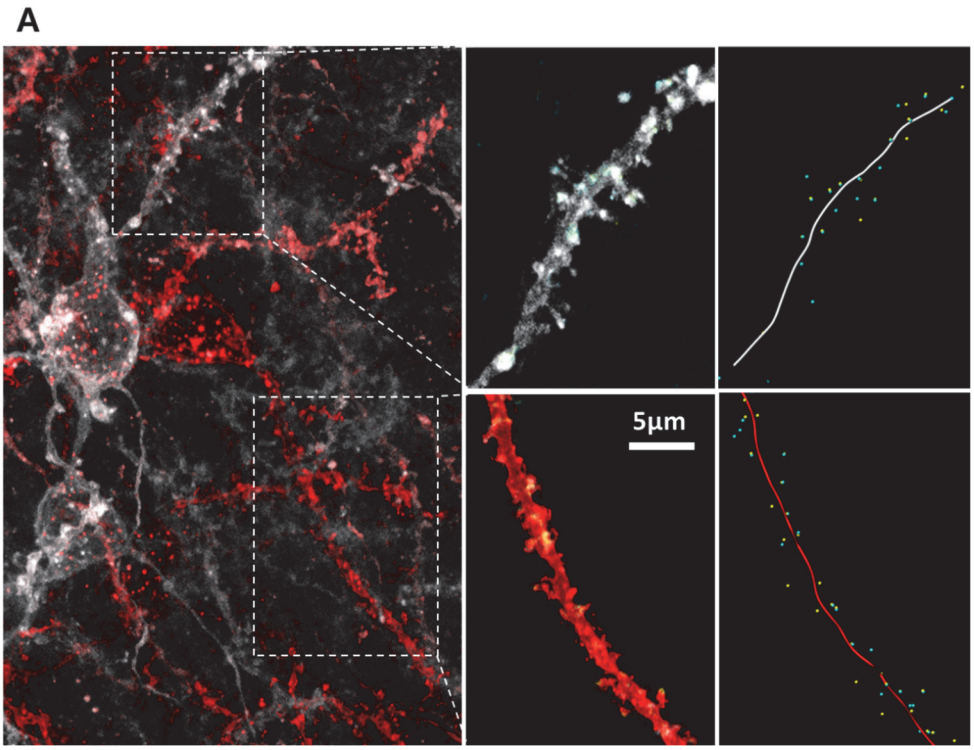


**Figure 18. Representative images of 3D modeling for analysis.**

*(in collaboration with Dong Il Choi)*

(A) All reconstructions were produced through IMARIS. $NAc^{sh}$ dendrites were reconstructed as filaments, myristoylated mScarlet-I dendrites into red filaments and myristoylated iRFP670 dendrites into gray filaments. Yellow eGRASP and cyan eGRASP puncta were marked as yellow sphere and cyan sphere, respectively.

## Male-specific increase of synaptic density between isolation-activated $DRN^{TH}$ and $NAc^{sh}$ neurons.

First, I checked whether the number of isolation-activated neurons were increased compared to the number of group-housed-activated neurons. Interestingly, social isolation did not induce an increase in the number of activated neurons in $DRN^{TH}$ and $NAc^{sh}$ of both sexes (Figure 19A and 19B).

Next, I investigated whether synaptic changes were observed when mice were socially isolated for 24 hours. I injected pre-eGRASP virus cocktails into the DRN of TH-cre mice and post-eGRASP virus cocktails bilaterally into the $NAc^{sh}$ (Figure 16A, 16B, 16C and 20A). Surprisingly, the spine density was significantly increased by social isolation in the male mice (Figure 20D). In contrast, strikingly, the isolated female mice did not show any increased spine density (Figure 20E). These synapse-level results were consistent with all the previous data in this study, suggesting the synaptic involvement of $DRN^{TH}$-$NAc^{sh}$ circuit in sexual dimorphism following social isolation. Importantly, this dual-eGRASP data go together with the electrophysiological results (Figure 15B and 15C) in which the excitability of the neuron is critical for synaptic strengthening and further more implicating the sexual dimorphism in $DRN^{TH}$ to $NAc^{sh}$ circuit.

Here, I show that 24-hours of social isolation facilitates synaptic strengthening between $DRN^{TH}$ and $NAc^{sh}$, in which further affects male-specific social-isolation-induced sociability increase. Whereas no synaptic strengthening has

occurred in the isolated female, isolation did not induce sociability increase.

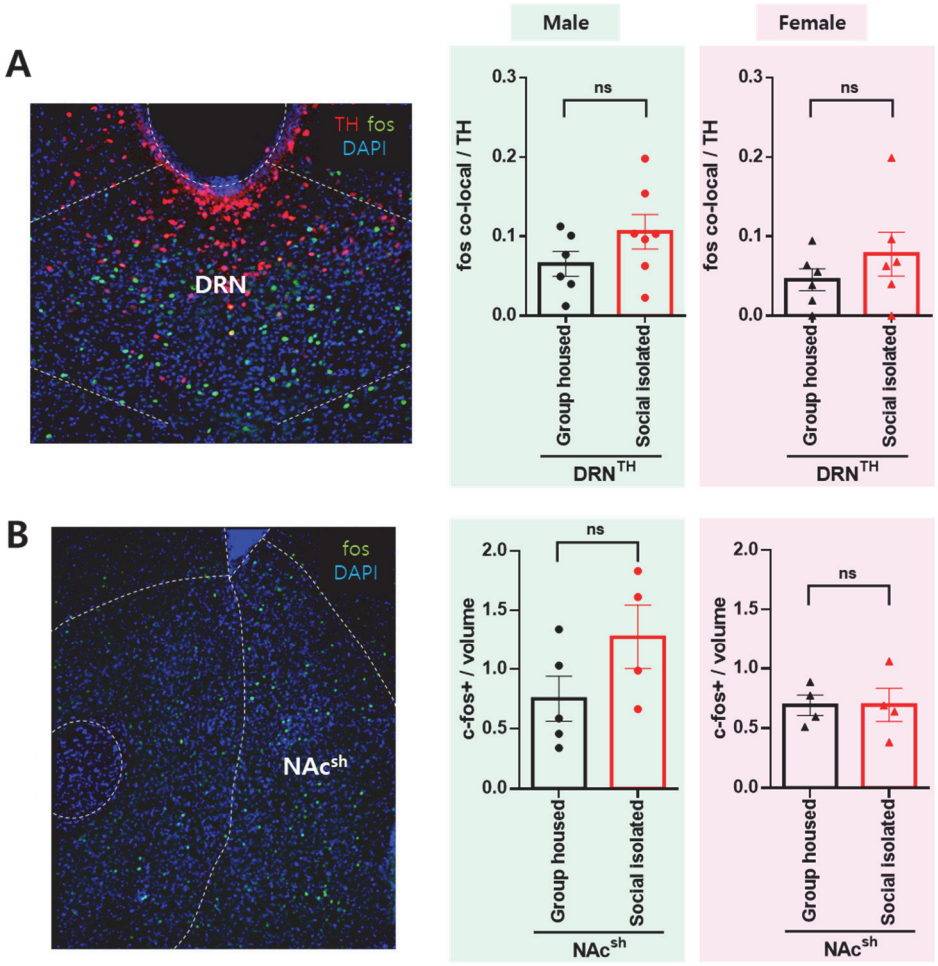


**Figure 19. The number of activated neurons in DRN$^{TH}$ and NAc$^{sh}$ are comparable between group housed and social isolated state.**

(A) Both male and females, social isolation did not affect the number of c-fos positive cells in the DRN$^{TH}$. (male in green, female in pink; group housed male, 0.06543 ± 0.01563, n=6; social isolated male, 0.1058 ± 0.02163, n=7; unpaired *t*-test; $p = 0.1711$; group housed female, 0.04536 ± 0.01372, n=6; social isolated female, 0.07771 ± 0.02759, n=6; unpaired *t*-test; $p = 0.3186$)

(B) Both male and females, social isolation did not affect the number of c-fos positive cells in the $NAc^{sh}$. (male in green, female in pink; group housed male, 0.7514 ± 0.1878, n=5; social isolated male, 1.274 ± 0.2706, n=4; unpaired *t*-test; $p = 0.1454$; group housed female, 0.6913 ± 0.08466, n=4; social isolated female, 0.6930 ± 0.1396, n=4; unpaired *t*-test; $p = 0.9918$)

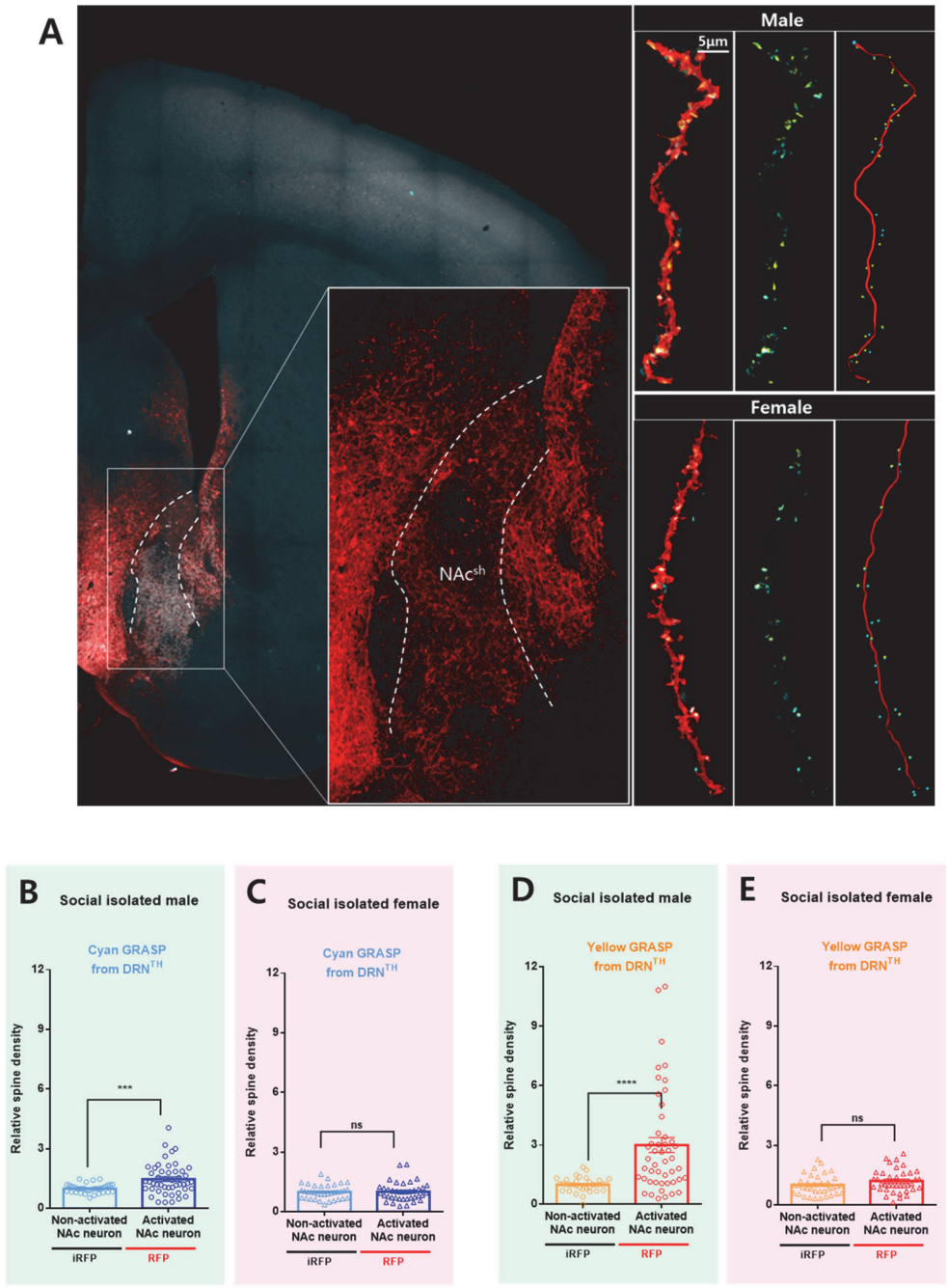


**Figure 20. Sexual dimorphism is observed between synaptic connections of isolation-activated DRN$^{TH}$ and NAc$^{sh}$ neurons.**

*(in collaboration with Dong Il Choi)*

(A) Representative image of $NAc^{sh}$ expressing dual-eGRASP.

(B, C, D and E) Isolation-induced spine density changes. The densities of cyan eGRASP (B and C) or yellow eGRASP (D and E) on mScarlet-I positive dendrites are normalized to the corresponding cyan eGRASP or yellow eGRASP on iRFP670 positive dendrites from the same images. Each data point represents a dendrite.

(B) (n = 36 for NAc non-activated dendrites, n = 59 for NAc activated dendrites, from 18 mice; Mann Whitney two-tailed test; ***$p = 0.0008$)

(C) (n = 36 for NAc non-activated dendrites, n = 38 for NAc activated dendrites, from 6 mice; Mann Whitney two-tailed test; $p = 0.9165$)

(D) (n = 36 for NAc non-activated dendrites, n = 59 for NAc activated dendrites, from 18 mice; Mann Whitney two-tailed test; ****$p < 0.0001$)

(E) (n = 36 for NAc non-activated dendrites, n = 38 for NAc activated dendrites, from 6 mice; Mann Whitney two-tailed test; $p = 0.1231$).

## $DRN^{TH}$ neurons showed a sharp increase in excitability following social isolation.

I found that the increased sociability reflects the strength of neural connectivity between $DRN^{TH}$ and $NAc^{sh}$ cells. This result can be further suggested that the activated synapses between the activated neurons indicate the degree of social interaction after 24-hours of social isolation. Therefore, I hypothesized that increased sociability will not be detected if the synaptic connectivity was blocked during social isolation.

To inhibit the $DRN^{TH}$ neurons from being isolated, I used the DREADD system. Since the plasma CNO levels peak with the maximum concentration at 30 minutes and fall to the baseline within 360 minutes (MacLaren et al., 2016), I needed to examined the excitability of $DRN^{TH}$ neurons after different time points during social isolation (Figure 21A). Thus, I performed whole-cell patch-clamp recording for measuring neuronal excitability in social isolated mice, at 2 hours, 4 hours, and 24 hours after social isolation. Interestingly, a robust increase in excitability was observed in 2 hours after social isolation and sharply decreased from 4 hours which continued to 24 hours (Figure 21B and 21C). Since the excitability peak by social isolation was during the working time of CNO, I could perform experiments to block the synaptic potentiation.

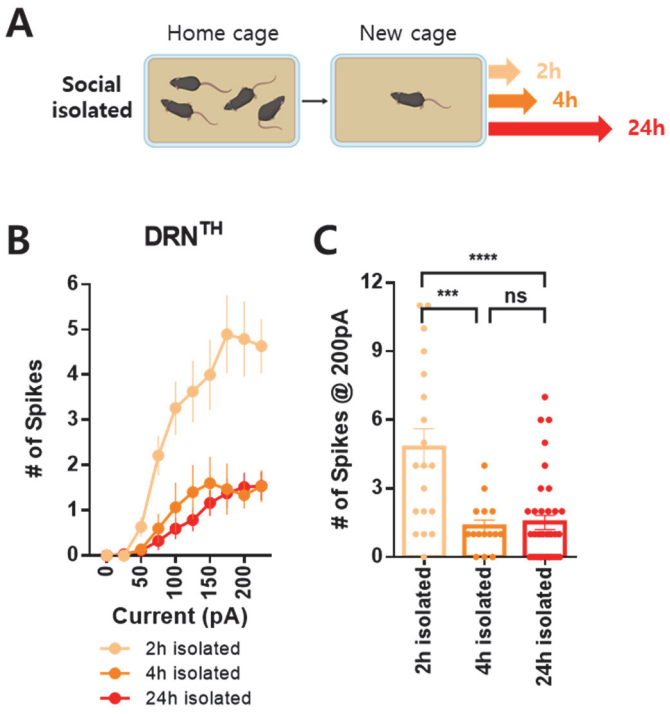


**Figure 21. The neuronal excitability of DRN$^{TH}$ neurons peak at 2 hours of social isolation.**

(A) Schematic image of social isolated male mice at three different time points.

(B) When male mice were social isolated for 2 hours, the DRN$^{TH}$ neurons showed a robust increase in excitability, in which the effect was disappeared from 4 hours and maintained to 24 hours.

(C) The number of spikes at 200pA showed a significant increase at 2-hour isolated males, compared with 4-hour and 24-hour. (2h isolated, n=19; 4h isolated, n=15; 24h isolated, n=37; one-way ANOVA Bonferroni's multiple comparisons test; ***$p$ = 0.0002; ****$p < 0.0001$; $p > 0.9999$)

## Activity of $DRN^{TH}$ neurons during isolation is necessary for isolation-induced sociability increase.

I expressed hM4Di in dopaminergic neurons of the DRN and the neural activity was inhibited by CNO injection when being social isolated (Figure 22A). Surprisingly, isolation-induced sociability increase disappeared when $DRN^{TH}$ neurons were inhibited during isolation (Figure 22B). This change was not due to the change in anxiety, as inhibition of $DRN^{TH}$ had no influence on velocity and total distance moved in three-chamber test (Figure 22C). I further performed open field test to examine the anxiety level more precisely. Even though $DRN^{TH}$ neurons were inhibited during 24-hours of social isolation, the time spent in center, velocity and total distance moved were unchanged (Figure 22D and 22E), in which means that the alterations were specific to sociability. Therefore, these results imply that the activation of $DRN^{TH}$ neurons are needed during isolation in order to increase the sociability.

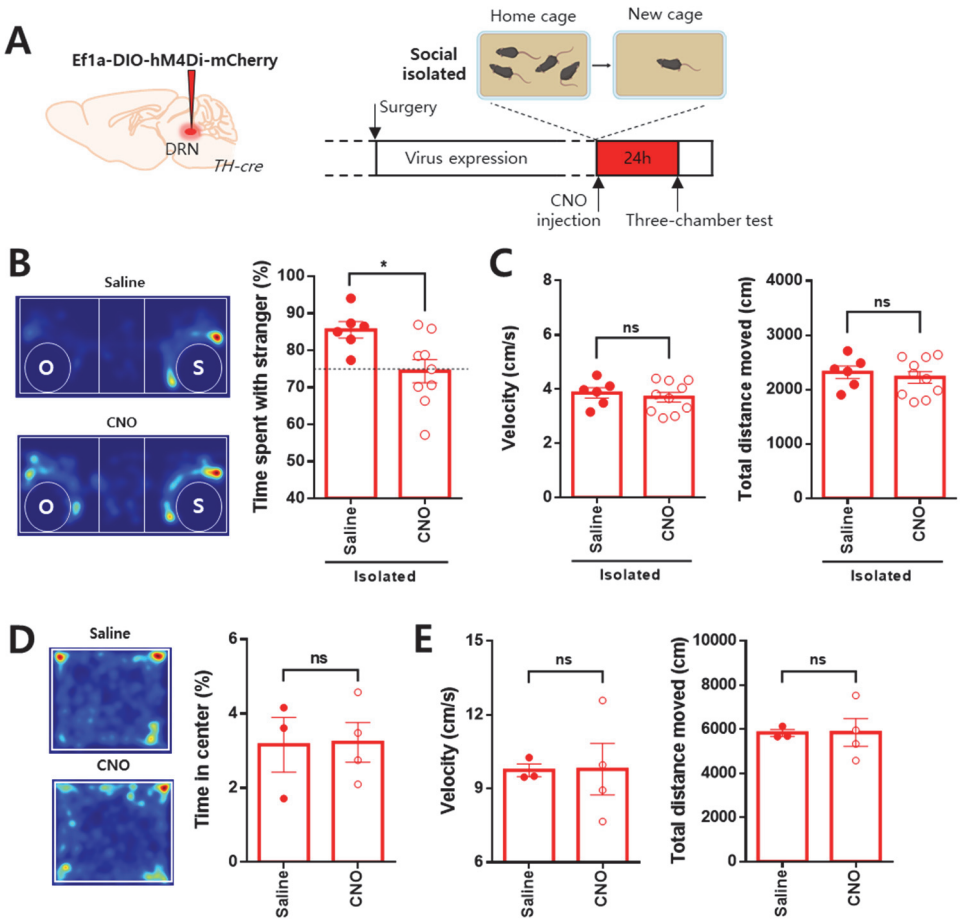


**Figure 22. Activity of DRN$^{TH}$ neurons during isolation is necessary for isolation-induced sociability increase.**

(A) Experimental scheme for virus injection site and timeline of behavioral tasks.

(B) Inhibition of DRN$^{TH}$ neurons during social isolation decreases isolation-induced sociability increase. When same DRN$^{TH}$ neurons were inhibited during group housing, it had no effect on sociability. (Saline, n=6, 85.51 ± 2.237; CNO, n=9, 74.35 ± 3.157; unpaired *t*-test; **p* = 0.0224)

(C) Velocity and total distance moved were not affected when inhibiting $DRN^{TH}$ neurons during social isolation. (Velocity; saline, n=6, 3.860 ± 0.1942; CNO, n=10, 3.700 ± 0.1787; unpaired *t*-test; $p = 0.5718$; Total distance moved; saline, n=6, 2316 ± 116.5; CNO, n=10, 2222 ± 108.1; unpaired *t*-test; $p = 0.5816$)

(D) No effect in anxiety level through open field test. (saline, n=3, 3.161 ± 0.7410; CNO, n=4, 3.224 ± 0.5310; unpaired *t*-test; $p = 0.9458$)

(E) Velocity and total distance moved were not affected by inhibition of $DRN^{TH}$ during 24-hours of social isolation. (Velocity; saline, n=3, 9.740 ± 0.2586; CNO, n=4, 9.784 ± 1.045; unpaired *t*-test; $p = 0.9735$; Total distance moved; saline, n=3, 5829 ± 152.9; CNO, n=4, 5853 ± 625.4; unpaired *t*-test; $p = 0.9757$)

# DISCUSSION

This chapter demonstrates that social isolation recruit isolation-activated neurons in $DRN^{TH}$ and $NAc^{sh}$. By strengthening the synaptic connections between these neuronal ensembles, increase in social interaction occurs.

After labeling isolation-activated or group-house-activated $DRN^{TH}$ neurons, I inhibited these neuronal ensembles when examining the sociability. Even though the number of activated neurons in both states are comparable, strikingly, only inhibiting the isolation-activated neurons could attenuate the isolation-induced sociability increase. These results strongly indicate that isolation-induced sociability increase requires the activated neuronal ensembles of $DRN^{TH}$ to be intact. Furthermore, the isolation-activated neuronal ensembles of the isolated male mice exhibited higher excitability. However, even though isolation induced the fos expression in female mice, no increase in neuronal excitability was detected. This sexual dimorphism results indicate that the fos and excitability do not always correlate. The neuronal excitability is one of the well revealed neuronal properties in the memory field, that the increased neuronal excitability has the necessity and sufficiency for memory expression (Han et al., 2009; Yiu et al., 2014). Whereas CREB is the mechanism of excitability in the field of memory, isolation-activated neurons may share the basis but further experiments are needed to clarify.

Based on chemogenetic modulation and electrophysiological data, I far

narrowed down to the synaptic level. Interestingly, the synaptic density between the activated neuronal ensembles were significantly increased only in the isolated male mice. This increase occurred by just being social isolated for just 24-hours. In addition, this synaptic strengthening was not detected in the isolated females, which also correlates with the unchanged sociability after being social isolated. This is the first study to visualize the isolation-activated synapses, in which correlates with the sociability degree.

Many researchers now focus down to the synaptic level to reveal the underlying mechanisms of various phenotypes. One paper from Medendorp et al. has reported that 3-month social isolated mice shows abnormal social behaviors with immature spine morphology in the prefrontal cortex (Medendorp et al., 2018). Despite the interesting results, we do not know whether the changes are circuit-specific nor activated-neuron-specific. The approach using dual-eGRASP will guide future studies in further narrowing down their previous results.

# CHAPTER IV

# CONCLUSION

# CONCLUSION

This study answered to where and how isolation-induced sociability changes occur in a sex-dependent manner. Through optogenetics, chemogenetics, patch clamp recording and dual-eGRASP technique, I could narrow down the underlying mechanism to the synaptic level. Sexual dimorphism following 24-hours of social isolation starts by activation of $DRN^{TH}$ neurons, in which then triggers synaptic strengthening with $NAc^{sh}$ neurons during the 24-hours. Thus, these modulations generate increased sociability. In contrast, in isolated females, since synaptic strengthening did not occur, isolation-induced sociability was not triggered.

In Chapter II, I detected sex-dependent isolation-induced sociability increase. Then I further manipulated $DRN^{TH}$-$NAc^{sh}$ circuit to examine whether this circuit is modulating the sociability, both in males and females. When I inhibited the circuit, the increased sociability by isolation was attenuated only in the males. To examine female's resilience to social isolation, I performed ovariectomy to see if female sex hormones are the cause. However, ovariectomized females did not show any isolation-induced sociability increase, which indicates that the resilient phenotype was not from sex hormones.

In Chapter III, I narrowed down the neuronal population of manipulation, from total to "isolation-activated" neurons. By combining fos-based labeling system with chemogenetics, I could modulate the activated neuronal ensembles.

Surprisingly, inhibition of isolation-activated neurons lowered the interaction time, whereas inhibition of group-house-activated neurons did not alter the sociability. Furthermore, 24-hours of social isolation facilitated the synaptic strengthening between the isolation-activated neurons. When $DRN^{TH}$ neurons' activity was blocked during isolation, sociability increase was not detected. This result implies that $DRN^{TH}$ neurons should be triggered in order to induce synaptic strengthening and sociability increase.

In human studies, sexual dimorphism in sociability is also observed. Sexual dimorphisms exist from brain anatomy (Ruigrok et al., 2014) to psychological processes and in various neurological disorders (Bálint et al., 2009; Gillberg et al., 2006; Wooten et al., 2004). It is reported that social isolation affects men and women differently (McLean et al., 2011). Moreover, a research by Vandervoort observed that men are more isolated than women (Vandervoort, 2000). It is further known that evidence from animal models reproduce the sex differences observed in humans (Leranth et al., 2000). According to previous studies and this thesis, social isolation mediates sociability changes in human and in mice. However due to the extensive differences in biology and social system, it is hard to classify into one basis. Even though the dissimilarities, it is known that neuromodulatory systems have coevolved to modulate social behaviors. Therefore, I expect this study will provide valuable set of data for future sociability studies with gender factor. The final aim of this study is to help develop therapeutics for sociability disorders such as autism spectrum disease.

This study, for the first time, revealed that one of the intrinsic mechanisms

in sociability, moreover the sex differences in sociability, is on the synapse. By applying dual-eGRASP technique to neuromodulatory system of the mouse brain, I further provided the visualization of neuromodulatory synapses that are activated during social isolation. I hope that the findings will provide us with groundwork for the synaptic manipulation of sociability. This approach can be modified by applying to different types of social behavior and to various brain regions.

# REFERENCES

Asher, M., and Aderka, I.M. (2018). Gender differences in social anxiety disorder. *74*, 1730-1741.

Badiani, A., Oates, M.M., Day, H.E., Watson, S.J., Akil, H., and Robinson, T.E. (1998). Amphetamine-induced behavior, dopamine release, and c-fos mRNA expression: modulation by environmental novelty. J Neurosci *18*, 10579-10593.

Bálint, S., Czobor, P., Komlósi, S., Mészáros, Á., Simon, V., and Bitter, I. (2009). Attention deficit hyperactivity disorder (ADHD): gender- and age-related differences in neurocognition. Psychological Medicine *39*, 1337-1345.

Barik, J., Marti, F., Morel, C., Fernandez, S.P., Lanteri, C., Godeheu, G., Tassin, J.-P., Mombereau, C., Faure, P., and Tronche, F. (2013). Chronic Stress Triggers Social Aversion via Glucocorticoid Receptor in Dopaminoceptive Neurons. Science *339*, 332.

Baumeister, R.F., and Leary, M.R. (1995). The Need to Belong: Desire for Interpersonal Attachments as a Fundamental Human Motivation. Psychological Bulletin *117*, 497-529.

Becker, J.B. (1999). Gender Differences in Dopaminergic Function in Striatum and Nucleus Accumbens. Pharmacology Biochemistry and Behavior *64*, 803-812.

Berkman, L.F., Vaccarino, V., and Seeman, T.J.A.o.B.M. (1993). Gender differences in cardiovascular morbidity and mortality: The contribution of social networks and support.

Bertran-Gonzalez, J., Bosch, C., Maroteaux, M., Matamales, M., Herve, D., Valjent, E., and Girault, J.A. (2008). Opposing patterns of signaling activation in dopamine D1 and D2 receptor-expressing striatal neurons in response to cocaine and haloperidol. J Neurosci *28*, 5671-5685.

Borland, J.M., Aiani, L.M., Norvelle, A., Grantham, K.N., O'Laughlin, K., Terranova, J.I., Frantz, K.J., and Albers, H.E. (2019). Sex-dependent regulation of social reward by oxytocin receptors in the ventral tegmental area. Neuropsychopharmacology *44*, 785-792.

Bourque, M., Dluzen, D.E., and Di Paolo, T.J.F.i.n. (2012). Signaling pathways mediating the neuroprotective effects of sex steroids and SERMs in Parkinson's disease. *33*, 169-178.

Brancato, A., Bregman, D., Ahn, H.F., Pfau, M.L., Menard, C., Cannizzaro, C., Russo, S.J., and Hodes, G.E. (2017). Sub-chronic variable stress induces sex-specific effects on glutamatergic synapses in the nucleus accumbens. Neuroscience *350*, 180-189.

Calipari, E.S., Juarez, B., Morel, C., Walker, D.M., Cahill, M.E., Ribeiro, E., Roman-Ortiz, C., Ramakrishnan, C., Deisseroth, K., Han, M.H.*, et al.* (2017). Dopaminergic dynamics underlying sex-specific cocaine reward. Nat Commun *8*, 13877.

Calizo, L.H., Akanwa, A., Ma, X., Pan, Y.-z., Lemos, J.C., Craige, C., Heemstra, L.A., and Beck, S.G. (2011). Raphe serotonin neurons are not homogenous: Electrophysiological, morphological and neurochemical evidence. Neuropharmacology *61*, 524-543.

Chandra, R., Francis, T.C., Konkalmatt, P., Amgalan, A., Gancarz, A.M., Dietz, D.M., and Lobo, M.K. (2015). Opposing role for Egr3 in nucleus accumbens cell subtypes in cocaine action. J Neurosci *35*, 7927-7937.

Choi, J.-H., Sim, S.-E., Kim, J.-i., Choi, D.I., Oh, J., Ye, S., Lee, J., Kim, T., Ko, H.-G., and Lim, C.-S.J.S. (2018). Interregional synaptic maps among engram cells underlie memory formation. *360*, 430-435.

Di Ciano, P., Robbins, T.W., and Everitt, B.J. (2008). Differential effects of nucleus accumbens core, shell, or dorsal striatal inactivations on the persistence, reacquisition, or reinstatement of responding for a drug-paired conditioned reinforcer. Neuropsychopharmacology *33*, 1413-1425.

Dolen, G., Darvishzadeh, A., Huang, K.W., and Malenka, R.C. (2013). Social reward requires coordinated activity of nucleus accumbens oxytocin and serotonin. Nature *501*, 179-184.

Eisenberger, N.I. (2012). The pain of social disconnection: examining the shared neural underpinnings of physical and social pain. Nat Rev Neurosci *13*, 421-434.

Ekstrand, M.I., Nectow, A.R., Knight, Z.A., Latcha, K.N., Pomeranz, L.E., and Friedman, J.M. (2014). Molecular profiling of neurons based on connectivity. Cell *157*, 1230-1242.

Ferguson, S.M., and Robinson, T.E. (2004). Amphetamine-evoked gene expression in striatopallidal neurons: regulation by corticostriatal afferents and the ERK/MAPK signaling cascade. Journal of neurochemistry *91*, 337-348.

Fernandez, S.P., Cauli, B., Cabezas, C., Muzerelle, A., Poncer, J.C., and Gaspar, P. (2016). Multiscale single-cell analysis reveals unique phenotypes of raphe 5-HT

neurons projecting to the forebrain. Brain Struct Funct *221*, 4007-4025.

Gillberg, C., Cederlund, M., Lamberg, K., and Zeijlon, L. (2006). Brief Report: "The Autism Epidemic". The Registered Prevalence of Autism in a Swedish Urban Area. Journal of Autism and Developmental Disorders *36*, 429.

Gillies, G.E., and McArthur, S. (2010). Estrogen Actions in the Brain and the Basis for Differential Action in Men and Women: A Case for Sex-Specific Medicines. Pharmacological Reviews *62*, 155-198.

Greenberg, G.D., Laman-Maharg, A., Campi, K.L., Voigt, H., Orr, V.N., Schaal, L., and Trainor, B.C. (2013). Sex differences in stress-induced social withdrawal: role of brain derived neurotrophic factor in the bed nucleus of the stria terminalis. Front Behav Neurosci *7*, 223.

Grueter, B.A., Robison, A.J., Neve, R.L., Nestler, E.J., and Malenka, R.C. (2013). FosB differentially modulates nucleus accumbens direct and indirect pathway function. Proc Natl Acad Sci U S A *110*, 1923-1928.

Gunaydin, L.A., Grosenick, L., Finkelstein, J.C., Kauvar, I.V., Fenno, L.E., Adhikari, A., Lammel, S., Mirzabekov, J.J., Airan, R.D., Zalocusky, K.A.*, et al.* (2014). Natural neural projection dynamics underlying social behavior. Cell *157*, 1535-1551.

Haasteren, G.v., Li, S., Ryser, S., and Schlegel, W. (2000). Essential Contribution of Intron Sequences to Ca2+-Dependent Activation of c-fos Transcription in Pituitary Cells. NEN *72*, 368-378.

Han, J.-H., Kushner, S., Yiu, A., Hsiang, H.-L., Buch, T., Waisman, A., Bontempi, B., Neve, R., Frankland, P., and Josselyn, S. (2009). Selective Erasure of a Fear

Memory. Science (New York, NY) *323*, 1492-1496.

Hasbi, A., Nguyen, T., Rahal, H., Manduca, J.D., Miksys, S., Tyndale, R.F., Madras, B.K., Perreault, M.L., and George, S.R. (2020). Sex difference in dopamine D1-D2 receptor complex expression and signaling affects depression- and anxiety-like behaviors. Biol Sex Differ *11*, 8.

Hille, B. (1978). Ionic channels in excitable membranes. Current problems and biophysical approaches. Biophys J *22*, 283-294.

Huang, K.W., Ochandarena, N.E., Philson, A.C., Hyun, M., Birnbaum, J.E., Cicconet, M., and Sabatini, B.L. (2019). Molecular and anatomical organization of the dorsal raphe nucleus. Elife *8*.

Huang, Q., Zhou, Y., and Liu, L.Y. (2017). Effect of post-weaning isolation on anxiety- and depressive-like behaviors of C57BL/6J mice. Exp Brain Res *235*, 2893-2899.

Ishimura, K., Takeuchi, Y., Fujiwara, K., Tominaga, M., Yoshioka, H., and Sawada, T. (1988). Quantitative analysis of the distribution of serotonin-immunoreactive cell bodies in the mouse brain. Neuroscience Letters *91*, 265-270.

Jung, H., Kim, S.W., Kim, M., Hong, J., Yu, D., Kim, J.H., Lee, Y., Kim, S., Woo, D., Shin, H.S.*, et al.* (2019). Noninvasive optical activation of Flp recombinase for genetic manipulation in deep mouse brain regions. Nat Commun *10*, 314.

Kang, S.J., Kwak, C., Lee, J., Sim, S.E., Shim, J., Choi, T., Collingridge, G.L., Zhuo, M., and Kaang, B.K. (2015). Bidirectional modulation of hyperalgesia via the specific control of excitatory and inhibitory neuronal activity in the ACC. Mol Brain *8*, 81.

Karkhanis, A.N., Locke, J.L., McCool, B.A., Weiner, J.L., and Jones, S.R. (2014). Social isolation rearing increases nucleus accumbens dopamine and norepinephrine responses to acute ethanol in adulthood. Alcohol Clin Exp Res *38*, 2770-2779.

Ke, M.T., Nakai, Y., Fujimoto, S., Takayama, R., Yoshida, S., Kitajima, T.S., Sato, M., and Imai, T. (2016). Super-Resolution Mapping of Neuronal Circuitry With an Index-Optimized Clearing Agent. Cell Rep *14*, 2718-2732.

Krishnan, V., Han, M.H., Graham, D.L., Berton, O., Renthal, W., Russo, S.J., Laplant, Q., Graham, A., Lutter, M., Lagace, D.C*., et al.* (2007). Molecular adaptations underlying susceptibility and resistance to social defeat in brain reward regions. Cell *131*, 391-404.

Kronman, H., Richter, F., Labonte, B., Chandra, R., Zhao, S., Hoffman, G., Lobo, M.K., Schadt, E.E., and Nestler, E.J. (2019). Biology and Bias in Cell Type-Specific RNAseq of Nucleus Accumbens Medium Spiny Neurons. Sci Rep *9*, 8350.

Krupina, N.A., Khlebnikova, N.N., Narkevich, V.B., Naplekova, P.L., and Kudrin, V.S. (2020). The Levels of Monoamines and Their Metabolites in the Brain Structures of Rats Subjected to Two- and Three-Month-Long Social Isolation. Bull Exp Biol Med *168*, 605-609.

Leranth, C., Roth, R.H., Elsworth, J.D., Naftolin, F., Horvath, T.L., and Redmond, D.E. (2000). Estrogen Is Essential for Maintaining Nigrostriatal Dopamine Neurons in Primates: Implications for Parkinson's Disease and Memory. The Journal of Neuroscience *20*, 8604.

Li, B.J., Liu, P., Chu, Z., Shang, Y., Huan, M.X., Dang, Y.H., and Gao, C.G.

(2017). Social isolation induces schizophrenia-like behavior potentially associated with HINT1, NMDA receptor 1, and dopamine receptor 2. Neuroreport *28*, 462-469.

Lin, R., Liang, J., Wang, R., Yan, T., Zhou, Y., Liu, Y., Feng, Q., Sun, F., Li, Y., Li, A.*, et al.* (2020). The Raphe Dopamine System Controls the Expression of Incentive Memory. Neuron.

Loew, R., Heinz, N., Hampf, M., Bujard, H., and Gossen, M. (2010). Improved Tet-responsive promoters with minimized background expression. BMC Biotechnol *10*, 81.

MacLaren, D., Browne, R., Shaw, J., Radhakrishnan, S., Khare, P., España, R., and Clark, S. (2016). Clozapine N-Oxide Administration Produces Behavioral Effects in Long–Evans Rats: Implications for Designing DREADD Experiments. eNeuro *3*.

Matthews, G.A., Nieh, E.H., Vander Weele, C.M., Halbert, S.A., Pradhan, R.V., Yosafat, A.S., Glober, G.F., Izadmehr, E.M., Thomas, R.E., Lacy, G.D.*, et al.* (2016). Dorsal Raphe Dopamine Neurons Represent the Experience of Social Isolation. Cell *164*, 617-631.

McLean, C.P., Asnaani, A., Litz, B.T., and Hofmann, S.G. (2011). Gender differences in anxiety disorders: prevalence, course of illness, comorbidity and burden of illness. J Psychiatr Res *45*, 1027-1035.

Medendorp, W.E., Petersen, E.D., Pal, A., Wagner, L.M., Myers, A.R., Hochgeschwender, U., and Jenrow, K.A. (2018). Altered Behavior in Mice Socially Isolated During Adolescence Corresponds With Immature Dendritic Spine

Morphology and Impaired Plasticity in the Prefrontal Cortex. Front Behav Neurosci *12*, 87.

Nelson, R.J., and Trainor, B.C. (2007). Neural mechanisms of aggression. Nature Reviews Neuroscience *8*, 536-546.

Newmann, J.P.J.J.o.H., and Behavior, S. (1986). Gender, life strains, and depression. 161-178.

Oliver, D.K., Intson, K., Sargin, D., Power, S.K., McNabb, J., Ramsey, A.J., and Lambe, E.K. (2020). Chronic social isolation exerts opposing sex-specific consequences on serotonin neuronal excitability and behaviour. Neuropharmacology *168*, 108015.

Raymond, V., Beaulieu, M., Labrie, F., and Boissier, J.J.S. (1978). Potent antidopaminergic activity of estradiol at the pituitary level on prolactin release. *200*, 1173-1175.

Reijmers, L.G., Perkins, B.L., Matsuo, N., and Mayford, M. (2007). Localization of a stable neural correlate of associative memory. Science *317*, 1230-1233.

Ren, J., Friedmann, D., Xiong, J., Liu, C.D., Ferguson, B.R., Weerakkody, T., DeLoach, K.E., Ran, C., Pun, A., Sun, Y.*, et al.* (2018). Anatomically Defined and Functionally Distinct Dorsal Raphe Serotonin Sub-systems. Cell *175*, 472-487 e420.

Riecher-Rössler, A., Häfner, H., Stumbaum, M., Maurer, K., and Schmidt, R. (1994). Can Estradiol Modulate Schizophrenic Symptomatology? Schizophrenia Bulletin *20*, 203-214.

Ruigrok, A.N.V., Salimi-Khorshidi, G., Lai, M.-C., Baron-Cohen, S., Lombardo,

M.V., Tait, R.J., and Suckling, J. (2014). A meta-analysis of sex differences in human brain structure. Neuroscience & Biobehavioral Reviews *39*, 34-50.

Sagoshi, S., Maejima, S., Morishita, M., Takenawa, S., Otubo, A., Takanami, K., Sakamoto, T., Sakamoto, H., Tsukahara, S., and Ogawa, S. (2020). Detection and characterization of estrogen receptor beta expression in the brain with newly developed transgenic mice. Neuroscience.

Seo, C., Guru, A., Jin, M., Ito, B., Sleezer, B.J., Ho, Y.-Y., Wang, E., Boada, C., Krupa, N.A., Kullakanda, D.S.*, et al.* (2019). Intense threat switches dorsal raphe serotonin neurons to a paradoxical operational mode. Science *363*, 538.

Smith, R.J., Lobo, M.K., Spencer, S., and Kalivas, P.W. (2013). Cocaine-induced adaptations in D1 and D2 accumbens projection neurons (a dichotomy not necessarily synonymous with direct and indirect pathways). Curr Opin Neurobiol *23*, 546-552.

Stratford, T.R., and Wirtshafter, D.J.B.r. (1990). Ascending dopaminergic projections from the dorsal raphe nucleus in the rat. *511*, 173-176.

Trainor, B.C. (2011). Stress responses and the mesolimbic dopamine system: social contexts and sex differences. Horm Behav *60*, 457-469.

Trulson, M.E., Cannon, M.S., and Raese, J.D.J.B.r.b. (1985). Identification of dopamine-containing cell bodies in the dorsal and median raphe nuclei of the rat brain using tyrosine hydroxylase immunochemistry. *15*, 229-234.

Vandervoort, D. (2000). Social isolation and gender. Current Psychology *19*, 229-236.

Wallace, D.L., Han, M.H., Graham, D.L., Green, T.A., Vialou, V., Iniguez, S.D.,

Cao, J.L., Kirk, A., Chakravarty, S., Kumar, A.*, et al.* (2009). CREB regulation of nucleus accumbens excitability mediates social isolation-induced behavioral deficits. Nat Neurosci *12*, 200-209.

Walsh, J.J., Christoffel, D.J., Heifets, B.D., Ben-Dor, G.A., Selimbeyoglu, A., Hung, L.W., Deisseroth, K., and Malenka, R.C. (2018). 5-HT release in nucleus accumbens rescues social deficits in mouse autism model. Nature *560*, 589-594.

Wooten, G.F., Currie, L.J., Bovbjerg, V.E., Lee, J.K., and Patrie, J. (2004). Are men at greater risk for Parkinson's disease than women? Journal of Neurology, Neurosurgery & Psychiatry *75*, 637-639.

Yiu, A.P., Mercaldo, V., Yan, C., Richards, B., Rashid, A.J., Hsiang, H.L., Pressey, J., Mahadevan, V., Tran, M.M., Kushner, S.A.*, et al.* (2014). Neurons are recruited to a memory trace based on relative neuronal excitability immediately before training. Neuron *83*, 722-735.

Zelikowsky, M., Hui, M., Karigo, T., Choe, A., Yang, B., Blanco, M.R., Beadle, K., Gradinaru, V., Deverman, B.E., and Anderson, D.J. (2018). The Neuropeptide Tac2 Controls a Distributed Brain State Induced by Chronic Social Isolation Stress. Cell *173*, 1265-1279 e1219.

Zhang, J., Zhang, L., Jiao, H., Zhang, Q., Zhang, D., Lou, D., Katz, J.L., and Xu, M. (2006). c-Fos facilitates the acquisition and extinction of cocaine-induced persistent changes. J Neurosci *26*, 13287-13296.

Zhou, X., Vink, M., Klaver, B., Berkhout, B., and Das, A.T. (2006). Optimization of the Tet-On system for regulated gene expression through viral evolution. Gene Ther *13*, 1382-1390.

# 국문초록

사회적 동물에서의 사회성은 매우 중요한 부분이며, 따라서 사회적 연결을 유지하기 위해 많은 노력을 한다. 사회적으로 단절이 되면 사회적 고통을 느끼게 되며, “사회적 고립”은 사회적 연결 고리가 끊어지는 종류 중 하나에 속한다. 사회적 고립에 의한 사회성 변화와 불안 수준에 대한 연구는 오랜 기간 동안 다양한 분야에서 연구가 진행되어 왔다. 주로 사회적 고립 상태를 몇 달 이상 유지하는 장기적인 영향에 대한 연구들이 이루어져왔지만, 하루 동안 사회적 고립이 되었을 때의 사회성 변화와 이러한 변화가 어떠한 메커니즘으로 이루어지는지에 대한 연구가 필요하였다.

본 연구는, 사회적 고립 시 성별에 따라 사회성이 다르게 변한다는 것을 발견하였으며, 수컷 생쥐에서만 사회적 고립에 의한 사회성 증가를 관찰하였다. 이러한 행동학적 변화가 나타나는 메커니즘을 밝히기 위해, 배측봉선핵에 존재하는 도파민 신경세포와 측좌핵에 초점을 맞춰 연구를 진행하였다. 광유전학을 활용하여 두 부위 간의 신경회로를 조절하였으며, 억제 시켰을 때 사회적 고립에 의한 사회성 증가가 나타나지 않는다는 것을 확인하였다. 더 나아가 사회적 고립에 의해 활성화를 보이는 신경세포만을 표지 하여 화학유전체학을 통해 신경세포의 활성 상

태를 조절하였다. 이를 통해, 사회적 고립에 의한 사회성 증가는 사회적 고립에 의해 활성화된 신경세포를 필요로 한다는 것을 밝혔다. 더 나아가 활성화된 신경세포 사이의 시냅스 변화를 시각화하여, 배측봉선핵의 도파민 신경세포와 측좌핵 신경세포 간의 시냅스 밀도가 증가했다는 것을 발견하였다. 이는 행동학적으로 관찰하고 조절한 실험 결과와 일치한다.

따라서, 성별에 따른 사회적 고립에 의한 사회성 변화의 원인을 시냅스 수준부터 행동학적 수준까지 밝혀, 사회적 고립에 의한 사회성 증가의 메커니즘을 밝혀내었다.

.....

주요어 : 사회적 고립, 사회성, 배측봉선핵, 측좌핵, 시냅스

학번 : 2015-20451